

1 **Transverse energy analysis of**
2 **relativistic heavy ion collisions**
3 **through the use of identified particles**
4 **spectra**

5 A Thesis Presented for the
6 Master of Science
7 Degree
8 The University of Tennessee, Knoxville

9 Biswas Sharma

10 May 2018

11

© by Biswas Sharma, 2018

12

All Rights Reserved.

13 Table of Contents

14	1 Introduction	1
15	2 Theoretical Background	3
16	2.1 Quantum Chromodynamics	3
17	2.2 Phase Transitions	4
18	2.3 Quark-Gluon Plasma	5
19	3 Relativistic Heavy Ion Collisions	7
20	3.1 RHIC and LHC	7
21	3.2 Collision Energy and Geometry	9
22	3.3 Kinematic Variables (will go into Appendix)	10
23	3.4 QGP Evolution	13
24	3.5 Detection of Collision Products	14
25	3.6 Detection of QGP Signatures	15
26	3.6.1 Bjorken Energy Density	15
27	3.6.2 Elliptic Flow	15
28	3.6.3 Direct and Thermal Photons	17
29	3.6.4 Strangeness Enhancement	18
30	3.6.5 Jet Quenching	19
31	3.7 The Beam Energy Scan Program	19
32	4 Measurement of Transverse Energy	21
33	4.1 Definition of Transverse Energy	21

34	4.2	E_T Measurement with Calorimeters	22
35	4.2.1	Calorimeter	22
36	4.2.2	E_T from PHENIX Calorimetry	23
37	4.3	E_T Measurement with Tracking Detectors	24
38	4.3.1	Tracking and Particle Identification	24
39	4.3.2	Calculation of $\frac{dE_T}{d\eta}$ from p_T spectra	25
40	4.3.3	Tracking Detectors in STAR	26
41	5	Data Analysis	28
42	5.0.1	STAR p_T spectra	28
43	5.1	Extrapolation of Spectra	29
44	5.1.1	Boltzmann-Gibbs Blast Wave	29
45	5.1.2	Fitting Spectra to BGBW	30
46	5.2	Calculations from the Spectral Fits	31
47	5.2.1	Calculation of $\frac{dE_T}{dy}$, $\frac{dE_T}{d\eta}$, $\frac{dN_{ch}}{dy}$, and $\frac{dN_{ch}}{d\eta}$	31
48	5.2.2	Corrections for Unidentified Particles and Estimation of Total E_T . .	31
49	5.2.3	Lambdas Centralitiy Adjustments and E_T Interpolations	31
50	5.3	Uncertainties	31
51	6	Results	32
52	7	Conclusion	39
53	8	Future Work	40
54	8.1	Goodness of Fit	40
55	8.2	Bjorken Energy Density Estimate	40
56	8.3	Asymmetric beams	41
57		Bibliography	42
58		Appendices	75

59 List of Tables

<small>60</small>	3.1 Colliding species and associated collision energies at RHIC [26].	10
<small>61</small>	5.1 Isospin states of different identified particles.	31

List of Figures

63	2.1	Schematic of the QCD phase diagram [9].	6
64	3.1	Initial layout of the RHIC [28].	8
65	3.2	An illustration of a mid-central collision of two nuclei traveling in the z	
66		direction. The X-axis is parallel to the line joining the centers of the two	
67		nuclei at the time of collision [14].	11
68	3.3	An illustration of a collision consisting of participants (solid red) and	
69		spectators (open blue) within the colliding nuclei labeled A and B. t_c denotes	
70		the time of maximum overlap of the two nuclei. The apparent narrowing of	
71		the volumes of the nuclei in the z-direction is due to Lorentz contraction [39].	12
72	3.4	Evolution of the QGP represented in a lightcone diagram. τ_0 denotes the	
73		formation time of the QGP. T_c is the critical temperature of the transition	
74		from the QGP to the hadron gas phase. T_{ch} and T_{fo} stand for the temperatures	
75		at, respectively, chemical freeze-out and thermal freeze-out [14].	13
76	3.5	Minimum-bias Au+Au ($\sqrt{s_{NN}} = 200\text{GeV}$) elliptic flow spectra for identified	
77		particles: (a) v_2 vs p_T and (b) v_2 vs KE_T [4].	16
78	3.6	Minimum-bias Au+Au ($\sqrt{s_{NN}} = 200\text{GeV}$) elliptic flow spectra for identified	
79		particles: (a) $\frac{v_2}{n_q}$ vs $\frac{p_T}{n_q}$ and (b) $\frac{v_2}{n_q}$ vs $\frac{KE_T}{n_q}$ [4].	17
80	3.7	Feynman diagram representing the production of photons from quarks and	
81		gluons. (a) and (b) represent annihilation processes, whereas (c) and (d)	
82		represent Compton processes [41].	18

83	3.8	Illustration of jet quenching. Two jets are produced from each of the hard	
84		scatterings occuring at the locations of the solid dots. Jets originating closer	
85		to the initial surface are more probable to propagate outside the medium, as	
86		shown. Jets opposite to them interact with the medium, losing their energy	
87		and resulting in bow front shock waves [38].	20
88	4.1	Energy loss distribution in the STAR TPC for primary and secondary particles	
89		[21].	27
90	5.1	Transverse momentum spectra for π^+ , π^- , K^+ , K^- , p , and \bar{p} at midrapidity	
91		($ y < 0.1$) from 39 GeV Au+Au collisions at RHIC. The fitting curves	
92		on the 0-5% central collision spectra for pions, kaons, and protons/anti-	
93		protons represent, respectively, the Bose-Einstein, m_T -exponential, and	
94		double-exponential functions [2].	29
95	5.2	Red curve shows the Boltzmann-Gibbs blast wave functional fit on the PRE-	
96		LIMINARY transverse momentum spectrum for lambda particles identified	
97		by the STAR detector for 19.6 GeV Au+Au collisions (10-15% central).	
98		Parameters extracted from the chi-square goodness-of-fit test, as well as other	
99		statistics, are shown in the box on the top right.	30
100	6.1	Parallel coordinates plot for 270 different spectra relating 6 different identified	
101		particles (color-coded) to their respective collision centrality classes, good-fit	
102		parameters, and the transverse energy calculated using said parameters. . . .	32
103	6.2	$(dE_T/d\eta)/0.5N_{part}$ at midrapidity as a function of $\sqrt{s_{NN}}$ for different central-	
104		ities. The dashed line represents a power-law fit to the 0-5% central data in	
105		the form $y = ax^{2b}$, where x and y are the placeholders for the quantities in	
106		the plot axes. $\chi^2/n.d.f$ for the fit was 1.806, and the good-fit parameters were	
107		$a = 0.4838 \pm 0.0429$ and $b = 0.2005 \pm 0.01466$. The shaded area represents	
108		the uncertainty bounds for the 0-5% central PHENIX data from [3].	33
109	6.3	$(dE_T/d\eta)/(dN_{ch}/d\eta)$ at midrapidity as a function of $\sqrt{s_{NN}}$ for different	
110		centralities.	34

111	6.4	$(dE_T/d\eta)/0.5N_{part}$ at midrapidity as a function of N_{part} for different collision	
112		energies.	35
113	6.5	$(dE_T/d\eta)/(dN_{ch}/d\eta)$ at midrapidity as a function of N_{part} for different collision	
114		energies.	35
115	6.6	$(dE_T/dy)/0.5N_{part}$ at midrapidity as a function of $\sqrt{s_{NN}}$ for different centralities.	36
116	6.7	$(dE_T/dy)/(dN_{ch}/dy)$ at midrapidity as a function of $\sqrt{s_{NN}}$ for different	
117		centralities.	36
118	6.8	$(dE_T/dy)/0.5N_{part}$ at midrapidity as a function of N_{part} for different collision	
119		energies.	37
120	6.9	$(dE_T/dy)/(dN_{ch}/dy)$ at midrapidity as a function of N_{part} for different collision	
121		energies.	37
122	6.10	$\frac{dE_T}{d\eta}/0.5N_{part}$ for 0-5% central collisions at midrapidity as a function of $\sqrt{s_{NN}}$.	
123		The PHENIX data are from [3]. The error bars represent the total statistical	
124		and systematic uncertainties.	38

Chapter 1

Introduction

The Big Bang model is based on observational evidence, such as the cosmic microwave background radiation and the cosmological expansion, and suggests that at the beginning the universe must have been at a state of really high density and temperature. As the universe expanded, it went through several stages of cooling characterized by the formation of matters with different compositions. The matter we mostly observe today exists at temperatures and densities much lower compared to those in the early universe.

The Large Hadron Collider (LHC) at CERN and the Relativistic Heavy Ion Collider (RHIC) at the Brookhaven National Laboratory have the ability to collide heavy nuclei, such as those of gold and uranium, at nearly the speed of light, reaching temperatures of trillions of degrees Celcius. These laboratories have provided evidence of the formation of an exotic state of matter, called the quark-gluon plasma (QGP). It only exists for a brief amount of time after such collisions and instantly freezes out into a plethora of new particles, which carry the signatures we can use to deduct QGP properties. Its properties suggest that it should be similar to the matter that existed within microseconds of the genesis of the universe.[?].

One of the methods to probe the properties of this matter is by analyzing the conversion of the beam-direction energy at the time of collision into transverse energy after the collision. These measurements can be used to estimate the energy density of the QGP. This analysis is generally done by using data from the calorimeters placed around the collision site. In this

thesis, I use the data collected by tracking detectors, instead of the conventional calorimeters, to calculate the transverse energy.

This thesis is structured as follows. chapter 2 touches on the theoretical background associated with the concept of the quark-gluon plasma. In chapter 3, I summarize the experimental concepts pertaining to relativistic heavy-ion collisions and the production and detection of QGP. chapter 4 consists of the formalism of the measurement of transverse energy using calorimeters as well as tracking detectors. It also describes what has been done using calorimeters. chapter 5 describes the data used to perform the analysis in this thesis and notes the relevant details of the analysis. In chapter 6, I present the results and compare them to the ones in literature obtained using a different method. Chapter ??ch:conclusion) concludes the thesis and discusses its implications. Finally, in chapter 8, I present arguments on what can be done in the future using the results of and the software developed for this analysis.

Chapter 2

Theoretical Background

2.1 Quantum Chromodynamics

The strong force is one of the four fundamental interactions in physics. At large scales, it is also known as the residual strong force, and it is responsible for binding the nucleons together to give the nucleus its structure. At smaller scales, it is called the fundamental nuclear force, and it binds the fundamental units of subnuclear matter, the quarks, together to form the nucleons. The force carriers of the interaction are the mesons at the former scale and the gluons at the latter. The electrodynamic interaction between charged particles such as protons and electrons is described by quantum electrodynamics (QED) as mediated by photons; the strong interaction, albeit more complicated, is explained under the framework of quantum chromodynamics (QCD) [24, 34]. The quarks and gluons of QCD are collectively known as partons. Gluons are the gauge bosons of the Yang-Mills theory.

The Yang-Mills theory is a non-Abelian gauge theory. It has a Lagrangian with several degrees of freedom, some of which are redundant and need to be gauged. This is done by a mathematical treatment as prescribed under a gauge theory [7]. The gauge theory associated with the Yang-Mills theory is based on the $SU(N)$ group. It is non-Abelian as represented by the non-commutative transformations. QCD is a gauge theory that describes the application of the $SU(3)$ symmetry transformations on the triplet (what does the tripleness imply?????????) of color charges, namely red, blue, and green. The electroweak interaction,

179 on the other hand, can be formalized under the gauge group $SU(2) \times U(1)$. Together, they
 180 form the $SU(3) \times SU(2) \times (U(1))$ gauge theory called the standard model.

181 One of the ways QCD is different from QED is the confinement of partons. In QED, the
 182 fundamental particles are bound together by the Coulomb potential, which diminishes with
 183 distance between the charge-carrying particles, as demonstrated by the relation 2.1:

$$V_C \propto \frac{1}{r} \quad (2.1)$$

184 where V_C is the Coulomb potential, and r is the spatial separation between the particles.
 185 This means that bound QED particles can be isolated by increasing their spatial separation.
 186 The QCD potential, on the other hand, has an extra linear term in it:

$$V_{QCD} = -\frac{4}{3} \frac{\alpha_S}{r} + kr \quad (2.2)$$

187 where α_S is the QCD fine-structure constant and k is the strength of the color interaction
 188 [?]. This means that the potential increases linearly with distance at large distances, and so
 189 an infinite amount of energy is required to separate quarks. Hence, we never observe isolated
 190 quarks and they are said to be confined, not just bound, to form composite structures called
 191 hadrons [31]. A quark and an anti-quark forms a meson and three quarks forms a baryon.
 192 In addition to having a color charge, a quark also carries a flavor. There are six different
 193 quarks based on the flavors they carry: up, down, top, bottom, beauty, and strange.

194 2.2 Phase Transitions

195 In everyday life, we observe matter existing in four distinct phases: solid, liquid, gas, and
 196 plasma. Changes in physical conditions can lead to a transition from one of these phases
 197 to another, exemplified by the commonly observed conversion of ice to water. Distinctions
 198 among the various phases can be represented in a chart called the phase diagram.

199 The phase diagram consists of thermodynamic observables such as temperature and
 200 density on its axes. Curves in the phase diagram represent boundaries of physical conditions
 201 at which two or more phases of matter can coexist in equilibrium. Crossing a boundary

represents an abrupt transition from one phase to another; this abruptness is mathematically characterized by the discontinuity in the change of the derivative of the free energy – a thermodynamic variable – with respect to the physical quantities in the axes. There can also be regions in the diagram representing the ranges of physical conditions in which a smooth phase transition can take place. Christine believes this is only for a first order phase transition.....

One of the main focuses of current experimental and theoretical nuclear physics research is the study of the phase diagram of strongly interacting matter at a range of temperatures and baryon chemical potentials. In experiments involving the collisions of heavy ions at high and low energies, different regions of the phase diagram can be probed by varying the collision energy [3]. For instance, the high-baryon chemical potential regime corresponds to lower beam energies and higher temperatures correspond to higher beam energies. The results of these experiments and model calculations can be used to study the nature of transitions in the QCD phase diagram.

A schematic representing the QCD phase diagram as a function of the temperature (T) and quark chemical potential (μ) is shown in Figure 2.1 [9]. A second-order transition is predicted at low baryon chemical potentials (close to baryon-antibaryon symmetry) and high temperatures reminiscent of the early universe. Methods to study this region of the phase space will be explored in this thesis. At low temperatures and high net baryon densities, loose predictions have been made regarding the existence of exotic phases of high density matter, and programs, such as the Compressed Baryonic Matter experiment at the Facility for Antiproton and Ion Research in Germany, are being designed to study this region of the phase diagram [20].

2.3 Quark-Gluon Plasma

The confinement of quarks into the hadronic phase of QCD matter, as described in section 2.1, has its limitations. At very high densities, when the wave function of a single hadron overlaps with the spatial regions covered by multiple such hadrons, it is impossible to classify which pair or triplet of quarks belongs to which meson or baryon. As long as a particular

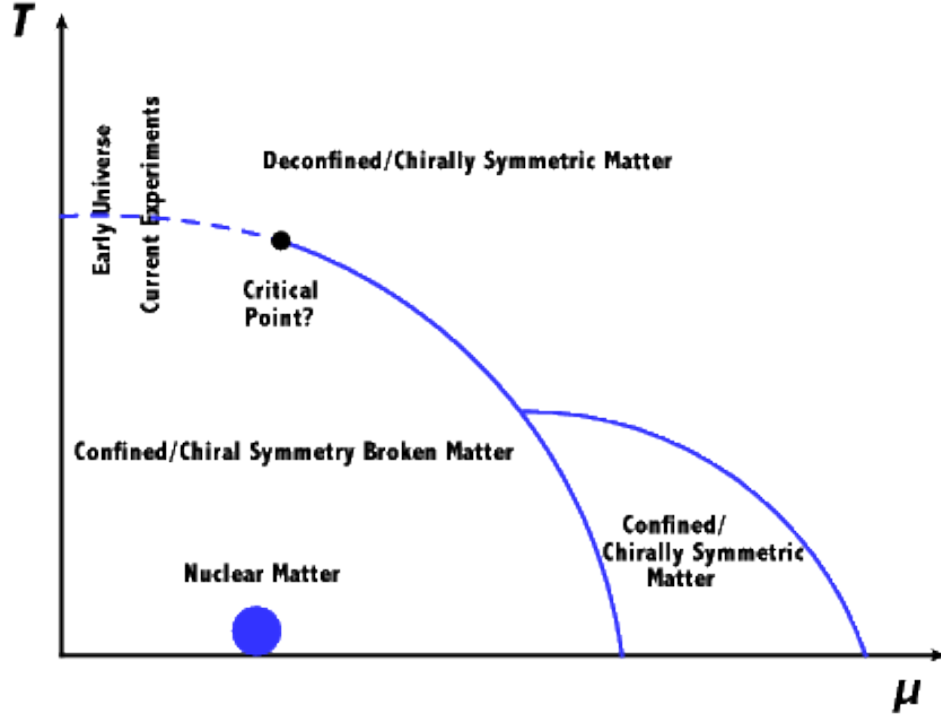


Figure 2.1: Schematic of the QCD phase diagram [9].

230 quark is close enough to the other quarks in the volume, it is deconfined in such a way that it
 231 can freely move anywhere in the volume [31]. QCD predicts such phase transition, at energy
 232 densities above $0.2\text{-}1\text{ GeV}/\text{fm}^3$ [1] and around a critical temperature of about 160 MeV [17],
 233 of strongly interacting matter to a phase with quarks and gluons in thermal and chemical
 234 equilibrium representing the relevant degrees of freedom and behaving like an almost perfect
 235 fluid [12]. This deconfined state of quarks and gluons is termed the quark-gluon plasma
 236 (QGP) in analogy to the quantum electrodynamical plasma phase of matter.

Chapter 3

Relativistic Heavy Ion Collisions

The experimental evidence for the QGP come from the collisions of heavy nuclei. The signatures of such evidence are described in section 3.6. Physicists proposed the existence of such matter since as far back as 1984, when nuclei were accelerated and collided with stationary targets [19]. They were able to agree on a conclusive discovery of this matter during the 2000s, after colliding accelerated nuclei with other such nuclei or smaller species (protons, deuterons) at unprecedented energies and with improved detection schemes [36]. With further increases in collision energies and enhancements in detector technology, modern accelerator facilities provided additional evidence and estimates of some of the properties as well as the dynamics of the evolution of the QGP. The following sections describe two such facilities, the physics of the collisions and what happens after the collisions.

3.1 RHIC and LHC

The Relativistic Heavy Ion Collider (RHIC) is located in Upton, New York in the premises of the Brookhaven National Laboratory (BNL). Its construction started in 1991 and was completed in 1999. Figure 3.1 shows the layout, at the time of construction, of the collider along with the Alternating Gradient Synchrotron (AGS) complex and the locations of the original four detectors: Solenoidal Tracker At RHIC (STAR), Pioneering High Energy Nuclear Interaction eXperiment (PHENIX), Phobos and BRAHMS (Broad RAnge Hadron Magnetic Spectrometers). Phobos, BRAHMS, and PHENIX were decommissioned after the

257 completion of their science objectives, but STAR is still functional. The AGS was part of
 258 BNL before the construction of the RHIC, and its capabilities were augmented with the
 construction of the AGS Booster in 1991.

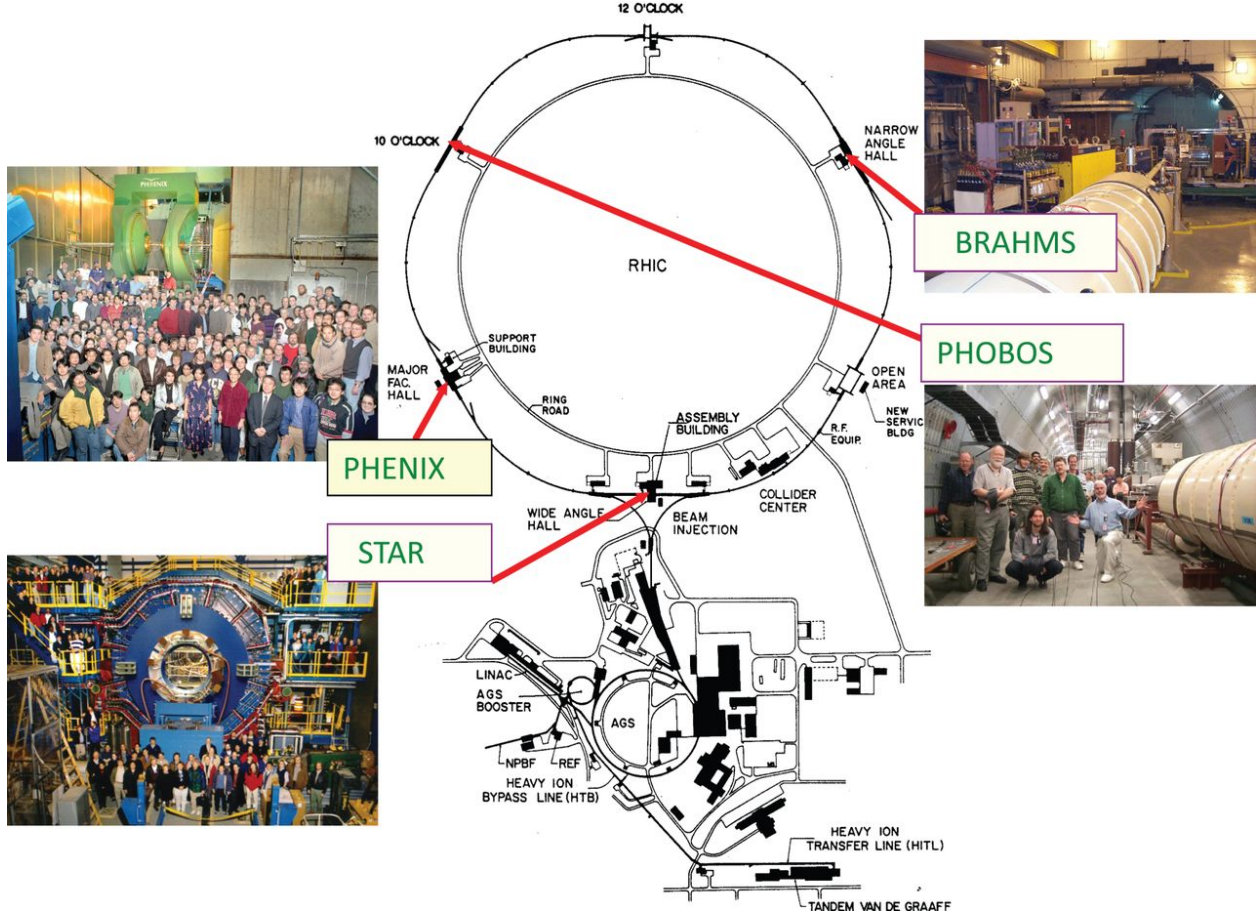


Figure 3.1: Initial layout of the RHIC [28].

259

260 Heavy ion beams in RHIC are created in a series of steps before collision. In case of gold
 261 ions, a pulsed sputter source produces negatively charged ions, which are stripped of some of
 262 their electrons with a foil on the positive end of the high-voltage Tandem Van de Graaff. The
 263 ions are now positively charged and are accelerated to 1MeV/u toward the negative terminal
 264 of the Tandem. Upon exiting it, some more stripping takes place. The bending magnets then
 265 selectively deliver +32 charge states of the ions to the Booster Synchrotron, which accelerates
 266 them to 95MeV/u and strips them to a +77 charge state before injecting them to the AGS.
 267 The AGS accelerates them to 10.8 GeV/u and strips them of the remaining two electrons at
 268 the exit. The gold ions are then injected through the AGS-to-RHIC Beam Transfer Line to

the two RHIC rings. These rings carry beams moving in opposite directions and intersect at six symmetric locations in the 3.8 km circumference. The original four detectors are located in four of these six locations where the beams undergo head-on collisions.

The Large Hadron Collider (LHC) is located underground (between 45m and 170m) beneath the France-Switzerland border near the city of Geneva. The two rings of the collider were constructed between 1998 and 2008 by the European Organization for Nuclear Research (CERN) in the 26.7 km circular tunnel originally housing CERN's Large Electron-Positron collider. Analogous to the RHIC, the LHC gets its beams prepared by a series of machines in the CERN accelerator complex. The collisions occur at the locations of the four big LHC experiments: Compact Muon Solenoid (CMS), A Toroidal LHC ApparatuS (ATLAS), Large Hadron Collider beauty (LHCb) experiment, and A Large Ion Collider Experiment (ALICE). ALICE is dedicated to the study of heavy-ion collisions [16].

3.2 Collision Energy and Geometry

What happens in the aftermath of a collision depends on how much energy is available at the time of the collision as well as the geometry of the collision. The collision energy is determined by the collider configuration. The geometry of the collision is deduced from the constraints imposed by the static (eg. rest mass) and dynamic (eg. trajectory) properties of the detected products.

In collision experiments, it is convenient to use a reference frame in which the net momentum of the pair of colliding species is zero. This frame is called the center-of-mass frame. In this frame, the total energy of the species in the two beams is a function of the number of nucleons and the center-of-mass energy per nucleon. The collision energy is reported as the center-of-mass energy per nucleon pair, $\sqrt{s_{NN}}$.

RHIC has the unique capability of colliding species at a range of energies spanning almost two orders of magnitude. Table 3.1 lists the collision energies produced so far at RHIC for various collision systems. The LHC boasts the highest amount of collision energy for any collider on earth. It collided species (p+p, p+A, Pb+Pb) at a center of mass energy upto

296 2.76 TeV per nucleon pair at the end of 2010. At the end of 2015, 5.02 TeV Pb+Pb (13 TeV
297 p+p) collisions were successfully completed [18].

Collision system	$\sqrt{s_{NN}}(GeV)$
p+p	200, 500
d+Au	200
Cu+Cu	62, 200
Au+Au	9, 20, 62, 130, 200

Table 3.1: Colliding species and associated collision energies at RHIC [26].

298 In general, any collision between two nuclei is not perfectly head-on. Some collisions are
299 close to being head-on and are called central collisions. Some are glancing and are called
300 peripheral collisions. By convention, 0% is the centrality of a perfectly head-on collision
301 and 100% is that of the least head-on, i.e., the most peripheral collision. In practice, each
302 collision event is deducted to belong to a specific centrality bin. For instance, 0-5% would
303 be the centrality for an identified N_{ch} value which would be the minimum charged particle
304 multiplicity produced by at most 5% of the total number of collisions. This identification of
305 the N_{ch} value is often achieved by using the Glauber models [?]. Figure 3.2 illustrates the
306 aftermath of a mid-central collision, i.e, a collision in which about half of the volume of each
307 of the nuclei intersects the other..... add brief discussion of Glauber model and STAR
308 centrality determination.....

309 The collision of two nuclei can be modeled as collisions of the constituents that make
310 up the nuclei. The nucleons that take part in the collisions and are called participants.
311 The rest of the nucleons are known as spectators. Figure 3.3 illustrates the distribution of
312 participants and spectators in two colliding nuclei.

313 3.3 Kinematic Variables (will go into Appendix)

314 The description of the collision physics and the interpretation of its results are aided by the
315 construction of variables that undergo simple transformations under a change of reference
316 frame. Two such variables, rapidity and pseudorapidity, are described in this section.

317 The rapidity, y , of a particle is defined as:

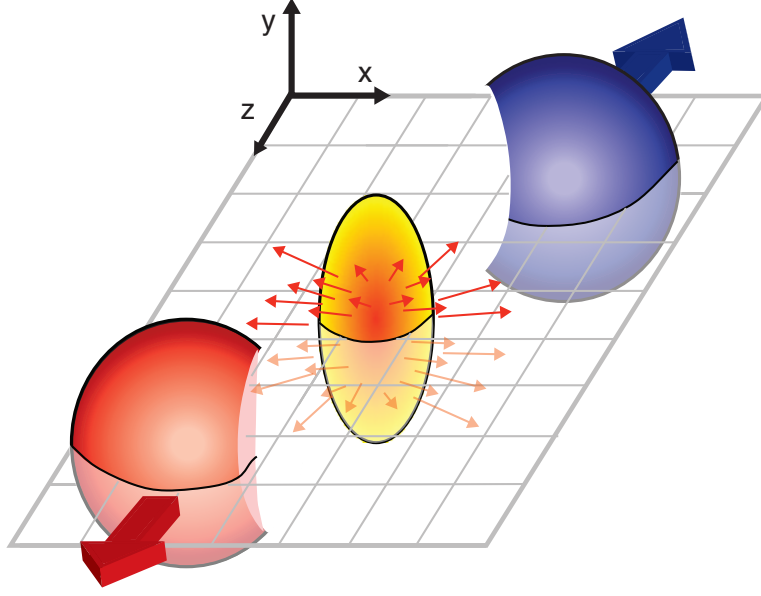


Figure 3.2: An illustration of a mid-central collision of two nuclei traveling in the z direction. The X -axis is parallel to the line joining the centers of the two nuclei at the time of collision [14].

$$y \equiv \frac{1}{2} \ln \frac{p_0 + p_z}{p_0 - p_z} \quad (3.1)$$

$$= \frac{1}{2} \ln \frac{E + p_z}{E - p_z}, \quad (3.2)$$

where p_0 and p_z are the components of its contravariant four-momentum $p = (p_0, p_x, p_y, p_z)$ with $p_0 = \frac{E}{c}$, E being the relativistic energy of the particle and c , the speed of light, being equal to 1 in natural units.

The rapidity of a particle is used as a relativistic description of its velocity. Unlike the canonical velocity of a particle, its rapidity transforms simply additively under a Lorentz boost of the frame of reference. For example, suppose a particle has a rapidity y in the laboratory frame. Let y' denote its rapidity as measured in a frame that is Lorentz boosted with a velocity β in the z -direction with respect to the laboratory frame. Then the

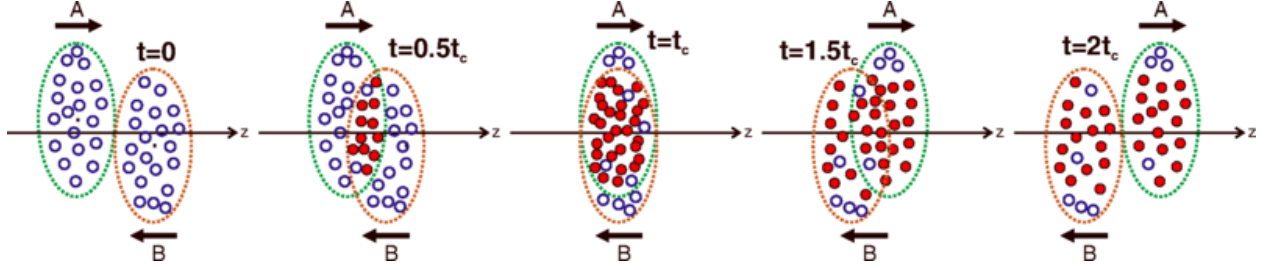


Figure 3.3: An illustration of a collision consisting of participants (solid red) and spectators (open blue) within the colliding nuclei labeled A and B. t_c denotes the time of maximum overlap of the two nuclei. The apparent narrowing of the volumes of the nuclei in the z -direction is due to Lorentz contraction [39].

relationship between the rapidities in the two different frames is simply

$$y' = y - y_\beta \quad (3.3)$$

Here,

$$y_\beta = \frac{1}{2} \ln \frac{1 + \beta}{1 - \beta} \quad (3.4)$$

is the rapidity the particle would have in the laboratory frame if it were moving with a velocity β in the z -direction with respect to the laboratory frame, as can be verified from equation 3.1 with $p_0 = \gamma m$ and $p_z = \gamma \beta m$, γ being the Lorentz factor $\frac{1}{\sqrt{1-\beta^2}}$ [41].

The convenience provided by this construct comes with a cost. As evident from equation 3.1, the calculation of the rapidity of a particle requires the measurement of two different observables associated with it, such as the energy and the z -direction momentum. However, experimental constraints may sometimes only facilitate the measurement of the direction of the detected particle with respect to the beam axis. What's more convenient in such a case is the use of another variable construct called pseudorapidity, η , defined as:

$$\eta \equiv -\ln \tan \frac{\theta}{2}, \quad (3.5)$$

where θ is the angle the particle's momentum vector, \mathbf{p} , makes with the z -direction. The above equation can also be written in terms of the momentum as:

$$\eta = \frac{1}{2} \ln \frac{|\mathbf{p}| + p_z}{|\mathbf{p}| - p_z} \quad (3.6)$$

From equations 3.1 and 3.6, it is evident that $\eta \approx y$ when $|\mathbf{p}| \approx p_0$, i.e., when the momentum is large. The transformation of the particle distribution from the y -space to the η -space is discussed in section 4.3.2.

3.4 QGP Evolution

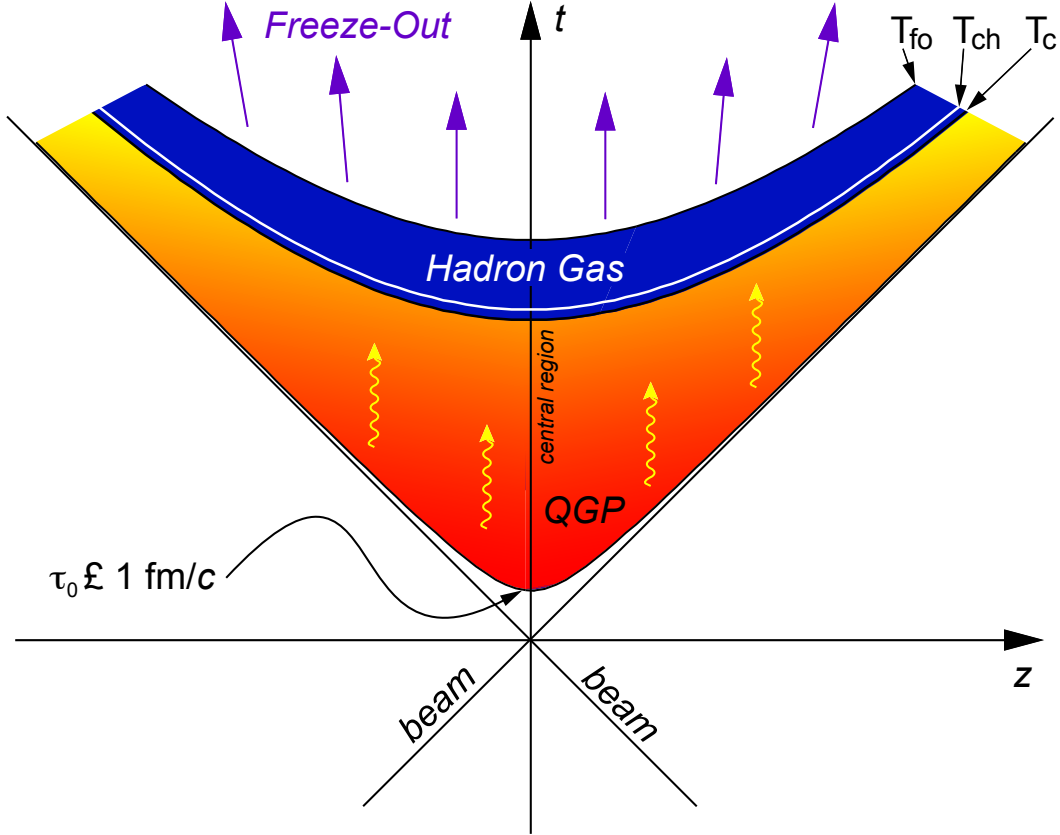


Figure 3.4: Evolution of the QGP represented in a lightcone diagram. τ_0 denotes the formation time of the QGP. T_c is the critical temperature of the transition from the QGP to the hadron gas phase. T_{ch} and T_{fo} stand for the temperatures at, respectively, chemical freeze-out and thermal freeze-out [14].

The evolution of the QGP is shown in a lightcone diagram in figure 3.4 [14]. The initial state of the colliding nuclei is not well known and is the topic of research for upcoming experiments. During the collision, the participants scatter off of each other while the spectators keep traveling almost unperturbed in their original direction. The immediate aftermath of a central collision of heavy ions at RHIC and LHC energies is the formation of a hot fireball. This fireball evolves in time to form a liquid-like medium of quarks and gluons. This medium attains a local equilibrium and remains in such a state, depending on the collision energy, for about 1-10 fm/c. This equilibrium is broken as the liquid QGP evolves by expanding and cooling to attain a density and temperature at which the deconfinement of quarks and gluons is lost and they undergo a chemical freeze-out to form a hadron gas. Collisions between the constituents of this gas become scant as it evolves with further expansion and cooling, and the hadrons undergo a thermal freeze-out to attain their final energies and momenta [14].

3.5 Detection of Collision Products

Detectors are placed around the collision site to perform measurements on the final state particles emitting from the thermal freeze-out of the medium. These measurements typically include the reconstruction of the particle tracks, estimation of the the types of particles, and the momenta and energies they carry.

Generally, a tracking detector surrounds the collision site, and there are particle identifiers followed by calorimeters around it. A magnetic field is applied parallel to the beam direction around the collision site. Due to this orientation of the magnetic field, the spectators traveling parallel to it move undeflected and the final state charged particles with components of velocity transverse to the beam axis get deflected around the beam axis with radius given by

$$r = \frac{p_T}{qB}, \quad (3.7)$$

where p_T is the transverse momentum of the particle, q is its electric charge, and B is the applied magnetic field. Two kinds of detectors most relevant to this thesis, tracking detectors and calorimeters, are described in chapter 4.

3.6 Detection of QGP Signatures

The existence and properties of the QGP in the aftermath of high-energy heavy-ion collisions can be probed using different techniques relevant to several theoretical characteristics of the medium. No signature can alone be used to claim the production of the QGP, and some of the probes, which should be interpreted together, are described below.

3.6.1 Bjorken Energy Density

In 1983, J.D. Bjorken[11] prescribed a formula to use the final state particles to estimate the initial energy density, ϵ_0 , in a nucleus-nucleus collision. With slight changes in the original formula, the energy density is given by:

$$\epsilon_0 = \frac{1}{\tau_0 A_T} \langle \frac{dE_T}{dy} \rangle, \quad (3.8)$$

where τ_0 is the formation time of QGP equilibration, A_T is the transverse area of the intersection of the two nuclei, and $\langle \frac{dE_T}{dy} \rangle$ is the mean transverse energy per unit rapidity. τ_0 is model-dependent and is normally estimated to be $1 fm/c$. A_T depends on the centrality of the collision and can be estimated using the Glauber models discussed earlier. $\langle \frac{dE_T}{dy} \rangle$ is found from the measurement of the transverse energy carried by the final state particles from the collision and is the central theme of this thesis. Details about it are in the following chapters. The estimate of the initial energy density from Bjorken formula can be compared with the QCD prediction of the critical energy density[1] to check if the results from a collision imply the achievement of the critical physical condition required for the phase transition [23].

3.6.2 Elliptic Flow

The evolution of the medium produced after relativistic heavy ion collisions can be well described under the framework of relativistic hydrodynamics [32, 37]. This description indicates the presence of a collective flow, and hence a liquid-like (awkward?????) and thermalized nature, of the constituents that make up the system. The momentum distribution of the final state particles emitted out of the collectively flowing system can

394 be decomposed into its azimuthal Fourier components. The second harmonic coefficient,
 395 $\nu_2(y, p_T)$, of this decomposition characterizes what is known as the elliptic flow [22]. The
 396 magnitude of the elliptic flow from a non-central collision represents the anisotropy in
 397 azimuthal momentum space of the thermalized post-collision system [35]. The elliptic flow
 398 of the medium, as a function of the momentum or the kinetic energy in the transverse
 399 direction, points towards quarks, rather than hadrons, being the relevant degrees of freedom
 400 in the QGP. Figure 3.5 shows ν_2 as a function of the transverse momentum and the transverse
 401 kinetic energy for identified particles. The spectra scale consistently at lower values of both
 402 p_T and KE_T . However, they branch out at higher values: $p_T \gtrsim 2\text{GeV}/c$ and $KE_T \gtrsim 1\text{GeV}$.
 403 Figure 3.6, on the other hand, is similar to figure 3.5, with the exception that both the
 404 axes have quantities that are normalized by the number of quarks, n_q . In this case, the
 405 KE_T spectra strongly exhibits a scaling which is more comprehensively consistent with the
 406 number of quarks than in case of figure 3.5. This universal quark-number scaling can be
 interpreted as the degrees of freedom of the system being quark-like [4].

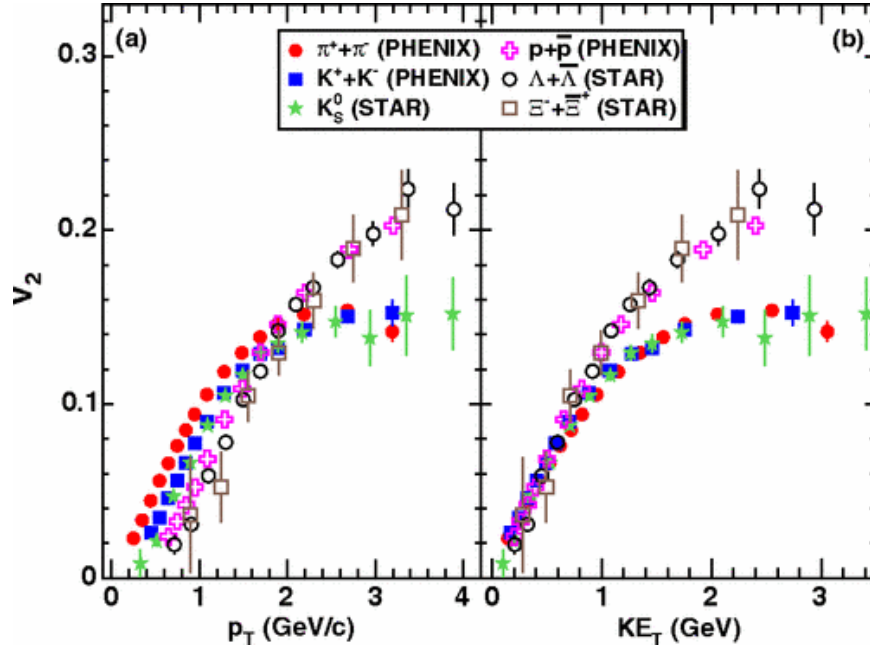


Figure 3.5: Minimum-bias Au+Au ($\sqrt{s_{NN}} = 200\text{GeV}$) elliptic flow spectra for identified particles: (a) ν_2 vs p_T and (b) ν_2 vs KE_T [4].

407

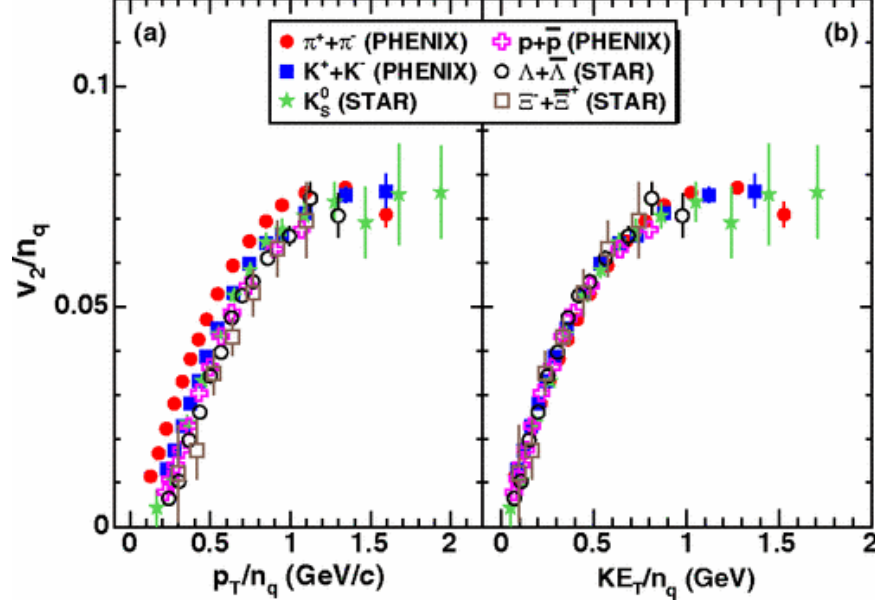


Figure 3.6: Minimum-bias Au+Au ($\sqrt{s_{NN}} = 200\text{GeV}$) elliptic flow spectra for identified particles: (a) $\frac{v_2}{n_q}$ vs $\frac{p_T}{n_q}$ and (b) $\frac{v_2}{n_q}$ vs $\frac{KE_T}{n_q}$ [4].

3.6.3 Direct and Thermal Photons

In the QGP, a quark and an antiquark can annihilate to produce a photon and a gluon. It is also possible for the pair to annihilate and produce two photons, but the probability of this process is smaller than the former by about two orders of magnitude. Furthermore, a quark (or an antiquark) can interact with a gluon to produce an antiquark (or a quark) and a photon, a process analogous to Compton scattering in QED. Just like the leptons described in the previous section, the photons produced in the QGP can only interact with the medium electromagnetically. Therefore, they undergo minimal scattering before being detected, and hence can be used to probe the thermodynamical state of the medium at the time of their creation [41]. Photons can also be produced after hadronization as a result of the scattering of the hadrons within the evolved medium. However, the nature of the p_T distribution is different in this case, and this difference helps distinguish these photons from the direct photons produced by partonic interactions [40].

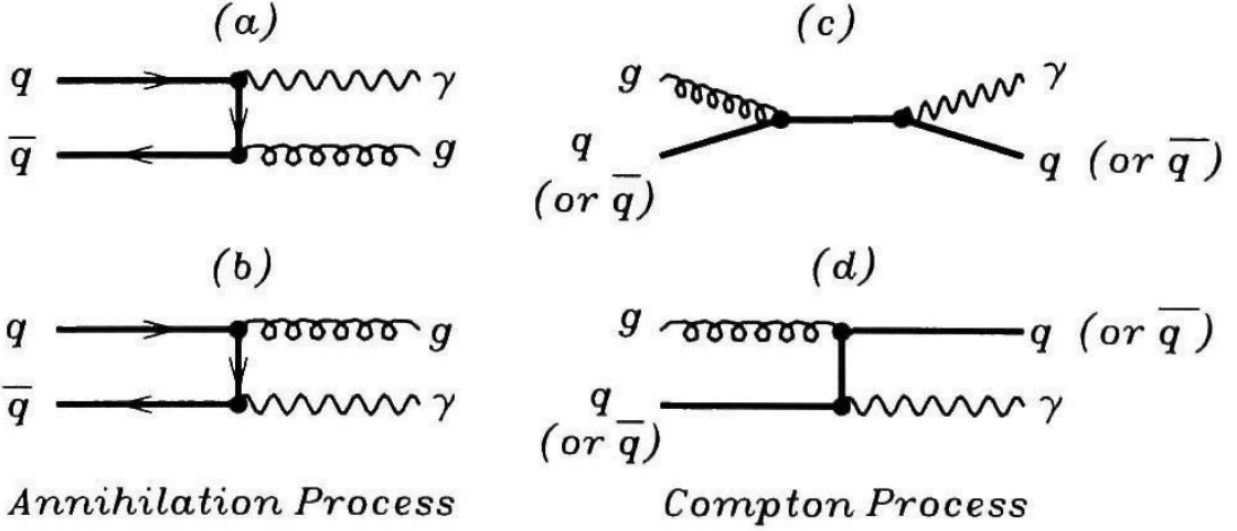


Figure 3.7: Feynman diagram representing the production of photons from quarks and gluons. (a) and (b) represent annihilation processes, whereas (c) and (d) represent Compton processes [41].

3.6.4 Strangeness Enhancement

One of the implications of the formation of QGP is chiral symmetry restoration. At the energy scale of this phenomenon, strange quarks lose their masses, and hence it is feasible to produce a lot of them. The interacting nuclei carry no net strangeness before colliding, and so an observation of strange and multi-strange particles after the collision can be used to probe the properties of the post-collision medium [15]. Strangeness can also be produced in hadron-hadron collisions. However, it is enhanced in nucleus-nucleus collisions in which a large number of hadrons are produced and are in chemical equilibrium at very high temperatures. The enhancement is exemplified by the ratio of the production of the strange kaons to that of the non-strange pions, which are the most abundant hadrons produced from nucleus-nucleus collisions. Kaon yield increases more rapidly than does pion yield as the temperature increases. This can be shown mathematically by treating the system as a hadron gas in thermal and chemical equilibrium that follows the Bose-Einstein distribution, but it is beyond the scope of this thesis [41]. connect to big picture... why is strangeness enhancement interesting? phase space suppression? chiral symmetry restoration.....?

3.6.5 Jet Quenching

A scattering event in which the participants transfer a large amount of their original momenta is called hard scattering. The products of the scattering are called jets. Ultimately, jets are what are recognized by a jet finder algorithm as jets. In heavy-ion collisions, most hard scatterings are the results of two partons from the opposite nuclei scattering off of each other. These partons can lose their momenta by strongly interacting with a medium made of deconfined quarks and gluons. Therefore, the properties of the jets, as carried by the final state hadrons, should be different for collisions that produce the QGP as compared to those that [don't]????????, and hence they can be used as signatures and probes of QGP. Figure 3.8 illustrates the quenching of jets that have to travel long distances in the medium. Formalisms developed to study jet quenching due to radiative and collisional energy losses are detailed in [30].

3.7 The Beam Energy Scan Program

The RHIC, in 2010, started a multi-phase Beam Energy Scan (BES) program to study the QCD phase diagram. Between 2010 and 2011, during the exploratory phase I of the BES program, the collider provided Au+Au collisions at 7.7, 11.5 (not completed in PHENIX), 19.6, 27, and 39 GeV. Together with the data formerly collected by the RHIC at higher collision energies, BES phase I data can scan the interval from 450 MeV to 20 MeV in μ_B space [27, 25]. One of the things that can be studied with the data associated with this region of the phase space is the possibility of a “turn-off of new phenomena already established at higher RHIC energies” [27]. Results corresponding to the high- μ_B region might provide evidence of a first order phase transition, and possibly the critical point [25].

The manifestation of such phenomena would be in terms of the fluctuations or other properties of the post-collision system. One can, for instance, study the scaling of the transverse energy after the collision with the longitudinal energy at the time of the collision, $\sqrt{s_{NN}}$. This can be done in multiple ways using a detector like STAR or PHENIX that is made up of sub-systems such as the Time Of Flight (TOF) detectors, Time Projection Chambers (TPCs)/Time Expansion Chambers, as well as calorimeters. The next chapter

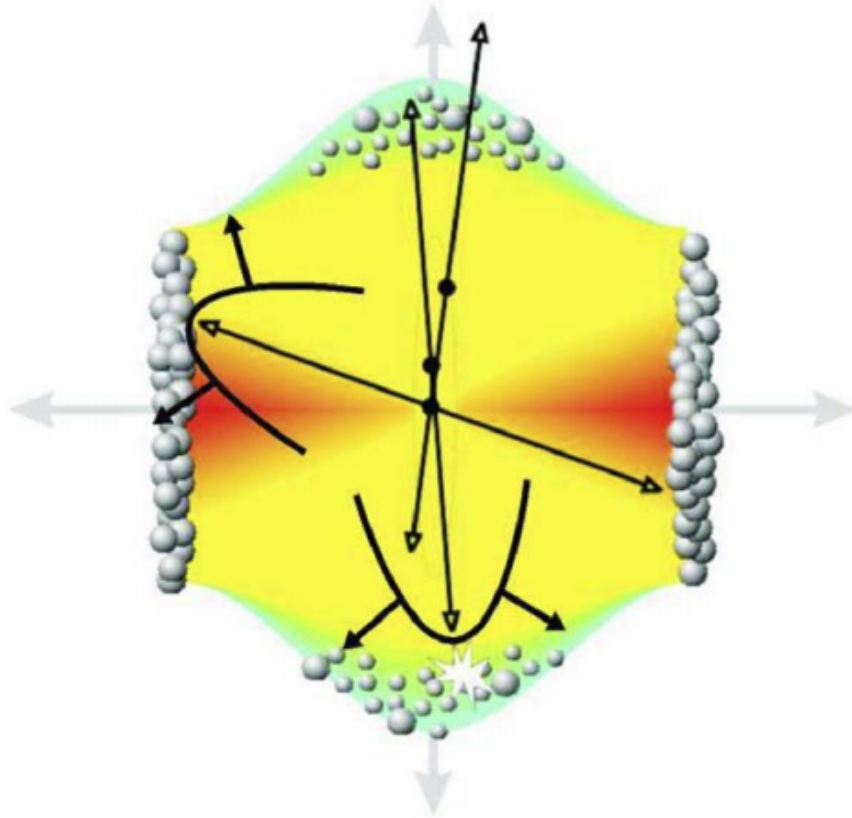


Figure 3.8: Illustration of jet quenching. Two jets are produced from each of the hard scatterings occurring at the locations of the solid dots. Jets originating closer to the initial surface are more probable to propagate outside the medium, as shown. Jets opposite to them interact with the medium, losing their energy and resulting in bow front shock waves [38].

464 describes the measurement of transverse energy using BES data from PHENIX calorimeters.
 465 Also, the next chapter and the ones after it contain the procedures and the results of the
 466 analysis of the BES data from STAR using the identified particles spectra.

Chapter 4

Measurement of Transverse Energy

This chapter introduces the definitions of transverse energy, ways to measure it using different detectors, and particular examples for the detectors at the RHIC.

4.1 Definition of Transverse Energy

The transverse energy, E_T , from a collision can be defined as the sum of the transverse masses, m_T , of all the particles produced in the collision, i.e.,

$$E_T \equiv \sum_i m_{T,i} \quad (4.1)$$

with

$$m_T \equiv \sqrt{p_T^2 + m^2} \quad (4.2)$$

where m is the rest mass of the particle and p_T is its transverse momentum. Using this definition to calculate the E_T requires perfect identification of all the particles. It has not been possible to do so in experiments, and so a more feasible, operational definition of E_T is used. A commonly accepted definition in case of the feasibility of calorimetric measurements is [5, 12]:

$$E_T = \sum_i E_i \sin \theta_i, \quad (4.3)$$

480

$$\frac{dE_T}{d\eta} = \sin\theta \frac{dE}{d\eta}, \quad (4.4)$$

481 where the index i runs over all the particles going into a fixed solid angle for each event,
 482 θ is the polar angle, i.e, the angle with respect to the beam axis, η is the pseudorapidity
 483 defined as

$$\eta \equiv -\ln \tan \frac{\theta}{2}, \quad (4.5)$$

484 and E_i is the energy deposited in the calorimeter by the i^{th} particle. E_i is considered to be,
 485 by convention [6], the following

$$E_i = \begin{cases} E_i^{tot} - m_0 & \text{for baryons} \\ E_i^{tot} + m_0 & \text{for anti-baryons} \\ E_i^{tot} & \text{otherwise} \end{cases} \quad (4.6)$$

486 where E_i^{tot} is the total energy of the i^{th} particle defined canonically as

$$E^{tot} \equiv \sqrt{p^2 + m_0^2} \quad (4.7)$$

487 and m_0 is the particle's rest mass.

488 E_i given by equation 4.6 is what would be observed by a calorimeter. In order to
 489 account for the portion of the emitted transverse energy not detected or overestimated by
 490 the calorimeters, corrections are made based on simulations.

491 **4.2 E_T Measurement with Calorimeters**

492 **4.2.1 Calorimeter**

493 A calorimeter in a particle or nuclear physics experiment is a device used to measure the
 494 energy carried by a particle by analyzing the signal generated by the shower of particles
 495 produced by the interaction of the incoming particle with the material of the device [? ,
 496 (<http://pdg.lbl.gov/2016/download/rpp-2016-booklet.pdf>)] In theory, a single calorimeter

can be made to measure the energy deposited by different kinds of particles. However, it makes more sense to have two different kinds of calorimeters: one optimized to measure the energy deposited by particles like electrons (or positrons) and photons, called an electromagnetic calorimeter (EMCal), and the other optimized to measure the energy deposited by hadronic particles, called a hadronic calorimeter (HCal). This is because of the difference in the particle showers that these two categories of particles generate. Electrons and photons mostly lose their energies in the calorimeter material via bremsstrahlung, Compton scattering and pair production. They generate particle showers made of electrons and photons which cannot travel much farther into the medium before losing all their energies in a series of interactions producing an avalanche of sequential showers. However, hadrons can interact inelastically with the nucleus generating a shower of hadrons. These secondary hadrons have much larger masses than the secondary electrons in the shower generated by the electrons and photons. This means they are not deflected nearly as much by the electric forces in the material and travel much farther into the calorimeter. For this reason, EMCals are comparably smaller in depth and are placed before the HCals in a detector assembly.

4.2.2 E_T from PHENIX Calorimetry

Adare et al. [3] use electromagnetic calorimetry in PHENIX to analyze the transverse energy corresponding to several different pairs of species colliding at a range of energies. They use the raw transverse energy measured by the EMCal, E_{TEMC} , to obtain the total E_T by making corrections in three different steps. They first scale the data by a constant factor calculated to account for the fiducial acceptance in azimuth and pseudorapidity. The second factor is calculated to adjust for the effects of the calorimeter towers that are disabled. The third factor, k , is computed as follows

$$k = k_{response} \times k_{inflow} \times k_{losses} \quad (4.8)$$

where $k_{response}$ corresponds to hadronic particles only depositing a fraction of their total energy while passing through the EMCal, k_{inflow} is attributable to the energy deposited by particles coming from outside the EMCal's fiducial aperture, and k_{losses} accounts for

the energy not registered in the EMCal due to energy thresholds, edge effects, and more importantly due to the particles that make it into the fiducial aperture but decay into products outside the aperture. Give some sense of what these corrections are... the first two probably have very small systematic uncertainties while the third likely has very large uncertainties.....

4.3 E_T Measurement with Tracking Detectors

Transverse energy analysis can be done using tracking detectors as well if they are able to produce measurements of other physical quantities that implicitly contain information about the transverse energy. Specifically, the charged particle multiplicity distributions with respect to the transverse momenta can be used, with assumptions involving particle ratios and mean p_T , to calculate the particle's transverse energy. Since the corrections related to the tracking detectors are very different from those related to the calorimeters, results from the two different methods can be used to test the assumptions involved in each.

4.3.1 Tracking and Particle Identification

The tracking detectors in experiments such as the STAR (Solenoidal Tracker At RHIC) experiment and ALICE (A Large Ion Collider Experiment) at CERN include Time Projection Chambers (TPCs) and Time-of-Flight (TOF) detectors that can be used to measure the p_T spectra, yields and particle ratios of the identified charged hadrons [29, 2]. The TPCs provide measurements of particle trajectories that can be used to determine the momenta for low-momentum particles. They also provide measurements of their specific energy loss, $\frac{dE}{dx}$, which can be used in combination with the momenta to identify particles using the Bethe-Bloch formula [10]. The particle identification (PID) capabilities of STAR are discussed in section 4.3.3. TOF detectors cover the high-momentum part of the measurements. In ALICE, the combination of the measurements of the TPC with those of the Inner Tracking System (ITS) effectively adds the tracking length, thereby improving the resolution of the measured p_T spectrum. Details about the PID and momentum determination capabilities of the detectors in ALICE can be found in [13].

550 The p_T spectra, reported as $\frac{d^2N}{dydp_T}$ as a function of p_T , can be used to calculate $\frac{dE_T}{d\eta}$ as
 551 formulated in the following section.

552 4.3.2 Calculation of $\frac{dE_T}{d\eta}$ from p_T spectra

553 In relativistic heavy ion collisions, rapidity (y) is defined as follows:

$$y \equiv \frac{1}{2} \ln \frac{E + p_z}{E - p_z}, \quad (4.9)$$

where E is given by equation 4.7 and p_z is the component of the momentum parallel to the beam axis. Pseudorapidity, η , is just y with $m_0 = 0$:

$$\begin{aligned} \eta &= \frac{1}{2} \ln \frac{p + p_z}{p - p_z} \\ &= \frac{1}{2} \ln \frac{1 + \cos \theta}{1 - \cos \theta} \\ &= \frac{1}{2} \ln \frac{2 \cos^2 \frac{\theta}{2}}{2 \sin^2 \frac{\theta}{2}} \end{aligned}$$

$$\therefore \eta = - \ln \left| \tan \frac{\theta}{2} \right| \quad (4.10)$$

554 The absolute value is not necessary for $0 \leq \theta \leq \pi$. Then, taking the exponential of both
 555 sides of the above equation and using Euler's formula, we get:

$$\sin \theta = \frac{1}{\cosh \eta}. \quad (4.11)$$

Hence,

$$\begin{aligned} p &= \frac{p_T}{\sin \theta} \\ &= p_T \cosh \eta, \end{aligned}$$

556 and so we have

$$E_T = E \sin \theta = \frac{\sqrt{p_T^2 \cosh^2 \eta + m_0^2}}{\cosh \eta} \quad (4.12)$$

The Jacobian for the transformation from y -space to η -space is derived to be:

$$\frac{\partial y}{\partial \eta} = \frac{p_T \cosh \eta}{\sqrt{m_0^2 + p_T^2 \cosh^2 \eta}} \quad (4.13)$$

From equations 4.12 and 4.13, we can see that the product of E_T with the Jacobian is equal to p_T . That leads to a formulation of $\frac{dE_T}{d\eta}$ as a function of only η and p_T :

$$\frac{dE_T}{d\eta} = \frac{1}{2a} \int_0^{10 \text{ GeV}/c} \int_{-a}^a p_T \frac{d^2 N}{dy dp_T} d\eta dp_T \quad (4.14)$$

where a and $-a$ are the bounds for η . The estimate for the upper limit of p_T makes sense in accordance with the mean p_T of the spectra being comfortably an order of magnitude less than 10 GeV/c as discussed in chapter 5.

4.3.3 Tracking Detectors in STAR

In the STAR experiment, the TPC is the primary tracking detector. It is 4.2 m long and it cylindrically encloses the accelerator beam pipe from its outside, with an inner diameter of 1 m and an outer diameter of 4 m [26]. It covers a pseudorapidity range of $|y| < 1.8$ in all of azimuth for charged particles. It can identify particles with momenta over 100 MeV/c up to about 1 GeV/c as well as measure their momenta from 100 MeV/c to 30 GeV/c [8]. Figure 4.1 shows the PID capability of the STAR TPC for very high-multiplicity events [21]. Separation of pions from protons is demonstrated up to a little more than 1 GeV/c. At higher momenta, separating particles is more difficult because their energy loss has lower dependence on the rest mass [8]. The TOF system in STAR, with a time resolution of $\lesssim 100$ ps, aids PID at higher momenta. However, at intermediate p_T , between ≈ 2.0 and 4.0 GeV/c, the TPC by itself cannot distinguish between pions and protons and the TOF by itself cannot separate pions from kaons. This problem is resolved by utilizing the fact that the dependence of the particle velocity on p_T – in case of the TPC – is different from that of the energy loss on p_T in case of the TPC; combining the results from the two, hence, makes PID feasible in this p_T range [33].



Figure 4.1: Energy loss distribution in the STAR TPC for primary and secondary particles [8].

Chapter 5

Data Analysis

The available spectra were extrapolated to calculate the transverse energies and charged particle multiplicities. Details follow.

5.0.1 STAR p_T spectra

This thesis details the method of transverse energy analysis through the use of p_T spectra from the STAR BES data. As described in section 4.3.3, the TPCs and TOF detectors in STAR can identify particles as well as their trajectories and ultimately measure their multiplicity distributions with respect to the momenta p_T . This report shows the results for the p_T spectra for six different identified hadrons, π^+ , π^- , K^+ , K^- , p , and \bar{p} , from the STAR experiment. The spectra come from Au+Au collisions at $\sqrt{s_{NN}} = 7.7$, 11.5, and 39 GeV in the year 2010 and at $\sqrt{s_{NN}} = 19.6$ and 27 GeV in 2011 as part of the BES Program. Figure 5.1 [2] shows the spectra corresponding to 39 GeV collisions categorized into seven different collision centrality classes. These spectra, and their counterparts for the rest of the energies, were used to calculate an estimate of the total transverse energy per event per particle species. This result was then used to estimate the total transverse energy due to all the collision products.

The corrections applied by Adamczyk et al. [2] to the raw data to obtain the spectra and the reported systematic uncertainties in their results are discussed below (under construction)

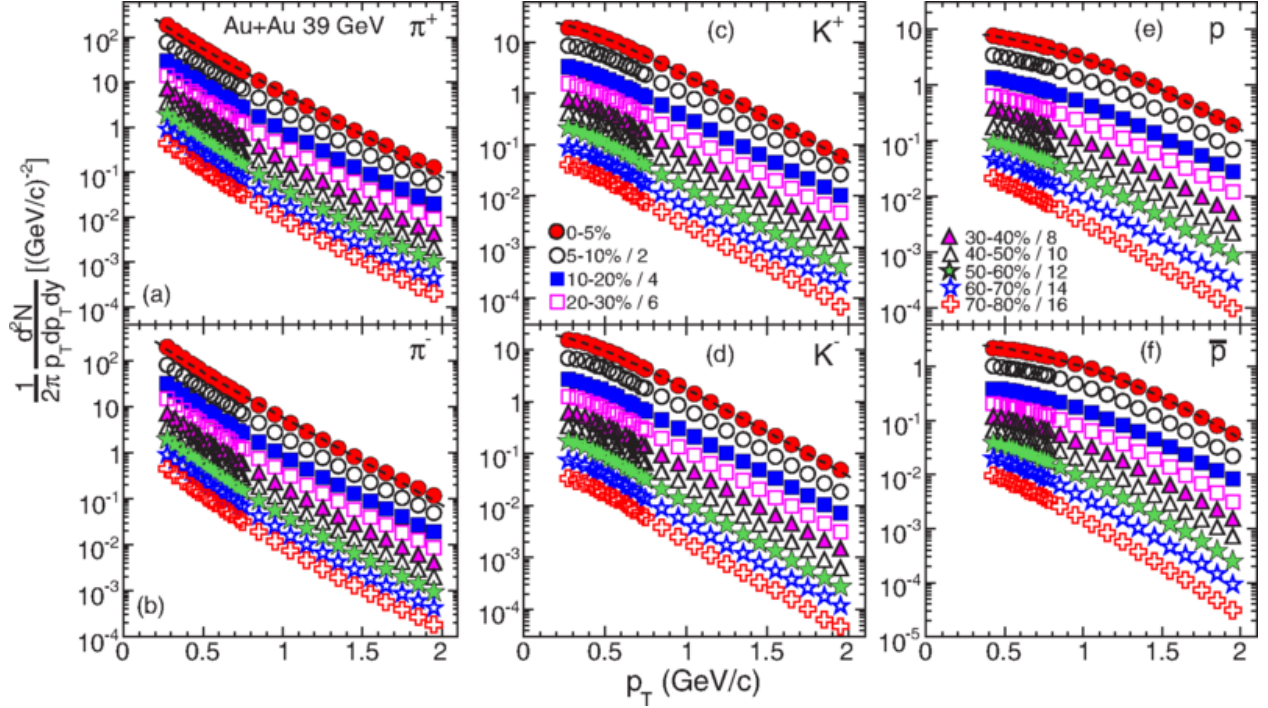


Figure 5.1: Transverse momentum spectra for π^+ , π^- , K^+ , K^- , p , and \bar{p} at midrapidity ($|y| < 0.1$) from 39 GeV Au+Au collisions at RHIC. The fitting curves on the 0-5% central collision spectra for pions, kaons, and protons/anti-protons represent, respectively, the Bose-Einstein, m_T -exponential, and double-exponential functions [2].

5.1 Extrapolation of Spectra

The available spectra were limited to a range of transverse momenta from around 0.25 GeV/c to around 2 GeV/c (for pions). To account for the transverse energy corresponding to the momenta for which there was no available data, an extrapolation had to be used. The model used for the extrapolation and the associated statistics are discussed below.

5.1.1 Boltzmann-Gibbs Blast Wave

The blast wave is a common model used in the analysis of the particle spectra.[????] The specific model used in this thesis is the Boltzmann-Gibbs blast wave (BGBW) as represented in equation ???. It has the parameters mass, temperature, beta, v, and n. I assume that any anomalies in the magnitude of the normalization parameter do not affect the results significantly insomuch as they don't lead to:

- (a) unreasonable relative errors in the extrapolated values of the transverse energy,

- 611 (b) any of the spectral fits having the extrapolated transverse energy more than that
612 calculated from just the available spectra, and
613 (c) for the 200 GeV collision samples, at least, the extrapolation at higher p_T being more
614 than that at lower p_T .

$$BGBW \tag{5.1}$$

615 5.1.2 Fitting Spectra to BGBW

616 Figure 5.2 presents an example of a Boltzmann-Gibbs Blast Wave (BGBW) fit on one of the
617 individual particle spectra with $\chi^2/\text{n.d.f}$ as well as other statistics and the associated errors.
618 A parallel-coordinates plot is presented in the next chapter in fig. 6.1, which shows the
619 measured centralities, two of the good-fit parameters, and the calculated transverse energies
620 for 270 different particles (lambdas not included).

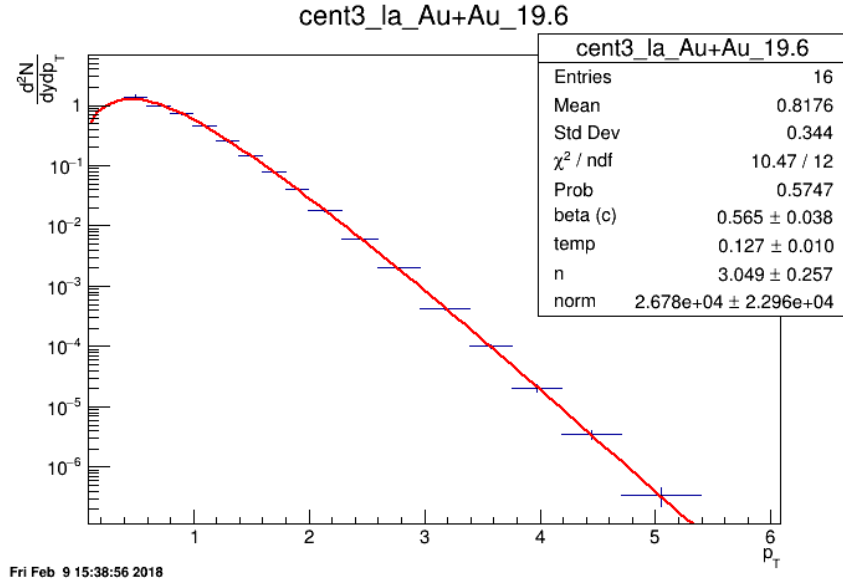


Figure 5.2: Red curve shows the Boltzmann-Gibbs blast wave functional fit on the PRELIMINARY transverse momentum spectrum for lambda particles identified by the STAR detector for 19.6 GeV Au+Au collisions (10-15% central). Parameters extracted from the chi-square goodness-of-fit test, as well as other statistics, are shown in the box on the top right.

5.2 Calculations from the Spectral Fits

5.2.1 Calculation of $\frac{dE_T}{dy}$, $\frac{dE_T}{d\eta}$, $\frac{dN_{ch}}{dy}$, and $\frac{dN_{ch}}{d\eta}$

5.2.2 Corrections for Unidentified Particles and Estimation of Total E_T

It is reasonable to assume that, at high energies, there should be roughly the same multiplicity of all the isospin states of a final state particle. Table 5.1 lists the isospin states associated with the pion, the kaon, the proton, and the lambda particles.

Particle	Isospin multiplets
pion	π^+, π^0, π^-
kaon	K^+, K^0, K^-, \bar{K}^0
proton	p, n
lambda	Λ

Table 5.1: Isospin states of different identified particles.

.....text content.....

$$E_T = 3E_T^\pi + 4E_T^K + 4E_T^p + 2E_T^\Lambda \tag{5.2}$$

.....text content.....

5.2.3 Lambdas Centralitiy Adjustments and E_T Interpolations

The centrality bins corresponding to the lambdas spectra were slightly different from those corresponding to the rest of the particles.....

5.3 Uncertainties

..... 100% correlated point-to-point and uncorrelated between particles..... ?

Chapter 6

Results

Present results and comparisons to Adare et al.....

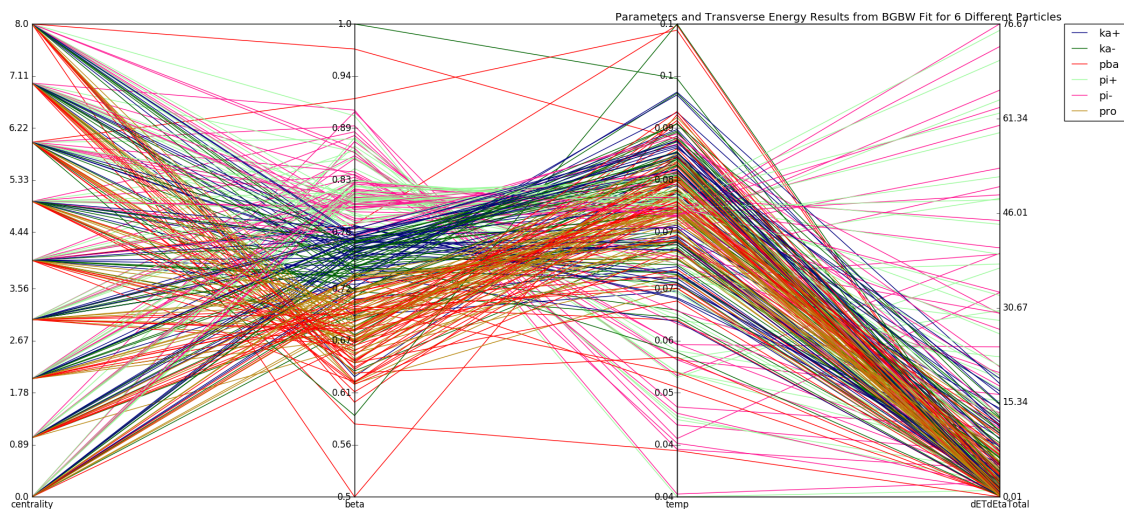


Figure 6.1: Parallel coordinates plot for 270 different spectra relating 6 different identified particles (color-coded) to their respective collision centrality classes, good-fit parameters, and the transverse energy calculated using said parameters.

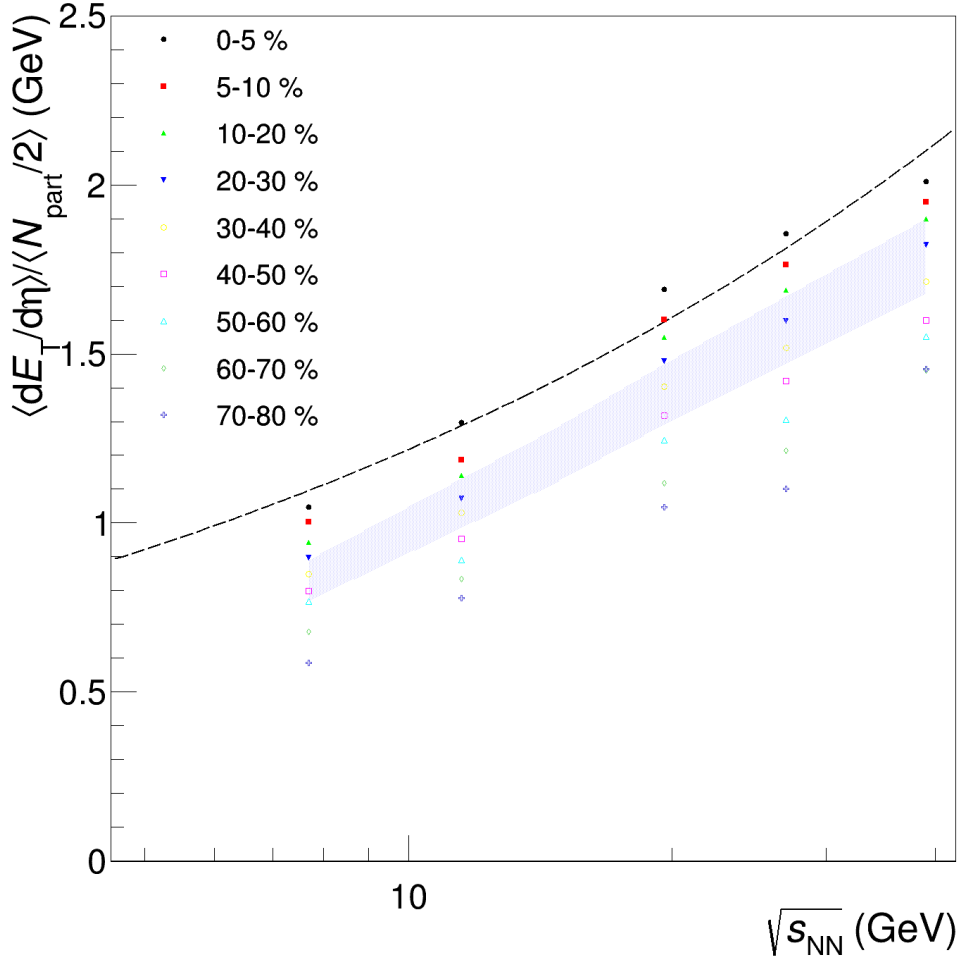


Figure 6.2: $(dE_T/d\eta)/0.5N_{part}$ at midrapidity as a function of $\sqrt{s_{NN}}$ for different centralities. The dashed line represents a power-law fit to the 0-5% central data in the form $y = ax^{2b}$, where x and y are the placeholders for the quantities in the plot axes. $\chi^2/n.d.f$ for the fit was 1.806, and the good-fit parameters were $a = 0.4838 \pm 0.0429$ and $b = 0.2005 \pm 0.01466$. The shaded area represents the uncertainty bounds for the 0-5% central PHENIX data from [3].

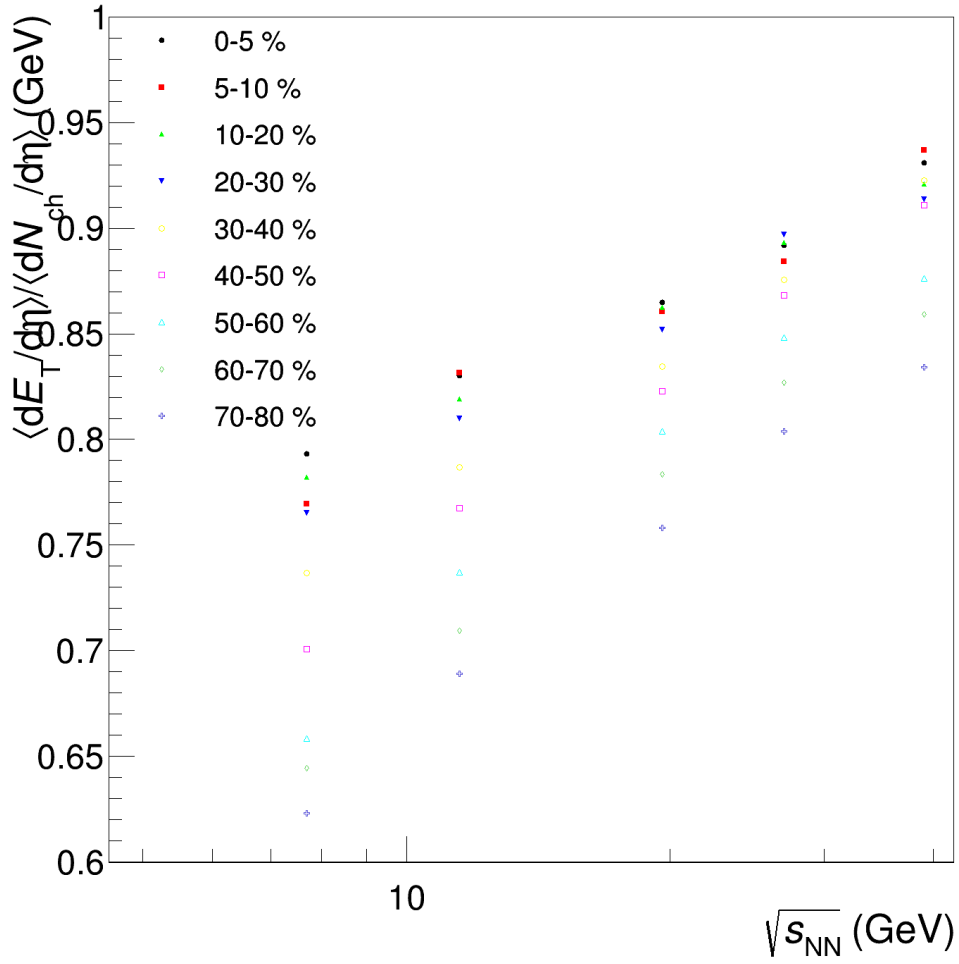


Figure 6.3: $(dE_T/d\eta)/(dN_{ch}/d\eta)$ at midrapidity as a function of $\sqrt{s_{NN}}$ for different centralities.

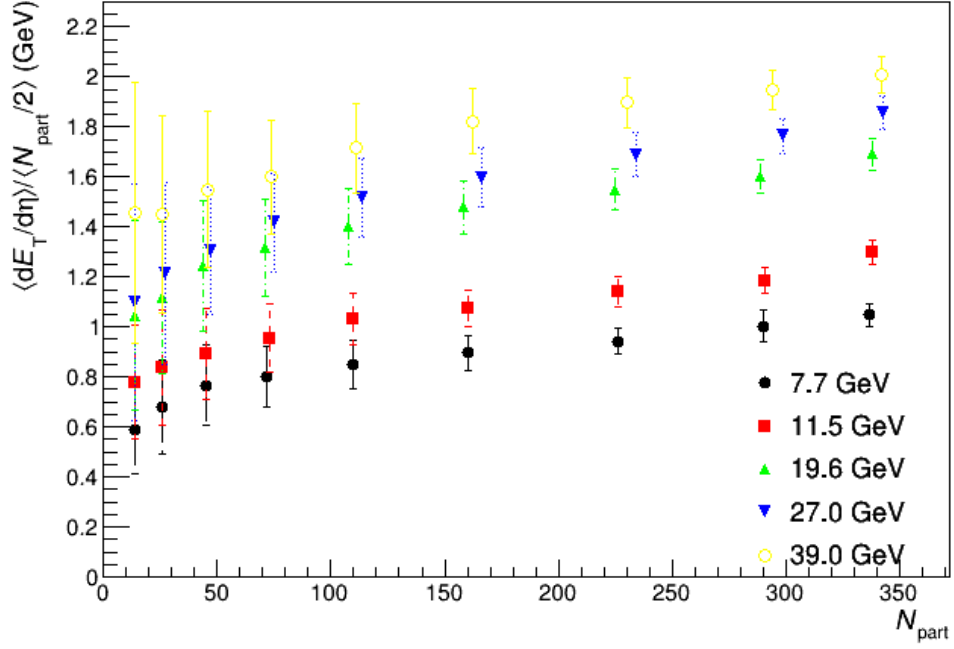


Figure 6.4: $\langle dE_T/d\eta \rangle / 0.5N_{part}$ at midrapidity as a function of N_{part} for different collision energies.

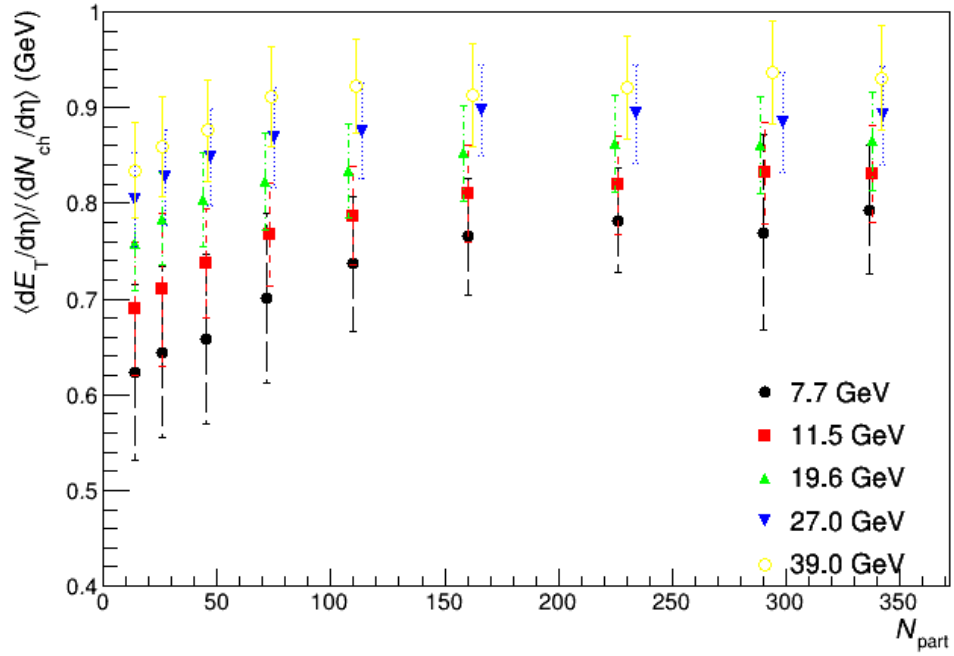


Figure 6.5: $\langle dE_T/d\eta \rangle / \langle dN_{ch}/d\eta \rangle$ at midrapidity as a function of N_{part} for different collision energies.

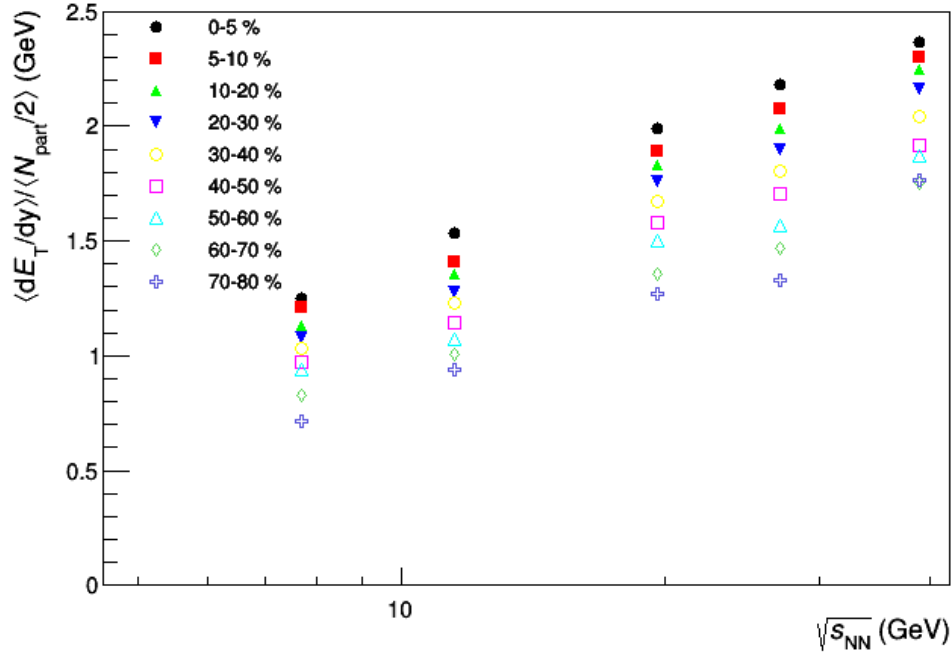


Figure 6.6: $\langle dE_T/dy \rangle / 0.5N_{part}$ at midrapidity as a function of $\sqrt{s_{NN}}$ for different centralities.

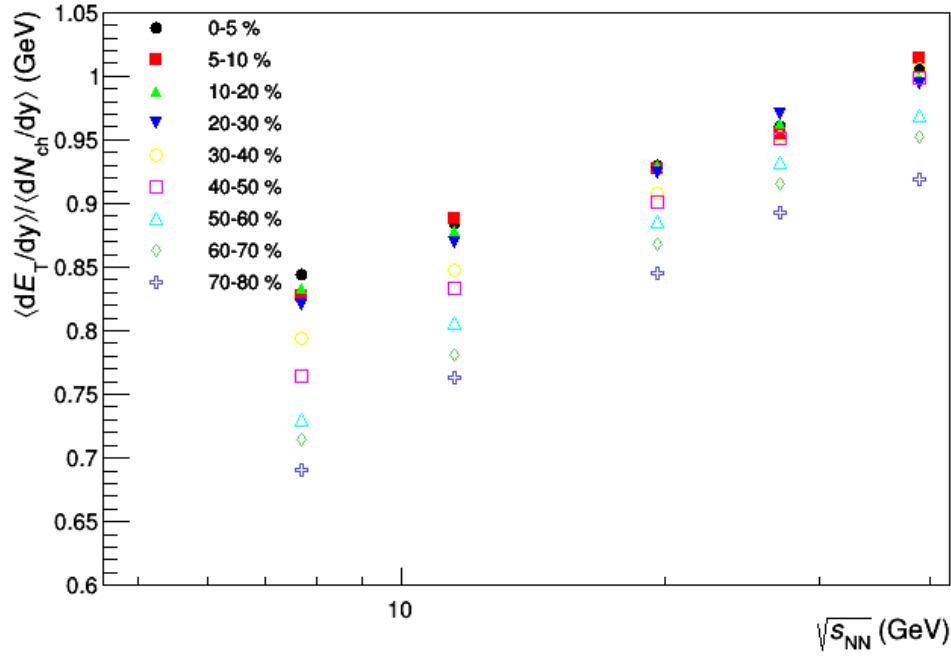


Figure 6.7: $\langle dE_T/dy \rangle / \langle dN_{ch}/dy \rangle$ at midrapidity as a function of $\sqrt{s_{NN}}$ for different centralities.

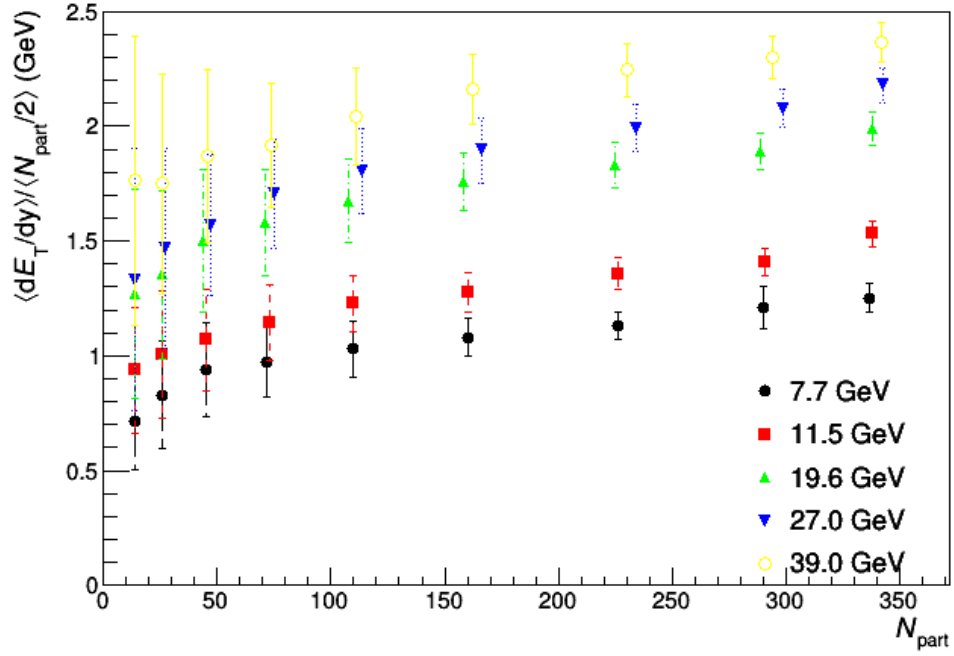


Figure 6.8: $\langle dE_T/dy \rangle / 0.5N_{part}$ at midrapidity as a function of N_{part} for different collision energies.

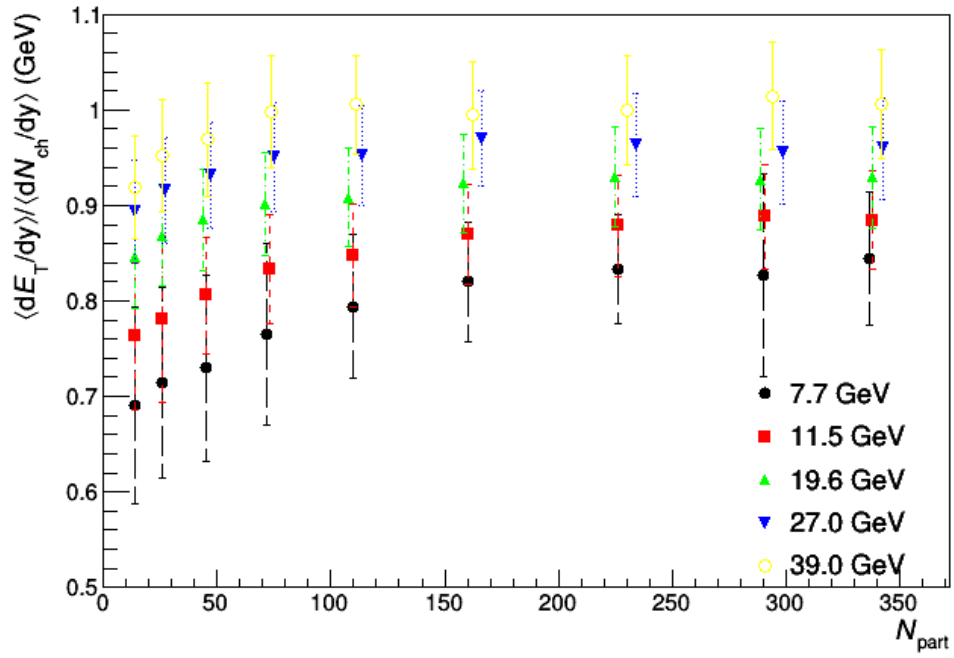


Figure 6.9: $\langle dE_T/dy \rangle / \langle dN_{ch}/dy \rangle$ at midrapidity as a function of N_{part} for different collision energies.

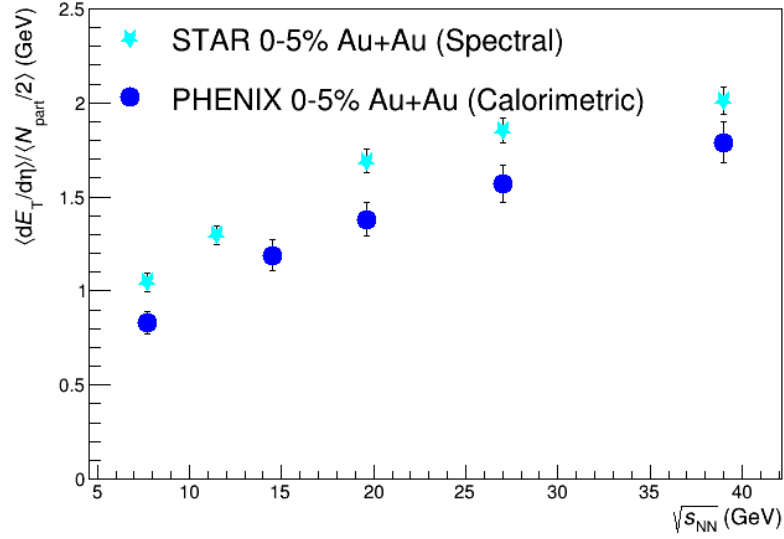


Figure 6.10: $\frac{dE_T}{d\eta} / 0.5N_{part}$ for 0-5% central collisions at midrapidity as a function of $\sqrt{s_{NN}}$. The PHENIX data are from [3]. The error bars represent the total statistical and systematic uncertainties.

638 **Chapter 7**

639 **Conclusion**

640 Summary and implications

Chapter 8

Future Work

8.1 Goodness of Fit

A maximum likelihood? fit method can be adopted to compare the results with those using the chi-squared fits.

8.2 Bjorken Energy Density Estimate

Apart from the transverse energy, the calculation of the initial energy density, ϵ , as given by the Bjorken formula in eq. 3.8, requires the estimate of other physical quantities. Adare et al.[3] use the Glauber model to determine A_T , the area of the intersection of the two nuclei in the transverse plane. Since the results in this thesis are cross-checked with those in [3], it would be reasonable to use the same model in the future work pertaining to this thesis. τ_0 , the proper time at the moment of QGP equilibration, also depends on the model of the collision. However, the product of ϵ and τ_0 is often used instead of just ϵ to study how the energy density scales with the collision energy and the number of participants.

655 **8.3 Asymmetric beams**

656 The codes in the repository can be used to analyze more data. In fact, since there is more
657 data available on collisions of asymmetric systems such as d+Au?, we can expect it to be a
658 test to tell if the assumptions? used in this analysis scale to such domains?

Bibliography

660 [1] Adam, J., Adamova, D., Aggarwal, M. M., Aglieri Rinella, G., Agnello, M., Agrawal,
 661 N., Ahammed, Z., Ahmad, S., Ahn, S. U., Aiola, S., Akindinov, A., Alam, S. N., Silva
 662 De Albuquerque, D., Aleksandrov, D., Alessandro, B., Alexandre, D., Alfaro Molina,
 663 J. R., Alici, A., Alkin, A., Millan Almaraz, J. R., Alme, J., Alt, T., Altinpinar, S.,
 664 Altsybeev, I., Alves Garcia Prado, C., Andrei, C., Andronic, A., Anguelov, V., Anticic,
 665 T., Antinori, F., Antonioli, P., Aphecetche, L. B., Appelshaeuser, H., Arcelli, S., Arnaldi,
 666 R., Arnold, O. W., Arsene, I. C., Arslanok, M., Audurier, B., Augustinus, A., Averbek,
 667 R. P., Azmi, M. D., Badala, A., Baek, Y. W., Bagnasco, S., Bailhache, R. M., Bala,
 668 R., Balasubramanian, S., Baldisseri, A., Baral, R. C., Barbano, A. M., Barbera, R.,
 669 Barile, F., Barnafoldi, G. G., Barnby, L. S., Ramillien Barret, V., Bartalini, P., Barth,
 670 K., Bartke, J. G., Bartsch, E., Basile, M., Bastid, N., Basu, S., Bathen, B., Batigne,
 671 G., Batista Camejo, A., Batyunya, B., Batzing, P. C., Bearden, I. G., Beck, H., Bedda,
 672 C., Behera, N. K., Belikov, I., Bellini, F., Bello Martinez, H., Bellwied, R., Belmont Iii,
 673 R. J., Belmont Moreno, E., Belyaev, V., Bencedi, G., Beole, S., Berceanu, I., Bercuci, A.,
 674 Berdnikov, Y., Berenyi, D., Bertens, R. A., Berzano, D., Betev, L., Bhasin, A., Bhat, I. R.,
 675 Bhati, A. K., Bhattacharjee, B., Bhom, J., Bianchi, L., Bianchi, N., Bianchin, C., Bielcik,
 676 J., Bielcikova, J., Bilandzic, A., Biro, G., Biswas, R., Biswas, S., Bjelogrljic, S., Blair, J. T.,
 677 Blau, D., Blume, C., Bock, F., Bogdanov, A., Boggild, H., Boldizar, L., Bombara, M.,
 678 Book, J. H., Borel, H., Borissov, A., Borri, M., Bossu, F., Botta, E., Bourjau, C., Braun-
 679 Munzinger, P., Bregant, M., Breitner, T. G., Broker, T. A., Browning, T. A., Broz, M.,
 680 Brucken, E. J., Bruna, E., Bruno, G. E., Budnikov, D., Buesching, H., Bufalino, S., Buncic,
 681 P., Busch, O., Buthelezi, E. Z., Bashir Butt, J., Buxton, J. T., Cabala, J., Caffarri, D.,
 682 Cai, X., Caines, H. L., Calero Diaz, L., Caliva, A., Calvo Villar, E., Camerini, P., Carena,
 683 F., Carena, W., Carnesecchi, F., Castillo Castellanos, J. E., Castro, A. J., Casula, E.
 684 A. R., Ceballos Sanchez, C., Cepila, J., Cerello, P., Cerkala, J., Chang, B., Chapeland,
 685 S., Chartier, M., Charvet, J.-L. F., Chattopadhyay, S., Chattopadhyay, S., Chauvin, A.,
 686 Chelnokov, V., Cherney, M. G., Cheshkov, C. V., Cheynis, B., Chibante Barroso, V. M.,
 687 Dobrigkeit Chinellato, D., Cho, S., Chochula, P., Choi, K., Chojnacki, M., Choudhury, S.,
 688 Christakoglou, P., Christensen, C. H., Christiansen, P., Chujo, T., Chung, S.-U., Cicalo,
 689 C., Cifarelli, L., Cindolo, F., Cleymans, J. W. A., Colamaria, F. F., Colella, D., Collu, A.,

690 Colocci, M., Conesa Balbastre, G., Conesa Del Valle, Z., Connors, M. E., Contreras Nuno,
 691 J. G., Cormier, T. M., Corrales Morales, Y., Cortes Maldonado, I., Cortese, P., Cosentino,
 692 M. R., Costa, F., Crochet, P., Cruz Albino, R., Cuautle Flores, E., Cunqueiro Mendez,
 693 L., Dahms, T., Dainese, A., Danisch, M. C., Danu, A., Das, D., Das, I., Das, S., Dash,
 694 A. K., Dash, S., De, S., De Caro, A., De Cataldo, G., De Conti, C., De Cuveland, J.,
 695 De Falco, A., De Gruttola, D., De Marco, N., De Pasquale, S., Deisting, A., Deloff,
 696 A., Denes, E. S., Deplano, C., Dhankher, P., Di Bari, D., Di Mauro, A., Di Nezza,
 697 P., Diaz Corchero, M. A., Dietel, T., Dillenseger, P., Divia, R., Djuvsland, O., Dobrin,
 698 A. F., Domenicis Gimenez, D., Donigus, B., Dordic, O., Drozhzhova, T., Dubey, A. K.,
 699 Dubla, A., Ducroux, L., Dupieux, P., Ehlers Iii, R. J., Elia, D., Endress, E., Engel, H.,
 700 Epple, E., Erasmus, B. E., Erdemir, I., Erhardt, F., Espagnon, B., Estienne, M. D.,
 701 Esumi, S., Eum, J., Evans, D., Evdokimov, S., Eyyubova, G., Fabbietti, L., Fabris, D.,
 702 Faivre, J., Fantoni, A., Fasel, M., Feldkamp, L., Feliciello, A., Feofilov, G., Ferencei, J.,
 703 Fernandez Tellez, A., Gonzalez Ferreiro, E., Ferretti, A., Festanti, A., Feuillard, V. J. G.,
 704 Figiel, J., Araujo Silva Figueredo, M., Filchagin, S., Finogeev, D., Fionda, F., Fiore, E. M.,
 705 Fleck, M. G., Floris, M., Foertsch, S. V., Foka, P., Fokin, S., Fragiacomio, E., Francescon,
 706 A., Frankenfeld, U. M., Fronze, G. G., Fuchs, U., Furget, C., Furs, A., Fusco Girard, M.,
 707 Gaardhoeje, J. J., Gagliardi, M., Gago Medina, A. M., Gallio, M., Gangadharan, D. R.,
 708 Ganoti, P., Gao, C., Garabatos Cuadrado, J., Garcia-Solis, E. J., Gargiulo, C., Gasik, P. J.,
 709 Gauger, E. F., Germain, M., Gheata, M., Ghosh, P., Ghosh, S. K., Gianotti, P., Giubellino,
 710 P., Giubilato, P., Gladysz-Dziadus, E., Glassel, P., Gomez Coral, D. M., Gomez Ramirez,
 711 A., Sanchez Gonzalez, A., Gonzalez, V., Gonzalez Zamora, P., Gorbunov, S., Gorlich,
 712 L. M., Gotovac, S., Grabski, V., Grachov, O. A., Graczykowski, L. K., Graham, K. L.,
 713 Grelli, A., Grigoras, A. G., Grigoras, C., Grigoryev, V., Grigoryan, A., Grigoryan, S.,
 714 Grynyov, B., Grion, N., Gronefeld, J. M., Grosse-Oetringhaus, J. F., Grosso, R., Guber,
 715 F., Guernane, R., Guerzoni, B., Gulbrandsen, K. H., Gunji, T., Gupta, A., Gupta, R.,
 716 Haake, R., Haaland, O. S., Hadjidakis, C. M., Haiduc, M., Hamagaki, H., Hamar, G.,
 717 Hamon, J. C., Harris, J. W., Harton, A. V., Hatzifotiadou, D., Hayashi, S., Heckel, S. T.,
 718 Hellbar, E., Helstrup, H., Herghelegiu, A. I., Herrera Corral, G. A., Hess, B. A., Hetland,
 719 K. F., Hillemanns, H., Hippolyte, B., Horak, D., Hosokawa, R., Hristov, P. Z., Humanic,

720 T., Hussain, N., Hussain, T., Hutter, D., Hwang, D. S., Ilkaev, R., Inaba, M., Incani,
 721 E., Ippolitov, M., Irfan, M., Ivanov, M., Ivanov, V., Izucheev, V., Jacazio, N., Jacobs,
 722 P. M., Jadhav, M. B., Jadlovská, S., Jadlovsky, J., Jahnke, C., Jakubowska, M. J., Jang,
 723 H. J., Janik, M. A., Pahula Hewage, S., Jena, C., Jena, S., Jimenez Bustamante, R. T.,
 724 Jones, P. G., Jusko, A., Kalinak, P., Kalweit, A. P., Kamin, J. A., Kang, J. H., Kaplin,
 725 V., Kar, S., Karasu Uysal, A., Karavichev, O., Karavicheva, T., Karayan, L., Karpechev,
 726 E., Kebschull, U. W., Keidel, R., Keijndener, D. L., Keil, M., Khan, M. M., Khan, P.,
 727 Khan, S. A., Khanzadeev, A., Kharlov, Y., Kileng, B., Kim, D. W., Kim, D. J., Kim,
 728 D., Kim, H., Kim, J., Kim, M., Kim, S. Y., Kim, T., Kirsch, S., Kisel, I., Kiselev,
 729 S., Kisiel, A. R., Kiss, G., Klay, J. L., Klein, C., Klein, J., Klein-Boesing, C., Klewin,
 730 S., Kluge, A., Knichel, M. L., Knospe, A. G., Kobdaj, C., Kofarago, M., Kollegger, T.,
 731 Kolozhvari, A., Kondratev, V., Kondratyeva, N., Kondratyuk, E., Konevskikh, A., Kopcik,
 732 M., Kostarakis, P., Kour, M., Kouzinopoulos, C., Kovalenko, O., Kovalenko, V., Kowalski,
 733 M., Koyithatta Meethalevedu, G., Kralik, I., Kravcakova, A., Krivda, M., Krizek, F.,
 734 Kryshen, E., Krzewicki, M., Kubera, A. M., Kucera, V., Kuhn, C. C., Kuijer, P. G.,
 735 Kumar, A., Kumar, J., Kumar, L., Kumar, S., Kurashvili, P., Kurepin, A., Kurepin, A.,
 736 Kuryakin, A., Kweon, M. J., Kwon, Y., La Pointe, S. L., La Rocca, P., Ladron De Guevara,
 737 P., Lagana Fernandes, C., Lakomov, I., Langoy, R., Lapidus, K., Lara Martinez, C. E.,
 738 Lardeux, A. X., Lattuca, A., Laudi, E., Lea, R., Leardini, L., Lee, G. R., Lee, S., Lehas, F.,
 739 Lemmon, R. C., Lenti, V., Leogrande, E., Leon Monzon, I., Leon Vargas, H., Leoncino, M.,
 740 Levai, P., Li, S., Li, X., Lien, J. A., Lietava, R., Lindal, S., Lindenstruth, V., Lippmann,
 741 C., Lisa, M. A., Ljunggren, H. M., Lodato, D. F., Lonne, P.-I., Loginov, V., Loizides, C.,
 742 Lopez, X. B., Lopez Torres, E., Lowe, A. J., Luettig, P. J., Lunardon, M., Luparello,
 743 G., Lutz, T. H., Maevskaya, A., Mager, M., Mahajan, S., Mahmood, S. M., Maire,
 744 A., Majka, R. D., Malaev, M., Maldonado Cervantes, I. A., Malinina, L., Mal'Kevich,
 745 D., Malzacher, P., Mamonov, A., Manko, V., Manso, F., Manzari, V., Marchisone, M.,
 746 Mares, J., Margagliotti, G. V., Margotti, A., Margutti, J., Marin, A. M., Markert, C.,
 747 Marquard, M., Martin, N. A., Martin Blanco, J., Martinengo, P., Martinez Hernandez,
 748 M. I., Martinez-Garcia, G., Martinez Pedreira, M., Mas, A. J.-M., Masciocchi, S., Masera,
 749 M., Masoni, A., Mastroserio, A., Matyja, A. T., Mayer, C., Mazer, J. A., Mazzoni,

750 A. M., Mcdonald, D., Meddi, F., Melikyan, Y., Menchaca-Rocha, A. A., Meninno, E.,
 751 Mercado-Perez, J., Meres, M., Miake, Y., Mieskolainen, M. M., Mikhaylov, K., Milano,
 752 L., Milosevic, J., Mischke, A., Mishra, A. N., Miskowiec, D. C., Mitra, J., Mitu, C. M.,
 753 Mohammadi, N., Mohanty, B., Molnar, L., Montano Zetina, L. M., Montes Prado, E.,
 754 Moreira De Godoy, D. A., Perez Moreno, L. A., Moretto, S., Morreale, A., Morsch, A.,
 755 Muccifora, V., Mudnic, E., Muhlheim, D. M., Muhuri, S., Mukherjee, M., Mulligan, J. D.,
 756 Gameiro Munhoz, M., Munzer, R. H., Murakami, H., Murray, S., Musa, L., Musinsky,
 757 J., Naik, B., Nair, R., Nandi, B. K., Nania, R., Nappi, E., Naru, M. U., Ferreira Natal
 758 Da Luz, P. H., Nattrass, C., Rosado Navarro, S., Nayak, K., Nayak, R., Nayak, T. K.,
 759 Nazarenko, S., Nedosekin, A., Nellen, L., Ng, F., Nicassio, M., Niculescu, M., Niedziela,
 760 J., Nielsen, B. S., Nikolaev, S., Nikulin, S., Nikulin, V., Noferini, F., Nomokonov, P.,
 761 Nooren, G., Cabanillas Noris, J. C., Norman, J., Nyanin, A., Nystrand, J. I., Oeschler,
 762 H. O., Oh, S., Oh, S. K., Ohlson, A. E., Okatan, A., Okubo, T., Olah, L., Oleniacz,
 763 J., Oliveira Da Silva, A. C., Oliver, M. H., Onderwaater, J., Oppedisano, C., Orava, R.,
 764 Oravec, M., Ortiz Velasquez, A., Oskarsson, A. N. E., Otwinowski, J. T., Oyama, K.,
 765 Ozdemir, M., Pachmayer, Y. C., Pagano, D., Pagano, P., Paic, G., Pal, S. K., Pan, J.,
 766 Pandey, A. K., Papikyan, V., Pappalardo, G., Pareek, P., Park, W., Parmar, S., Passfeld,
 767 A., Paticchio, V., Patra, R. N., Paul, B., Pei, H., Peitzmann, T., Pereira Da Costa, H.
 768 D. A., Peresunko, D. Y., Perez Lara, C. E., Perez Lezama, E., Peskov, V., Pestov, Y.,
 769 Petracek, V., Petrov, V., Petrovici, M., Petta, C., Piano, S., Pikna, M., Pillot, P., Ozelin
 770 De Lima Pimentel, L., Pinazza, O., Pinsky, L., Piyaathana, D., Ploskon, M. A., Planinic,
 771 M., Pluta, J. M., Pochybova, S., Podesta Lerma, P. L. M., Poghosyan, M., Polishchuk,
 772 B., Poljak, N., Poonsawat, W., Pop, A., Porteboeuf, S. J., Porter, R. J., Pospisil, J.,
 773 Prasad, S. K., Preghenella, R., Prino, F., Pruneau, C. A., Pshenichnov, I., Puccio, M.,
 774 Puddu, G., Pujahari, P. R., Punin, V., Putschke, J. H., Qvigstad, H., Rachevski, A., Raha,
 775 S., Rajput, S., Rak, J., Rakotozafindrabe, A. M., Ramello, L., Rami, F., Raniwala, R.,
 776 Raniwala, S., Rasanen, S. S., Rascanu, B. T., Rathee, D., Read, K. F., Redlich, K., Reed,
 777 R. J., Rehman, A. U., Reichelt, P. S., Reidt, F., Ren, X., Renfordt, R. A. E., Reolon, A. R.,
 778 Reshetin, A., Reygers, K. J., Riabov, V., Ricci, R. A., Richert, T. O. H., Richter, M. R.,
 779 Riedler, P., Riegler, W., Riggi, F., Ristea, C.-L., Rocco, E., Rodriguez Cahuantzi, M.,

780 Rodriguez Manso, A., Roeed, K., Rogochaya, E., Rohr, D. M., Roehrich, D., Ronchetti,
 781 F., Ronflette, L., Rosnet, P., Rossi, A., Roukoutakis, F., Roy, A., Roy, C. S., Roy, P. K.,
 782 Rubio Montero, A. J., Rui, R., Russo, R., Di Ruzza, B., Ryabinkin, E., Ryabov, Y.,
 783 Rybicki, A., Saarinen, S., Sadhu, S., Sadovskiy, S., Safarik, K., Sahlmuller, B., Sahoo, P.,
 784 Sahoo, R., Sahoo, S., Sahu, P. K., Saini, J., Sakai, S., Saleh, M. A., Salzwedel, J. S. N.,
 785 Sambyal, S. S., Samsonov, V., Sandor, L., Sandoval, A., Sano, M., Sarkar, D., Sarkar, N.,
 786 Sarma, P., Scapparone, E., Scarlassara, F., Schiaua, C. C., Schicker, R. M., Schmidt, C. J.,
 787 Schmidt, H. R., Schuchmann, S., Schukraft, J., Schulc, M., Schutz, Y. R., Schwarz, K. E.,
 788 Schweda, K. O., Scioli, G., Scomparin, E., Scott, R. M., Sefcik, M., Seger, J. E., Sekiguchi,
 789 Y., Sekihata, D., Selyuzhenkov, I., Senosi, K., Senyukov, S., Serradilla Rodriguez, E.,
 790 Sevcenco, A., Shabanov, A., Shabetai, A., Shadura, O., Shahoyan, R., Shahzad, M. I.,
 791 Shangaraev, A., Sharma, A., Sharma, M., Sharma, M., Sharma, N., Sheikh, A. I., Shigaki,
 792 K., Shou, Q., Shtejer Diaz, K., Sibiryak, Y., Siddhanta, S., Sielewicz, K. M., Siemiarczuk,
 793 T., Silvermyr, D. O. R., Silvestre, C. M., Simatovic, G., Simonetti, G., Singaraju, R. N.,
 794 Singh, R., Singha, S., Singhal, V., Sinha, B., Sarkar Sinha, T., Sitar, B., Sitta, M., Skaali,
 795 B., Slupecki, M., Smirnov, N., Snellings, R., Snellman, T. W., Song, J., Song, M., Song,
 796 Z., Soramel, F., Sorensen, S. P., Derradi De Souza, R., Sozzi, F., Spacek, M., Spiriti, E.,
 797 Sputowska, I. A., Spyropoulou-Stassinaki, M., Stachel, J., Stan, I., Stankus, P., Stenlund,
 798 E. A., Steyn, G. F., Stiller, J. H., Stocco, D., Strmen, P., Alarcon Do Passo Suaide, A.,
 799 Sugitate, T., Suire, C. P., Suleymanov, M. K. O., Suljic, M., Sultanov, R., Sumbera,
 800 M., Sumowidagdo, S., Szabo, A., Szanto De Toledo, A., Szarka, I., Szczepankiewicz, A.,
 801 Szymanski, M. P., Tabassam, U., Takahashi, J., Tambave, G. J., Tanaka, N., Tarhini,
 802 M., Tariq, M., Tarzila, M.-G., Tauro, A., Tejeda Munoz, G., Telesca, A., Terasaki, K.,
 803 Terrevoli, C., Teyssier, B., Thaeder, J. M., Thakur, D., Thomas, D., Tieulent, R. N.,
 804 Tikhonov, A., Timmins, A. R., Toia, A., Trogolo, S., Trombetta, G., Trubnikov, V.,
 805 Trzaska, W. H., Tsuji, T., Tumkin, A., Turrisi, R., Tveter, T. S., Ullaland, K., Uras, A.,
 806 Usai, G., Utrobicic, A., Vala, M., Valencia Palomo, L., Vallero, S., Van Der Maarel, J.,
 807 Van Hoorne, J. W., Van Leeuwen, M., Vanat, T., Vande Vyvre, P., Varga, D., Diozcora
 808 Vargas Trevino, A., Vargyas, M., Varma, R., Vasileiou, M., Vasiliev, A., Vauthier, A.,
 809 Vazquez Doce, O., Vechernin, V., Veen, A. M., Veldhoen, M., Velure, A., Vercellin, E.,

Vergara Limon, S., Vernet, R., Verweij, M., Vickovic, L., Viinikainen, J. S., Vilakazi, Z.,
Villalobos Baillie, O., Villatoro Tello, A., Vinogradov, A., Vinogradov, L., Vinogradov,
Y., Virgili, T., Vislavicius, V., Viyogi, Y., Vodopyanov, A., Volkl, M. A., Voloshin, K.,
Voloshin, S., Volpe, G., Von Haller, B., Vorobyev, I., Vranic, D., Vrlakova, J., Vulpescu,
B., Wagner, B., Wagner, J., Wang, H., Wang, M., Watanabe, D., Watanabe, Y., Weber,
M., Weber, S. G., Weiser, D. F., Wessels, J. P., Westerhoff, U., Whitehead, A. M.,
Wiechula, J., Wikne, J., Wilk, G. A., Wilkinson, J. J., Williams, C., Windelband, B. S.,
Winn, M. A., Yang, P., Yano, S., Yasin, Z., Yin, Z., Yokoyama, H., Yoo, I.-K., Yoon,
J. H., Yurchenko, V., Yushmanov, I., Zaborowska, A., Zaccolo, V., Zaman, A., Zampolli,
C., Correia Zanolli, H. J., Zaporozhets, S., Zardoshti, N., Zarochentsev, A., Zavada, P.,
Zavvalov, N., Zbroszczyk, H. P., Zgura, S. I., Zhalov, M., Zhang, H., Zhang, X., Zhang,
Y., Chunhui, Z., Zhang, Z., Zhao, C., Zhigareva, N., Zhou, D., Zhou, Y., Zhou, Z.,
Zhu, H., Zhu, J., Zichichi, A., Zimmermann, A., Zimmermann, M. B., Zinovjev, G., and
Zyzak, M. (2016). Measurement of transverse energy at midrapidity in Pb-Pb collisions at
 $\sqrt{s_{NN}} = 2.76$ TeV. *Phys. Rev. C*, 94(CERN-EP-2016-071. CERN-EP-2016-071):034903.
30 p. 30 pages, 14 captioned figures, 2 tables, authors from page 25, published version,
figures at <http://aliceinfo.cern.ch/ArtSubmission/node/2400>. 6, 15

[2] Adamczyk, L., Adkins, J. K., Agakishiev, G., Aggarwal, M. M., Ahammed, Z., Ajitanand,
N. N., Alekseev, I., Anderson, D. M., Aoyama, R., Aparin, A., Arkhipkin, D., Aschenauer,
E. C., Ashraf, M. U., Attri, A., Averichev, G. S., Bai, X., Bairathi, V., Behera, A.,
Bellwied, R., Bhasin, A., Bhati, A. K., Bhattarai, P., Bielcik, J., Bielcikova, J., Bland,
L. C., Bordyuzhin, I. G., Bouchet, J., Brandenburg, J. D., Brandin, A. V., Brown, D.,
Bunzarov, I., Butterworth, J., Caines, H., Calderón de la Barca Sánchez, M., Campbell,
J. M., Cebra, D., Chakaberia, I., Chaloupka, P., Chang, Z., Chankova-Bunzarova, N.,
Chatterjee, A., Chattopadhyay, S., Chen, X., Chen, J. H., Chen, X., Cheng, J., Cherney,
M., Christie, W., Contin, G., Crawford, H. J., Das, S., De Silva, L. C., Debbe, R. R.,
Dedovich, T. G., Deng, J., Derevschikov, A. A., Didenko, L., Dilks, C., Dong, X.,
Drachenberg, J. L., Draper, J. E., Dunkelberger, L. E., Dunlop, J. C., Efimov, L. G.,
Elsley, N., Engelage, J., Eppley, G., Esha, R., Esumi, S., Evdokimov, O., Ewigleben,

839 J., Eyser, O., Fatemi, R., Fazio, S., Federic, P., Federicova, P., Fedorisin, J., Feng, Z.,
 840 Filip, P., Finch, E., Fisyak, Y., Flores, C. E., Fulek, L., Gagliardi, C. A., Garand, D.,
 841 Geurts, F., Gibson, A., Girard, M., Grosnick, D., Gunarathne, D. S., Guo, Y., Gupta, A.,
 842 Gupta, S., Guryn, W., Hamad, A. I., Hamed, A., Harlenderova, A., Harris, J. W., He, L.,
 843 Heppelmann, S., Heppelmann, S., Hirsch, A., Hoffmann, G. W., Horvat, S., Huang, T.,
 844 Huang, B., Huang, X., Huang, H. Z., Humanic, T. J., Huo, P., Igo, G., Jacobs, W. W.,
 845 Jentsch, A., Jia, J., Jiang, K., Jowzaee, S., Judd, E. G., Kabana, S., Kalinkin, D., Kang,
 846 K., Kauder, K., Ke, H. W., Keane, D., Kechechyan, A., Khan, Z., Kikoła, D. P., Kisel,
 847 I., Kisiel, A., Kochenda, L., Kocmanek, M., Kollegger, T., Kosarzewski, L. K., Kraishan,
 848 A. F., Kravtsov, P., Krueger, K., Kulathunga, N., Kumar, L., Kvapil, J., Kwasizur, J. H.,
 849 Lacey, R., Landgraf, J. M., Landry, K. D., Lauret, J., Lebedev, A., Lednický, R., Lee,
 850 J. H., Li, X., Li, C., Li, W., Li, Y., Lidrych, J., Lin, T., Lisa, M. A., Liu, H., Liu,
 851 P., Liu, Y., Liu, F., Ljubicic, T., Llope, W. J., Lomnitz, M., Longacre, R. S., Luo, S.,
 852 Luo, X., Ma, G. L., Ma, L., Ma, Y. G., Ma, R., Magdy, N., Majka, R., Mallick, D.,
 853 Margetis, S., Markert, C., Matis, H. S., Meehan, K., Mei, J. C., Miller, Z. W., Minaev,
 854 N. G., Mioduszewski, S., Mishra, D., Mizuno, S., Mohanty, B., Mondal, M. M., Morozov,
 855 D. A., Mustafa, M. K., Nasim, M., Nayak, T. K., Nelson, J. M., Nie, M., Nigmatkulov,
 856 G., Niida, T., Nogach, L. V., Nonaka, T., Nurushev, S. B., Odyniec, G., Ogawa, A.,
 857 Oh, K., Okorokov, V. A., Olvitt, D., Page, B. S., Pak, R., Pandit, Y., Panebratsev, Y.,
 858 Pawlik, B., Pei, H., Perkins, C., Pile, P., Pluta, J., Poniatowska, K., Porter, J., Posik,
 859 M., Poskanzer, A. M., Pruthi, N. K., Przybycien, M., Putschke, J., Qiu, H., Quintero, A.,
 860 Ramachandran, S., Ray, R. L., Reed, R., Rehbein, M. J., Ritter, H. G., Roberts, J. B.,
 861 Rogachevskiy, O. V., Romero, J. L., Roth, J. D., Ruan, L., Rusnak, J., Rusnakova, O.,
 862 Sahoo, N. R., Sahu, P. K., Salur, S., Sandweiss, J., Saur, M., Schambach, J., Schmah,
 863 A. M., Schmidke, W. B., Schmitz, N., Schweid, B. R., Seger, J., Sergeeva, M., Seyboth, P.,
 864 Shah, N., Shahaliev, E., Shanmuganathan, P. V., Shao, M., Sharma, A., Sharma, M. K.,
 865 Shen, W. Q., Shi, Z., Shi, S. S., Shou, Q. Y., Sichtermann, E. P., Sikora, R., Simko,
 866 M., Singha, S., Skoby, M. J., Smirnov, N., Smirnov, D., Solyst, W., Song, L., Sorensen,
 867 P., Spinka, H. M., Srivastava, B., Stanislaus, T. D. S., Strikhanov, M., Stringfellow, B.,
 868 Sugiura, T., Sumbera, M., Summa, B., Sun, Y., Sun, X. M., Sun, X., Surrow, B., Svirida,

D. N., Tang, A. H., Tang, Z., Taranenko, A., Tarnowsky, T., Tawfik, A., Thäder, J., Thomas, J. H., Timmins, A. R., Tlusty, D., Todoroki, T., Tokarev, M., Trentalange, S., Tribble, R. E., Tribedy, P., Tripathy, S. K., Trzeciak, B. A., Tsai, O. D., Ullrich, T., Underwood, D. G., Upsal, I., Van Buren, G., van Nieuwenhuizen, G., Vasiliev, A. N., Videbæk, F., Vokal, S., Voloshin, S. A., Vossen, A., Wang, G., Wang, Y., Wang, F., Wang, Y., Webb, J. C., Webb, G., Wen, L., Westfall, G. D., Wieman, H., Wissink, S. W., Witt, R., Wu, Y., Xiao, Z. G., Xie, W., Xie, G., Xu, J., Xu, N., Xu, Q. H., Xu, Y. F., Xu, Z., Yang, Y., Yang, Q., Yang, C., Yang, S., Ye, Z., Ye, Z., Yi, L., Yip, K., Yoo, I.-K., Yu, N., Zbroszczyk, H., Zha, W., Zhang, Z., Zhang, X. P., Zhang, J. B., Zhang, S., Zhang, J., Zhang, Y., Zhang, J., Zhang, S., Zhao, J., Zhong, C., Zhou, L., Zhou, C., Zhu, X., Zhu, Z., and Zyzak, M. (2017). Bulk properties of the medium produced in relativistic heavy-ion collisions from the beam energy scan program. *Phys. Rev. C*, 96:044904. vii, 24, 28, 29

[3] Adare, A., Afanasiev, S., Aidala, C., Ajitanand, N. N., Akiba, Y., Akimoto, R., Al-Bataineh, H., Alexander, J., Alfred, M., Al-Jamel, A., Al-Ta'ani, H., Angerami, A., Aoki, K., Apadula, N., Aphecetche, L., Aramaki, Y., Armendariz, R., Aronson, S. H., Asai, J., Asano, H., Aschenauer, E. C., Atomssa, E. T., Auerbeck, R., Awes, T. C., Azmoun, B., Babintsev, V., Bai, M., Bai, X., Baksay, G., Baksay, L., Baldisseri, A., Bandara, N. S., Bannier, B., Barish, K. N., Barnes, P. D., Bassalleck, B., Basye, A. T., Bathe, S., Batsouli, S., Baublis, V., Bauer, F., Baumann, C., Baumgart, S., Bazilevsky, A., Beaumier, M., Beckman, S., Belikov, S., Belmont, R., Bennett, R., Berdnikov, A., Berdnikov, Y., Bhom, J. H., Bickley, A. A., Bjorndal, M. T., Black, D., Blau, D. S., Boissevain, J. G., Bok, J. S., Borel, H., Boyle, K., Brooks, M. L., Brown, D. S., Bryslawskyj, J., Bucher, D., Buesching, H., Bumazhnov, V., Bunce, G., Burward-Hoy, J. M., Butsyk, S., Campbell, S., Caringi, A., Castera, P., Chai, J.-S., Chang, B. S., Charvet, J.-L., Chen, C.-H., Chernichenko, S., Chi, C. Y., Chiba, J., Chiu, M., Choi, I. J., Choi, J. B., Choi, S., Choudhury, R. K., Christiansen, P., Chujo, T., Chung, P., Churn, A., Chvala, O., Cianciolo, V., Citron, Z., Cleven, C. R., Cobigo, Y., Cole, B. A., Comets, M. P., Conesa del Valle, Z., Connors, M., Constantin, P., Cronin, N., Crossette, N., Csanád, M., Csörgő, T., Dahms,

898 T., Dairaku, S., Danchev, I., Danley, T. W., Das, K., Datta, A., Daugherty, M. S.,
 899 David, G., Dayananda, M. K., Deaton, M. B., DeBlasio, K., Dehmelt, K., Delagrange,
 900 H., Denisov, A., d'Enterria, D., Deshpande, A., Desmond, E. J., Dharmawardane, K. V.,
 901 Dietzsch, O., Ding, L., Dion, A., Diss, P. B., Do, J. H., Donadelli, M., D'Orazio, L.,
 902 Drachenberg, J. L., Drapier, O., Drees, A., Drees, K. A., Dubey, A. K., Durham, J. M.,
 903 Durum, A., Dutta, D., Dzhordzhadze, V., Edwards, S., Efremenko, Y. V., Egdemir, J.,
 904 Ellinghaus, F., Emam, W. S., Engelmores, T., Enokizono, A., En'yo, H., Espagnon, B.,
 905 Esumi, S., Eyser, K. O., Fadem, B., Feege, N., Fields, D. E., Finger, M., Finger, M.,
 906 Fleuret, F., Fokin, S. L., Forestier, B., Fraenkel, Z., Frantz, J. E., Franz, A., Frawley,
 907 A. D., Fujiwara, K., Fukao, Y., Fung, S.-Y., Fusayasu, T., Gadrat, S., Gainey, K., Gal,
 908 C., Gallus, P., Garg, P., Garishvili, A., Garishvili, I., Gastineau, F., Ge, H., Germain, M.,
 909 Giordano, F., Glenn, A., Gong, H., Gong, X., Gonin, M., Gosset, J., Goto, Y., Granier de
 910 Cassagnac, R., Grau, N., Greene, S. V., Grim, G., Grosse Perdekamp, M., Gu, Y., Gunji,
 911 T., Guo, L., Guragain, H., Gustafsson, H.-A., Hachiya, T., Hadj Henni, A., Haegemann,
 912 C., Haggerty, J. S., Hagiwara, M. N., Hahn, K. I., Hamagaki, H., Hamblen, J., Hamilton,
 913 H. F., Han, R., Han, S. Y., Hanks, J., Harada, H., Hartouni, E. P., Haruna, K., Harvey,
 914 M., Hasegawa, S., Haseler, T. O. S., Hashimoto, K., Haslum, E., Hasuko, K., Hayano, R.,
 915 Hayashi, S., He, X., Heffner, M., Hemmick, T. K., Hester, T., Heuser, J. M., Hiejima, H.,
 916 Hill, J. C., Hobbs, R., Hohlmann, M., Hollis, R. S., Holmes, M., Holzmann, W., Homma,
 917 K., Hong, B., Horaguchi, T., Hori, Y., Hornback, D., Hoshino, T., Hotvedt, N., Huang, J.,
 918 Huang, S., Hur, M. G., Ichihara, T., Ichimiya, R., Inuma, H., Ikeda, Y., Imai, K., Imazu,
 919 Y., Imrek, J., Inaba, M., Inoue, Y., Iordanova, A., Isenhowe, D., Isenhowe, L., Ishihara,
 920 M., Isinhue, A., Isobe, T., Issah, M., Isupov, A., Ivanishchev, D., Iwanaga, Y., Jacak,
 921 B. V., Javani, M., Jeon, S. J., Jezghani, M., Jia, J., Jiang, X., Jin, J., Jinnouchi, O.,
 922 Johnson, B. M., Jones, T., Joo, K. S., Jouan, D., Jumper, D. S., Kajihara, F., Kametani,
 923 S., Kamihara, N., Kamin, J., Kanda, S., Kaneta, M., Kaneti, S., Kang, B. H., Kang, J. H.,
 924 Kang, J. S., Kanou, H., Kapustinsky, J., Karatsu, K., Kasai, M., Kawagishi, T., Kawall,
 925 D., Kawashima, M., Kazantsev, A. V., Kelly, S., Kempel, T., Key, J. A., Khachatryan, V.,
 926 Khandai, P. K., Khanzadeev, A., Kijima, K. M., Kikuchi, J., Kim, A., Kim, B. I., Kim, C.,
 927 Kim, D. H., Kim, D. J., Kim, E., Kim, E.-J., Kim, G. W., Kim, H. J., Kim, K.-B., Kim,

928 M., Kim, Y.-J., Kim, Y. K., Kim, Y.-S., Kimelman, B., Kinney, E., Kiss, A., Kistenev, E.,
 929 Kitamura, R., Kiyomichi, A., Klatsky, J., Klay, J., Klein-Boeing, C., Kleinjan, D., Kline,
 930 P., Koblesky, T., Kochenda, L., Kochetkov, V., Kofarago, M., Komatsu, Y., Komkov,
 931 B., Konno, M., Koster, J., Kotchetkov, D., Kotov, D., Kozlov, A., Král, A., Kravitz, A.,
 932 Krizek, F., Kroon, P. J., Kubart, J., Kunde, G. J., Kurihara, N., Kurita, K., Kurosawa,
 933 M., Kweon, M. J., Kwon, Y., Kyle, G. S., Lacey, R., Lai, Y. S., Lajoie, J. G., Lebedev,
 934 A., Le Bornec, Y., Leckey, S., Lee, B., Lee, D. M., Lee, G. H., Lee, J., Lee, K. B.,
 935 Lee, K. S., Lee, M. K., Lee, S., Lee, S. H., Lee, S. R., Lee, T., Leitch, M. J., Leite, M.
 936 A. L., Leitgab, M., Lenzi, B., Lewis, B., Li, X., Li, X. H., Lichtenwalner, P., Liebing, P.,
 937 Lim, H., Lim, S. H., Linden Levy, L. A., Liška, T., Litvinenko, A., Liu, H., Liu, M. X.,
 938 Love, B., Lynch, D., Maguire, C. F., Makdisi, Y. I., Makek, M., Malakhov, A., Malik,
 939 M. D., Manion, A., Manko, V. I., Mannel, E., Mao, Y., Maruyama, T., Mašek, L., Masui,
 940 H., Masumoto, S., Matathias, F., McCain, M. C., McCumber, M., McGaughey, P. L.,
 941 McGlinchey, D., McKinney, C., Means, N., Meles, A., Mendoza, M., Meredith, B., Miake,
 942 Y., Mibe, T., Midori, J., Mignerey, A. C., Mikeš, P., Miki, K., Miller, T. E., Milov, A.,
 943 Mioduszewski, S., Mishra, D. K., Mishra, G. C., Mishra, M., Mitchell, J. T., Mitrovski,
 944 M., Miyachi, Y., Miyasaka, S., Mizuno, S., Mohanty, A. K., Mohapatra, S., Montuenga,
 945 P., Moon, H. J., Moon, T., Morino, Y., Morreale, A., Morrison, D. P., Moskowitz, M.,
 946 Moss, J. M., Motschwiller, S., Moukhanova, T. V., Mukhopadhyay, D., Murakami, T.,
 947 Murata, J., Mwai, A., Nagae, T., Nagamiya, S., Nagashima, K., Nagata, Y., Nagle, J. L.,
 948 Naglis, M., Nagy, M. I., Nakagawa, I., Nakagomi, H., Nakamiya, Y., Nakamura, K. R.,
 949 Nakamura, T., Nakano, K., Nam, S., Nattrass, C., Nederlof, A., Netrakanti, P. K., Newby,
 950 J., Nguyen, M., Nihashi, M., Niida, T., Nishimura, S., Norman, B. E., Nouicer, R., Novák,
 951 T., Novitzky, N., Nukariya, A., Nyanin, A. S., Nystrand, J., Oakley, C., Obayashi, H.,
 952 O'Brien, E., Oda, S. X., Ogilvie, C. A., Ohnishi, H., Oide, H., Ojha, I. D., Oka, M.,
 953 Okada, K., Omiwade, O. O., Onuki, Y., Orjuela Koop, J. D., Osborn, J. D., Oskarsson,
 954 A., Otterlund, I., Ouchida, M., Ozawa, K., Pak, R., Pal, D., Palounek, A. P. T., Pantuev,
 955 V., Papavassiliou, V., Park, B. H., Park, I. H., Park, J., Park, J. S., Park, S., Park, S. K.,
 956 Park, W. J., Pate, S. F., Patel, L., Patel, M., Pei, H., Peng, J.-C., Pereira, H., Perepelitsa,
 957 D. V., Perera, G. D. N., Peresedov, V., Peressounko, D., Perry, J., Petti, R., Pinkenburg,

958 C., Pinson, R., Pisani, R. P., Proissl, M., Purschke, M. L., Purwar, A. K., Qu, H., Rak,
 959 J., Rakotozafindrabe, A., Ramson, B. J., Ravinovich, I., Read, K. F., Rembeczki, S.,
 960 Reuter, M., Reygers, K., Reynolds, D., Riabov, V., Riabov, Y., Richardson, E., Rinn, T.,
 961 Riveli, N., Roach, D., Roche, G., Rolnick, S. D., Romana, A., Rosati, M., Rosen, C. A.,
 962 Rosendahl, S. S. E., Rosnet, P., Rowan, Z., Rubin, J. G., Rukoyatkin, P., Ružička, P.,
 963 Rykov, V. L., Ryu, M. S., Ryu, S. S., Sahlmueller, B., Saito, N., Sakaguchi, T., Sakai, S.,
 964 Sakashita, K., Sakata, H., Sako, H., Samsonov, V., Sano, M., Sano, S., Sarsour, M., Sato,
 965 H. D., Sato, S., Sato, T., Sawada, S., Schaefer, B., Schmoll, B. K., Sedgwick, K., Seele,
 966 J., Seidl, R., Sekiguchi, Y., Semenov, V., Sen, A., Seto, R., Sett, P., Sexton, A., Sharma,
 967 D., Shaver, A., Shea, T. K., Shein, I., Shevel, A., Shibata, T.-A., Shigaki, K., Shimomura,
 968 M., Shohjoh, T., Shoji, K., Shukla, P., Sickles, A., Silva, C. L., Silvermyr, D., Silvestre,
 969 C., Sim, K. S., Singh, B. K., Singh, C. P., Singh, V., Skolnik, M., Skutnik, S., Slunečka,
 970 M., Smith, W. C., Snowball, M., Solano, S., Soldatov, A., Soltz, R. A., Sondheim, W. E.,
 971 Sorensen, S. P., Sourikova, I. V., Staley, F., Stankus, P. W., Steinberg, P., Stenlund, E.,
 972 Stepanov, M., Ster, A., Stoll, S. P., Stone, M. R., Sugitate, T., Suire, C., Sukhanov, A.,
 973 Sullivan, J. P., Sumita, T., Sun, J., Sziklai, J., Tabaru, T., Takagi, S., Takagui, E. M.,
 974 Takahara, A., Taketani, A., Tanabe, R., Tanaka, K. H., Tanaka, Y., Taneja, S., Tanida, K.,
 975 Tannenbaum, M. J., Tarafdar, S., Taranenko, A., Tarján, P., Tennant, E., Themann, H.,
 976 Thomas, D., Thomas, T. L., Tieulent, R., Timilsina, A., Todoroki, T., Togawa, M., Toia,
 977 A., Tojo, J., Tomášek, L., Tomášek, M., Torii, H., Towell, C. L., Towell, R., Towell, R. S.,
 978 Tram, V.-N., Tserruya, I., Tsuchimoto, Y., Tsuji, T., Tuli, S. K., Tydesjö, H., Tyurin,
 979 N., Vale, C., Valle, H., van Hecke, H. W., Vargyas, M., Vazquez-Zambrano, E., Veicht,
 980 A., Velkovska, J., Vértési, R., Vinogradov, A. A., Virius, M., Voas, B., Vossen, A., Vrba,
 981 V., Vznuzdaev, E., Wagner, M., Walker, D., Wang, X. R., Watanabe, D., Watanabe, K.,
 982 Watanabe, Y., Watanabe, Y. S., Wei, F., Wei, R., Wessels, J., Whitaker, S., White, A. S.,
 983 White, S. N., Willis, N., Winter, D., Wolin, S., Woody, C. L., Wright, R. M., Wysocki, M.,
 984 Xia, B., Xie, W., Xue, L., Yalcin, S., Yamaguchi, Y. L., Yamaura, K., Yang, R., Yanovich,
 985 A., Yasin, Z., Ying, J., Yokkaichi, S., Yoo, J. H., Yoon, I., You, Z., Young, G. R., Younus,
 986 I., Yu, H., Yushmanov, I. E., Zajc, W. A., Zaudtke, O., Zelenski, A., Zhang, C., Zhou, S.,

Zimanyi, J., Zolin, L., and Zou, L. (2016). Transverse energy production and charged-particle multiplicity at midrapidity in various systems from $\sqrt{s_{NN}} = 7.7$ to 200 gev. *Phys. Rev. C*, 93:024901. vii, viii, 5, 23, 33, 38, 40

[4] Adare, A., Afanasiev, S., Aidala, C., Ajitanand, N. N., Akiba, Y., Al-Bataineh, H., Alexander, J., Al-Jamel, A., Aoki, K., Aphecetche, L., and et al. (2007). Scaling Properties of Azimuthal Anisotropy in Au+Au and Cu+Cu Collisions at $s_{NN}=200\text{GeV}$. *Physical Review Letters*, 98(16):162301. vi, 16, 17

[5] Adler, S. S., Afanasiev, S., Aidala, C., Ajitanand, N. N., Akiba, Y., Al-Jamel, A., Alexander, J., Aoki, K., Aphecetche, L., Armendariz, R., Aronson, S. H., Auerbeck, R., Awes, T. C., Azmoun, B., Babintsev, V., Baldisseri, A., Barish, K. N., Barnes, P. D., Bassalleck, B., Bathe, S., Batsouli, S., Baublis, V., Bauer, F., Bazilevsky, A., Belikov, S., Bennett, R., Berdnikov, Y., Bjorndal, M. T., Boissevain, J. G., Borel, H., Boyle, K., Brooks, M. L., Brown, D. S., Bruner, N., Bucher, D., Buesching, H., Bumazhnov, V., Bunce, G., Burward-Hoy, J. M., Butsyk, S., Camard, X., Campbell, S., Chai, J.-S., Chand, P., Chang, W. C., Chernichenko, S., Chi, C. Y., Chiba, J., Chiu, M., Choi, I. J., Choudhury, R. K., Chujo, T., Cianciolo, V., Cleven, C. R., Cobigo, Y., Cole, B. A., Comets, M. P., Constantin, P., Csanád, M., Csörgő, T., Cussonneau, J. P., Dahms, T., Das, K., David, G., Deák, F., Delagrange, H., Denisov, A., d'Enterria, D., Deshpande, A., Desmond, E. J., Devismes, A., Dietzsch, O., Dion, A., Drachenberg, J. L., Drapier, O., Drees, A., Dubey, A. K., Durum, A., Dutta, D., Dzhordzhadze, V., Efremenko, Y. V., Egdemir, J., Enokizono, A., En'yo, H., Espagnon, B., Esumi, S., Fields, D. E., Finck, C., Fleuret, F., Fokin, S. L., Forestier, B., Fox, B. D., Fraenkel, Z., Frantz, J. E., Franz, A., Frawley, A. D., Fukao, Y., Fung, S.-Y., Gadrat, S., Gastineau, F., Germain, M., Glenn, A., Gonin, M., Gosset, J., Goto, Y., Granier de Cassagnac, R., Grau, N., Greene, S. V., Grosse Perdekamp, M., Gunji, T., Gustafsson, H.-A., Hachiya, T., Hadj Henni, A., Haggerty, J. S., Hagiwara, M. N., Hamagaki, H., Hansen, A. G., Harada, H., Hartouni, E. P., Haruna, K., Harvey, M., Haslum, E., Hasuko, K., Hayano, R., He, X., Heffner, M., Hemmick, T. K., Heuser, J. M., Hidas, P., Hiejima, H., Hill, J. C., Hobbs, R., Holmes, M., Holzmann, W., Homma, K., Hong, B., Hoover, A., Horaguchi, T., Hur, M. G., Ichihara, T.,

1016 Iinuma, H., Ikonnikov, V. V., Imai, K., Inaba, M., Inuzuka, M., Isenhowe, D., Isenhowe,
 1017 L., Ishihara, M., Isobe, T., Issah, M., Isupov, A., Jacak, B. V., Jia, J., Jin, J., Jinnouchi,
 1018 O., Johnson, B. M., Johnson, S. C., Joo, K. S., Jouan, D., Kajihara, F., Kametani,
 1019 S., Kamihara, N., Kaneta, M., Kang, J. H., Katou, K., Kawabata, T., Kawagishi, T.,
 1020 Kazantsev, A. V., Kelly, S., Khachaturov, B., Khanzadeev, A., Kikuchi, J., Kim, D. J.,
 1021 Kim, E., Kim, E. J., Kim, G.-B., Kim, H. J., Kim, Y.-S., Kinney, E., Kiss, A., Kistenev, E.,
 1022 Kiyomichi, A., Klein-Boesing, C., Kobayashi, H., Kochenda, L., Kochetkov, V., Kohara,
 1023 R., Komkov, B., Konno, M., Kotchetkov, D., Kozlov, A., Kroon, P. J., Kuberg, C. H.,
 1024 Kunde, G. J., Kurihara, N., Kurita, K., Kweon, M. J., Kwon, Y., Kyle, G. S., Lacey, R.,
 1025 Lajoie, J. G., Lebedev, A., Le Bornec, Y., Leckey, S., Lee, D. M., Lee, M. K., Leitch,
 1026 M. J., Leite, M. A. L., Li, X. H., Lim, H., Litvinenko, A., Liu, M. X., Maguire, C. F.,
 1027 Makdisi, Y. I., Malakhov, A., Malik, M. D., Manko, V. I., Mao, Y., Martinez, G., Masui,
 1028 H., Matathias, F., Matsumoto, T., McCain, M. C., McGaughey, P. L., Miake, Y., Miller,
 1029 T. E., Milov, A., Mioduszewski, S., Mishra, G. C., Mitchell, J. T., Mohanty, A. K.,
 1030 Morrison, D. P., Moss, J. M., Moukhanova, T. V., Mukhopadhyay, D., Muniruzzaman,
 1031 M., Murata, J., Nagamiya, S., Nagata, Y., Nagle, J. L., Naglis, M., Nakamura, T., Newby,
 1032 J., Nguyen, M., Norman, B. E., Nyanin, A. S., Nystrand, J., O'Brien, E., Ogilvie, C. A.,
 1033 Ohnishi, H., Ojha, I. D., Okada, K., Omiwade, O. O., Oskarsson, A., Otterlund, I., Oyama,
 1034 K., Ozawa, K., Pal, D., Palounek, A. P. T., Pantuev, V., Papavassiliou, V., Park, J., Park,
 1035 W. J., Pate, S. F., Pei, H., Penev, V., Peng, J.-C., Pereira, H., Peresedov, V., Peressounko,
 1036 D., Pierson, A., Pinkenburg, C., Pisani, R. P., Purschke, M. L., Purwar, A. K., Qu, H.,
 1037 Qualls, J. M., Rak, J., Ravinovich, I., Read, K. F., Reuter, M., Reygers, K., Riabov,
 1038 V., Riabov, Y., Roche, G., Romana, A., Rosati, M., Rosendahl, S. S. E., Rosnet, P.,
 1039 Rukoyatkin, P., Rykov, V. L., Ryu, S. S., Sahlmueller, B., Saito, N., Sakaguchi, T., Sakai,
 1040 S., Samsonov, V., Sanfratello, L., Santo, R., Sarsour, M., Sato, H. D., Sato, S., Sawada,
 1041 S., Schutz, Y., Semenov, V., Seto, R., Sharma, D., Shea, T. K., Shein, I., Shibata, T.-A.,
 1042 Shigaki, K., Shimomura, M., Shohjoh, T., Shoji, K., Sickles, A., Silva, C. L., Silvermyr, D.,
 1043 Sim, K. S., Singh, C. P., Singh, V., Skutnik, S., Smith, W. C., Soldatov, A., Soltz, R. A.,
 1044 Sondheim, W. E., Sorensen, S. P., Sourikova, I. V., Staley, F., Stankus, P. W., Stenlund,
 1045 E., Stepanov, M., Ster, A., Stoll, S. P., Sugitate, T., Suire, C., Sullivan, J. P., Sziklai, J.,

1046 Tabaru, T., Takagi, S., Takagui, E. M., Taketani, A., Tanaka, K. H., Tanaka, Y., Tanida,
 1047 K., Tannenbaum, M. J., Taranenko, A., Tarján, P., Thomas, T. L., Togawa, M., Tojo, J.,
 1048 Torii, H., Towell, R. S., Tram, V.-N., Tserruya, I., Tsuchimoto, Y., Tuli, S. K., Tydesjö,
 1049 H., Tyurin, N., Uam, T. J., Vale, C., Valle, H., van Hecke, H. W., Velkovska, J., Velkovsky,
 1050 M., Vértesi, R., Veszprémi, V., Vinogradov, A. A., Volkov, M. A., Vznuzdaev, E., Wagner,
 1051 M., Wang, X. R., Watanabe, Y., Wessels, J., White, S. N., Willis, N., Winter, D., Wohn,
 1052 F. K., Woody, C. L., Wysocki, M., Xie, W., Yanovich, A., Yokkaichi, S., Young, G. R.,
 1053 Younus, I., Yushmanov, I. E., Zajc, W. A., Zaudtke, O., Zhang, C., Zhou, S., Zimányi, J.,
 1054 Zolin, L., and Zong, X. (2014). Transverse-energy distributions at midrapidity in $p + p$,
 1055 $d + \text{Au}$, and $\text{Au} + \text{Au}$ collisions at $\sqrt{s_{\text{NN}}} = 62.4 \sim 200$ gev and implications for particle-
 1056 production models. *Phys. Rev. C*, 89:044905. 21

1057 [6] Adler, S. S., Afanasiev, S., Aidala, C., Ajitanand, N. N., Akiba, Y., Alexander, J.,
 1058 Amirikas, R., Aphecetche, L., Aronson, S. H., Auerbeck, R., Awes, T. C., Azmoun, R.,
 1059 Babintsev, V., Baldissieri, A., Barish, K. N., Barnes, P. D., Bassalleck, B., Bathe, S.,
 1060 Batsouli, S., Baublis, V., Bazilevsky, A., Belikov, S., Berdnikov, Y., Bhagavatula, S.,
 1061 Boissevain, J. G., Borel, H., Borenstein, S., Brooks, M. L., Brown, D. S., Bruner, N.,
 1062 Bucher, D., Buesching, H., Bumazhnov, V., Bunce, G., Burward-Hoy, J. M., Butsyk, S.,
 1063 Camard, X., Chai, J.-S., Chand, P., Chang, W. C., Chernichenko, S., Chi, C. Y., Chiba,
 1064 J., Chiu, M., Choi, I. J., Choi, J., Choudhury, R. K., Chujo, T., Cianciolo, V., Cobigo,
 1065 Y., Cole, B. A., Constantin, P., d’Enterria, D. G., David, G., Delagrange, H., Denisov, A.,
 1066 Deshpande, A., Desmond, E. J., Dietzsch, O., Drapier, O., Drees, A., Rietz, R. d., Durum,
 1067 A., Dutta, D., Efremenko, Y. V., Chenawi, K. E., Enokizono, A., En’yo, H., Esumi,
 1068 S., Ewell, L., Fields, D. E., Fleuret, F., Fokin, S. L., Fox, B. D., Fraenkel, Z., Frantz,
 1069 J. E., Franz, A., Frawley, A. D., Fung, S.-Y., Garpman, S., Ghosh, T. K., Glenn, A.,
 1070 Gogiberidze, G., Gonin, M., Gosset, J., Goto, Y., Cassagnac, R. G. d., Grau, N., Greene,
 1071 S. V., Perdekamp, M. G., Guryn, W., Gustafsson, H.-A., Hachiya, T., Haggerty, J. S.,
 1072 Hamagaki, H., Hansen, A. G., Hartouni, E. P., Harvey, M., Hayano, R., He, X., Heffner,
 1073 M., Hemmick, T. K., Heuser, J. M., Hibino, M., Hill, J. C., Holzmann, W., Homma, K.,
 1074 Hong, B., Hoover, A., Ichihara, T., Ikonnikov, V. V., Imai, K., Isenhower, D., Ishihara,

1075 M., Issah, M., Isupov, A., Jacak, B. V., Jang, W. Y., Jeong, Y., Jia, J., Jinnouchi, O.,
 1076 Johnson, B. M., Johnson, S. C., Joo, K. S., Jouan, D., Kametani, S., Kamihara, N.,
 1077 Kang, J. H., Kapoor, S. S., Katou, K., Kelly, S., Khachaturov, B., Khanzadeev, A.,
 1078 Kikuchi, J., Kim, D. H., Kim, D. J., Kim, D. W., Kim, E., Kim, G.-B., Kim, H. J.,
 1079 Kistenev, E., Kiyomichi, A., Kiyoyama, K., Klein-Boesing, C., Kobayashi, H., Kochenda,
 1080 L., Kochetkov, V., Koehler, D., Kohama, T., Kopytine, M., Kotchetkov, D., Kozlov, A.,
 1081 Kroon, P. J., Kuberg, C. H., Kurita, K., Kuroki, Y., Kweon, M. J., Kwon, Y., Kyle,
 1082 G. S., Lacey, R., Ladygin, V., Lajoie, J. G., Lebedev, A., Leckey, S., Lee, D. M., Lee, S.,
 1083 Leitch, M. J., Li, X. H., Lim, H., Litvinenko, A., Liu, M. X., Liu, Y., Maguire, C. F.,
 1084 Makdisi, Y. I., Malakhov, A., Manko, V. I., Mao, Y., Martinez, G., Marx, M. D., Masui,
 1085 H., Matathias, F., Matsumoto, T., McGaughey, P. L., Melnikov, E., Mendenhall, M.,
 1086 Messer, F., Miake, Y., Milan, J., Miller, T. E., Milov, A., Mioduszewski, S., Mischke,
 1087 R. E., Mishra, G. C., Mitchell, J. T., Mohanty, A. K., Morrison, D. P., Moss, J. M.,
 1088 Mühlbacher, F., Mukhopadhyay, D., Muniruzzaman, M., Murata, J., Nagamiya, S., Nagle,
 1089 J. L., Nakamura, T., Nandi, B. K., Nara, M., Newby, J., Nilsson, P., Nyanin, A. S.,
 1090 Nystrand, J., O'Brien, E., Ogilvie, C. A., Ohnishi, H., Ojha, I. D., Okada, K., Ono, M.,
 1091 Onuchin, V., Oskarsson, A., Otterlund, I., Oyama, K., Ozawa, K., Pal, D., Palounek, A.
 1092 P. T., Pantuev, V. S., Papavassiliou, V., Park, J., Parmar, A., Pate, S. F., Peitzmann,
 1093 T., Peng, J.-C., Peresedov, V., Pinkenburg, C., Pisani, R. P., Plasil, F., Purschke, M. L.,
 1094 Purwar, A. K., Rak, J., Ravinovich, I., Read, K. F., Reuter, M., Reygers, K., Riabov, V.,
 1095 Riabov, Y., Roche, G., Romana, A., Rosati, M., Rosnet, P., Ryu, S. S., Sadler, M. E.,
 1096 Saito, N., Sakaguchi, T., Sakai, M., Sakai, S., Samsonov, V., Sanfratello, L., Santo, R.,
 1097 Sato, H. D., Sato, S., Sawada, S., Schutz, Y., Semenov, V., Seto, R., Shaw, M. R., Shea,
 1098 T. K., Shibata, T.-A., Shigaki, K., Shiina, T., Silva, C. L., Silvermyr, D., Sim, K. S., Singh,
 1099 C. P., Singh, V., Sivertz, M., Soldatov, A., Soltz, R. A., Sondheim, W. E., Sorensen, S. P.,
 1100 Sourikova, I. V., Staley, F., Stankus, P. W., Stenlund, E., Stepanov, M., Ster, A., Stoll,
 1101 S. P., Sugitate, T., Sullivan, J. P., Takagui, E. M., Taketani, A., Tamai, M., Tanaka, K. H.,
 1102 Tanaka, Y., Tanida, K., Tannenbaum, M. J., Tarján, P., Tepe, J. D., Thomas, T. L., Tojo,
 1103 J., Torii, H., Towell, R. S., Tserruya, I., Tsuruoka, H., Tuli, S. K., Tydesjö, H., Tyurin,
 1104 N., Hecke, H. W. v., Velkovska, J., Velkovsky, M., Villatte, L., Vinogradov, A. A., Volkov,

- 1105 M. A., Vznuzdaev, E., Wang, X. R., Watanabe, Y., White, S. N., Wohn, F. K., Woody,
1106 C. L., Xie, W., Yang, Y., Yanovich, A., Yokkaichi, S., Young, G. R., Yushmanov, I. E.,
1107 Zajc, W. A., Zhang, C., Zhou, S., Zhou, S. J., and Zolin, L. (2005). Systematic studies of
1108 the centrality and $\sqrt{s_{NN}}$ dependence of the $de_T/d\eta$ and $dn_{ch}/d\eta$ in heavy ion collisions at
1109 midrapidity. *Phys. Rev. C*, 71:034908. 22
- 1110 [7] Aitchison, I. and Hey, A. (2003). *Gauge Theories in Particle Physics, Volume II: QCD*
1111 *and the Electroweak Theory, Third Edition*. Graduate Student Series in Physics. CRC
1112 Press. 3
- 1113 [8] Anderson, M. et al. (2003). The Star time projection chamber: A Unique tool for studying
1114 high multiplicity events at RHIC. *Nucl. Instrum. Meth.*, A499:659–678. 26
- 1115 [9] Ayala, A. (2016). Hadronic matter at the edge: A survey of some theoretical approaches
1116 to the physics of the qcd phase diagram. *Journal of Physics: Conference Series*,
1117 761(1):012066. vi, 5, 6
- 1118 [10] Bethe, H. A. and Ashkin, J. (1953). Passage of radiations through matter experimental
1119 nuclear physics vol 1 ed e segre. 24
- 1120 [11] Bjorken, J. D. (1983). Highly relativistic nucleus-nucleus collisions: The central rapidity
1121 region. *Phys. Rev. D*, 27:140–151. 15
- 1122 [12] Chatrchyan, S., Khachatryan, V., Sirunyan, A. M., Tumasyan, A., Adam, W., Bergauer,
1123 T., Dragicevic, M., Erö, J., Fabjan, C., Friedl, M., Frühwirth, R., Ghete, V. M., Hammer,
1124 J., Hörmann, N., Hrubec, J., Jeitler, M., Kiesenhofer, W., Knünz, V., Krammer, M., Liko,
1125 D., Mikulec, I., Pernicka, M., Rahbaran, B., Rohringer, C., Rohringer, H., Schöfbeck, R.,
1126 Strauss, J., Taurok, A., Wagner, P., Waltenberger, W., Walzel, G., Widl, E., Wulz, C.-E.,
1127 Mossolov, V., Shumeiko, N., Suarez Gonzalez, J., Bansal, S., Cornelis, T., De Wolf, E. A.,
1128 Janssen, X., Luyckx, S., Maes, T., Mucibello, L., Ochesanu, S., Roland, B., Rougny,
1129 R., Selvaggi, M., Staykova, Z., Van Haevermaet, H., Van Mechelen, P., Van Remortel,
1130 N., Van Spilbeeck, A., Blekman, F., Blyweert, S., D’Hondt, J., Gonzalez Suarez, R.,
1131 Kalogeropoulos, A., Maes, M., Olbrechts, A., Van Doninck, W., Van Mulders, P.,

1132 Van Onsem, G. P., Villella, I., Clerbaux, B., De Lentdecker, G., Dero, V., Gay, A. P. R.,
 1133 Hreus, T., Léonard, A., Marage, P. E., Reis, T., Thomas, L., Vander Velde, C., Vanlaer, P.,
 1134 Wang, J., Adler, V., Beernaert, K., Cimmino, A., Costantini, S., Garcia, G., Grunewald,
 1135 M., Klein, B., Lellouch, J., Marinov, A., McCartin, J., Ocampo Rios, A. A., Ryckbosch, D.,
 1136 Strobbe, N., Thyssen, F., Tytgat, M., Verwilligen, P., Walsh, S., Yazgan, E., Zaganidis,
 1137 N., Basegmez, S., Bruno, G., Castello, R., Ceard, L., Delaere, C., du Pree, T., Favart, D.,
 1138 Forthomme, L., Giammanco, A., Hollar, J., Lemaitre, V., Liao, J., Militaru, O., Nuttens,
 1139 C., Pagano, D., Pin, A., Piotrkowski, K., Schul, N., Vizan Garcia, J. M., Beliy, N.,
 1140 Caebegs, T., Daubie, E., Hammad, G. H., Alves, G. A., Correa Martins Junior, M.,
 1141 De Jesus Damiao, D., Martins, T., Pol, M. E., Souza, M. H. G., Aldá Júnior, W. L.,
 1142 Carvalho, W., Custódio, A., Da Costa, E. M., De Oliveira Martins, C., Fonseca De Souza,
 1143 S., Matos Figueiredo, D., Mundim, L., Nogima, H., Oguri, V., Prado Da Silva, W. L.,
 1144 Santoro, A., Soares Jorge, L., Sznajder, A., Bernardes, C. A., Dias, F. A., Fernandez
 1145 Perez Tomei, T. R., Gregores, E. M., Lagana, C., Marinho, F., Mercadante, P. G., Novaes,
 1146 S. F., Padula, S. S., Genchev, V., Iaydjiev, P., Piperov, S., Rodozov, M., Stoykova, S.,
 1147 Sultanov, G., Tcholakov, V., Trayanov, R., Vutova, M., Dimitrov, A., Hadjiiska, R.,
 1148 Kozhuharov, V., Litov, L., Pavlov, B., Petkov, P., Bian, J. G., Chen, G. M., Chen, H. S.,
 1149 Jiang, C. H., Liang, D., Liang, S., Meng, X., Tao, J., Wang, J., Wang, X., Wang, Z.,
 1150 Xiao, H., Xu, M., Zang, J., Zhang, Z., Asawatangtrakuldee, C., Ban, Y., Guo, S., Guo,
 1151 Y., Li, W., Liu, S., Mao, Y., Qian, S. J., Teng, H., Wang, S., Zhu, B., Zou, W., Avila,
 1152 C., Gomez, J. P., Gomez Moreno, B., Osorio Oliveros, A. F., Sanabria, J. C., Godinovic,
 1153 N., Lelas, D., Plestina, R., Polic, D., Puljak, I., Antunovic, Z., Kovac, M., Brigljevic, V.,
 1154 Duric, S., Kadija, K., Luetic, J., Morovic, S., Attikis, A., Galanti, M., Mavromanolakis,
 1155 G., Mousa, J., Nicolaou, C., Ptochos, F., Razis, P. A., Finger, M., Finger, M., Assran,
 1156 Y., Elgammal, S., Ellithi Kamel, A., Khalil, S., Mahmoud, M. A., Radi, A., Kadastik,
 1157 M., Müntel, M., Raidal, M., Rebane, L., Tiko, A., Azzolini, V., Eerola, P., Fedi, G.,
 1158 Voutilainen, M., Härkönen, J., Heikkinen, A., Karimäki, V., Kinnunen, R., Kortelainen,
 1159 M. J., Lampén, T., Lassila-Perini, K., Lehti, S., Lindén, T., Luukka, P., Mäenpää, T.,
 1160 Peltola, T., Tuominen, E., Tuominiemi, J., Tuovinen, E., Ungaro, D., Wendland, L.,
 1161 Banzuzi, K., Karjalainen, A., Korpela, A., Tuuva, T., Besancon, M., Choudhury, S.,

1162 Dejardin, M., Denegri, D., Fabbro, B., Faure, J. L., Ferri, F., Ganjour, S., Givernaud,
 1163 A., Gras, P., Hamel de Monchenault, G., Jarry, P., Locci, E., Malcles, J., Millischer, L.,
 1164 Nayak, A., Rander, J., Rosowsky, A., Shreyber, I., Titov, M., Baffioni, S., Beaudette,
 1165 F., Benhabib, L., Bianchini, L., Bluj, M., Broutin, C., Busson, P., Charlot, C., Daci,
 1166 N., Dahms, T., Dobrzynski, L., Granier de Cassagnac, R., Haguenaue, M., Miné, P.,
 1167 Mironov, C., Nguyen, M., Ochando, C., Paganini, P., Sabes, D., Salerno, R., Sirois, Y.,
 1168 Veelken, C., Zabi, A., Agram, J.-L., Andrea, J., Bloch, D., Bodin, D., Brom, J.-M.,
 1169 Cardaci, M., Chabert, E. C., Collard, C., Conte, E., Drouhin, F., Ferro, C., Fontaine, J.-
 1170 C., Gelé, D., Goerlach, U., Juillot, P., Le Bihan, A.-C., Van Hove, P., Fassi, F., Mercier,
 1171 D., Beauceron, S., Beaupere, N., Bondu, O., Boudoul, G., Chasserat, J., Chierici, R.,
 1172 Contardo, D., Depasse, P., El Mamouni, H., Fay, J., Gascon, S., Gouzevitch, M., Ille,
 1173 B., Kurca, T., Lethuillier, M., Mirabito, L., Perries, S., Sordini, V., Tosi, S., Tschudi,
 1174 Y., Verdier, P., Viret, S., Tsamalaidze, Z., Anagnostou, G., Beranek, S., Edelhoff, M.,
 1175 Feld, L., Heracleous, N., Hindrichs, O., Jussen, R., Klein, K., Merz, J., Ostapchuk, A.,
 1176 Perieanu, A., Raupach, F., Sammet, J., Schael, S., Sprenger, D., Weber, H., Wittmer,
 1177 B., Zhukov, V., Ata, M., Caudron, J., Dietz-Laursonn, E., Erdmann, M., Güth, A.,
 1178 Hebbeker, T., Heidemann, C., Hoepfner, K., Klingebiel, D., Kreuzer, P., Lingemann,
 1179 J., Magass, C., Merschmeyer, M., Meyer, A., Olschewski, M., Papacz, P., Pieta, H.,
 1180 Reithler, H., Schmitz, S. A., Sonnenschein, L., Steggemann, J., Teyssier, D., Weber, M.,
 1181 Bontenackels, M., Cherepanov, V., Flügge, G., Geenen, H., Geisler, M., Haj Ahmad, W.,
 1182 Hoehle, F., Kargoll, B., Kress, T., Kuessel, Y., Nowack, A., Perchalla, L., Pooth, O.,
 1183 Rennefeld, J., Sauerland, P., Stahl, A., Aldaya Martin, M., Behr, J., Behrenhoff, W.,
 1184 Behrens, U., Bergholz, M., Bethani, A., Borrás, K., Burgmeier, A., Cakir, A., Calligaris,
 1185 L., Campbell, A., Castro, E., Costanza, F., Dammann, D., Diez Pardos, C., Eckerlin, G.,
 1186 Eckstein, D., Flucke, G., Geiser, A., Glushkov, I., Gunnellini, P., Habib, S., Hauk, J.,
 1187 Jung, H., Kasemann, M., Katsas, P., Kleinwort, C., Kluge, H., Knutsson, A., Krämer, M.,
 1188 Krücker, D., Kuznetsova, E., Lange, W., Lohmann, W., Lutz, B., Mankel, R., Marfin, I.,
 1189 Marienfeld, M., Melzer-Pellmann, I.-A., Meyer, A. B., Mnich, J., Mussgiller, A., Naumann-
 1190 Emme, S., Olzem, J., Perrey, H., Petrukhin, A., Pitzl, D., Raspereza, A., Ribeiro Cipriano,
 1191 P. M., Riedl, C., Ron, E., Rosin, M., Salfeld-Nebgen, J., Schmidt, R., Schoerner-Sadenius,

1192 T., Sen, N., Spiridonov, A., Stein, M., Walsh, R., Wissing, C., Autermann, C., Blobel,
 1193 V., Draeger, J., Enderle, H., Erfle, J., Gebbert, U., Görner, M., Hermanns, T., Höing,
 1194 R. S., Kaschube, K., Kaussen, G., Kirschenmann, H., Klanner, R., Lange, J., Mura, B.,
 1195 Nowak, F., Peiffer, T., Pietsch, N., Sander, C., Schettler, H., Schleper, P., Schlieckau, E.,
 1196 Schmidt, A., Schröder, M., Schum, T., Sola, V., Stadie, H., Steinbrück, G., Thomsen,
 1197 J., Vanelderen, L., Barth, C., Berger, J., Chwalek, T., De Boer, W., Dierlamm, A.,
 1198 Feindt, M., Guthoff, M., Hackstein, C., Hartmann, F., Heinrich, M., Held, H., Hoffmann,
 1199 K. H., Honc, S., Katkov, I., Komaragiri, J. R., Lobelle Pardo, P., Martschei, D., Mueller,
 1200 S., Müller, T., Niegel, M., Nürnberg, A., Oberst, O., Oehler, A., Ott, J., Quast, G.,
 1201 Rabbertz, K., Ratnikov, F., Ratnikova, N., Röcker, S., Scheurer, A., Schilling, F.-P.,
 1202 Schott, G., Simonis, H. J., Stober, F. M., Troendle, D., Ulrich, R., Wagner-Kuhr, J.,
 1203 Weiler, T., Zeise, M., Daskalakis, G., Gerasis, T., Kesisoglou, S., Kyriakis, A., Loukas,
 1204 D., Manolakos, I., Markou, A., Markou, C., Mavrommatis, C., Ntomari, E., Gouskos, L.,
 1205 Mertzimekis, T. J., Panagiotou, A., Saoulidou, N., Evangelou, I., Foudas, C., Kokkas, P.,
 1206 Manthos, N., Papadopoulos, I., Patras, V., Bencze, G., Hajdu, C., Hidas, P., Horvath, D.,
 1207 Sikler, F., Veszpremi, V., Vesztergombi, G., Beni, N., Czellar, S., Molnar, J., Palinkas, J.,
 1208 Szillasi, Z., Karancsi, J., Raics, P., Trocsanyi, Z. L., Ujvari, B., Beri, S. B., Bhatnagar,
 1209 V., Dhingra, N., Gupta, R., Jindal, M., Kaur, M., Mehta, M. Z., Nishu, N., Saini, L. K.,
 1210 Sharma, A., Singh, J., Ahuja, S., Bhardwaj, A., Choudhary, B. C., Kumar, A., Kumar,
 1211 A., Malhotra, S., Naimuddin, M., Ranjan, K., Sharma, V., Shivpuri, R. K., Banerjee,
 1212 S., Bhattacharya, S., Dutta, S., Gomber, B., Jain, S., Jain, S., Khurana, R., Sarkar,
 1213 S., Sharan, M., Abdulsalam, A., Choudhury, R. K., Dutta, D., Kailas, S., Kumar, V.,
 1214 Mehta, P., Mohanty, A. K., Pant, L. M., Shukla, P., Aziz, T., Ganguly, S., Guchait, M.,
 1215 Maity, M., Majumder, G., Mazumdar, K., Mohanty, G. B., Parida, B., Sudhakar, K.,
 1216 Wickramage, N., Banerjee, S., Dugad, S., Arfaei, H., Bakhshiansohi, H., Etesami, S. M.,
 1217 Fahim, A., Hashemi, M., Hesari, H., Jafari, A., Khakzad, M., Mohammadi Najafabadi,
 1218 M., Paktinat Mehdiabadi, S., Safarzadeh, B., Zeinali, M., Abbrescia, M., Barbone, L.,
 1219 Calabria, C., Chhibra, S. S., Colaleo, A., Creanza, D., De Filippis, N., De Palma, M.,
 1220 Fiore, L., Iaselli, G., Lusito, L., Maggi, G., Maggi, M., Marangelli, B., My, S., Nuzzo,
 1221 S., Pacifico, N., Pompili, A., Pugliese, G., Selvaggi, G., Silvestris, L., Singh, G., Zito,

1222 G., Abbiendi, G., Benvenuti, A. C., Bonacorsi, D., Braibant-Giacomelli, S., Brigliadori,
 1223 L., Capiluppi, P., Castro, A., Cavallo, F. R., Cuffiani, M., Dallavalle, G. M., Fabbri, F.,
 1224 Fanfani, A., Fasanella, D., Giacomelli, P., Grandi, C., Guiducci, L., Marcellini, S., Masetti,
 1225 G., Meneghelli, M., Montanari, A., Navarria, F. L., Odorici, F., Perrotta, A., Primavera,
 1226 F., Rossi, A. M., Rovelli, T., Siroli, G., Travaglini, R., Albergo, S., Cappello, G., Chiorboli,
 1227 M., Costa, S., Potenza, R., Tricomi, A., Tuve, C., Barbagli, G., Ciulli, V., Civinini, C.,
 1228 D'Alessandro, R., Focardi, E., Frosali, S., Gallo, E., Gonzi, S., Meschini, M., Paoletti,
 1229 S., Sguazzoni, G., Tropiano, A., Benussi, L., Bianco, S., Colafranceschi, S., Fabbri, F.,
 1230 Piccolo, D., Fabbricatore, P., Musenich, R., Benaglia, A., De Guio, F., Di Matteo, L.,
 1231 Fiorendi, S., Gennai, S., Ghezzi, A., Malvezzi, S., Manzoni, R. A., Martelli, A., Massironi,
 1232 A., Menasce, D., Moroni, L., Paganoni, M., Pedrini, D., Ragazzi, S., Redaelli, N., Sala,
 1233 S., Tabarelli de Fatis, T., Buontempo, S., Carrillo Montoya, C. A., Cavallo, N., De Cosa,
 1234 A., Dogangun, O., Fabozzi, F., Iorio, A. O. M., Lista, L., Meola, S., Merola, M., Paolucci,
 1235 P., Azzi, P., Bacchetta, N., Bellan, P., Bisello, D., Branca, A., Carlin, R., Checchia, P.,
 1236 Dorigo, T., Dosselli, U., Gasparini, F., Gasparini, U., Gozzelino, A., Kanishchev, K.,
 1237 Lacaprara, S., Lazzizzera, I., Margoni, M., Meneguzzo, A. T., Nespolo, M., Ronchese,
 1238 P., Simonetto, F., Torassa, E., Vanini, S., Zotto, P., Zumerle, G., Gabusi, M., Ratti,
 1239 S. P., Riccardi, C., Torre, P., Vitulo, P., Biasini, M., Bilei, G. M., Fanò, L., Lariccia, P.,
 1240 Lucaroni, A., Mantovani, G., Menichelli, M., Nappi, A., Romeo, F., Saha, A., Santocchia,
 1241 A., Taroni, S., Azzurri, P., Bagliesi, G., Boccali, T., Broccolo, G., Castaldi, R., D'Agnolo,
 1242 R. T., Dell'Orso, R., Fiori, F., Foà, L., Giassi, A., Kraan, A., Ligabue, F., Lomtadze, T.,
 1243 Martini, L., Messineo, A., Palla, F., Rizzi, A., Serban, A. T., Spagnolo, P., Squillacioti, P.,
 1244 Tenchini, R., Tonelli, G., Venturi, A., Verdini, P. G., Barone, L., Cavallari, F., Del Re, D.,
 1245 Diemoz, M., Grassi, M., Longo, E., Meridiani, P., Micheli, F., Nourbakhsh, S., Organtini,
 1246 G., Paramatti, R., Rahatlou, S., Sigamani, M., Soffi, L., Amapane, N., Arcidiacono, R.,
 1247 Argiro, S., Arneodo, M., Biino, C., Cartiglia, N., Costa, M., Demaria, N., Graziano,
 1248 A., Mariotti, C., Maselli, S., Migliore, E., Monaco, V., Musich, M., Obertino, M. M.,
 1249 Pastrone, N., Pelliccioni, M., Potenza, A., Romero, A., Ruspa, M., Sacchi, R., Solano, A.,
 1250 Staiano, A., Vilela Pereira, A., Belforte, S., Candelise, V., Cossutti, F., Della Ricca, G.,
 1251 Gobbo, B., Marone, M., Montanino, D., Penzo, A., Schizzi, A., Heo, S. G., Kim, T. Y.,

1252 Nam, S. K., Chang, S., Kim, D. H., Kim, G. N., Kong, D. J., Park, H., Ro, S. R., Son,
 1253 D. C., Son, T., Kim, J. Y., Kim, Z. J., Song, S., Choi, S., Gyun, D., Hong, B., Jo, M.,
 1254 Kim, H., Kim, T. J., Lee, K. S., Moon, D. H., Park, S. K., Choi, M., Kim, J. H., Park,
 1255 C., Park, I. C., Park, S., Ryu, G., Cho, Y., Choi, Y., Choi, Y. K., Goh, J., Kim, M. S.,
 1256 Kwon, E., Lee, B., Lee, J., Lee, S., Seo, H., Yu, I., Bilinskas, M. J., Grigelionis, I., Janulis,
 1257 M., Juodagalvis, A., Castilla-Valdez, H., De La Cruz-Burelo, E., Heredia-de La Cruz, I.,
 1258 Lopez-Fernandez, R., Magaña Villalba, R., Martínez-Ortega, J., Sánchez-Hernández, A.,
 1259 Villasenor-Cendejas, L. M., Carrillo Moreno, S., Vazquez Valencia, F., Salazar Ibarguen,
 1260 H. A., Casimiro Linares, E., Morelos Pineda, A., Reyes-Santos, M. A., Krofcheck, D.,
 1261 Bell, A. J., Butler, P. H., Doesburg, R., Reucroft, S., Silverwood, H., Ahmad, M.,
 1262 Asghar, M. I., Hoorani, H. R., Khalid, S., Khan, W. A., Khurshid, T., Qazi, S., Shah,
 1263 M. A., Shoaib, M., Bialkowska, H., Boimska, B., Frueboes, T., Gokieli, R., Górski,
 1264 M., Kazana, M., Nawrocki, K., Romanowska-Rybinska, K., Szleper, M., Wrochna, G.,
 1265 Zalewski, P., Brona, G., Bunkowski, K., Cwiok, M., Dominik, W., Doroba, K., Kalinowski,
 1266 A., Konecki, M., Krolikowski, J., Almeida, N., Bargassa, P., David, A., Faccioli, P.,
 1267 Ferreira Parracho, P. G., Gallinaro, M., Seixas, J., Varela, J., Vischia, P., Belotelov,
 1268 I., Bunin, P., Gavrilenko, M., Golutvin, I., Gorbunov, I., Kamenev, A., Karjavin, V.,
 1269 Kozlov, G., Lanev, A., Malakhov, A., Moisenz, P., Palichik, V., Perelygin, V., Shmatov,
 1270 S., Smirnov, V., Volodko, A., Zarubin, A., Evstyukhin, S., Golovtsov, V., Ivanov, Y.,
 1271 Kim, V., Levchenko, P., Murzin, V., Oreshkin, V., Smirnov, I., Sulimov, V., Uvarov,
 1272 L., Vavilov, S., Vorobyev, A., Vorobyev, A., Andreev, Y., Dermenev, A., Gninenko,
 1273 S., Golubev, N., Kirsanov, M., Krasnikov, N., Matveev, V., Pashenkov, A., Tlisov, D.,
 1274 Toropin, A., Epshteyn, V., Erofeeva, M., Gavrilov, V., Kossov, M., Lychkovskaya, N.,
 1275 Popov, V., Safronov, G., Semenov, S., Stolin, V., Vlasov, E., Zhokin, A., Belyaev, A.,
 1276 Boos, E., Ershov, A., Gribushin, A., Klyukhin, V., Kodolova, O., Korotkikh, V., Lokhtin,
 1277 I., Markina, A., Obraztsov, S., Perfilov, M., Petrushanko, S., Popov, A., Sarycheva, L.,
 1278 Savrin, V., Snigirev, A., Vardanyan, I., Andreev, V., Azarkin, M., Dremine, I., Kirakosyan,
 1279 M., Leonidov, A., Mesyats, G., Rusakov, S. V., Vinogradov, A., Azhgirey, I., Bayshev, I.,
 1280 Bitioukov, S., Grishin, V., Kachanov, V., Konstantinov, D., Korablev, A., Krychkin,
 1281 V., Petrov, V., Ryutin, R., Sobol, A., Tourtchanovitch, L., Troshin, S., Tyurin, N.,

1282 Uzunian, A., Volkov, A., Adzic, P., Djordjevic, M., Ekmedzic, M., Krpic, D., Milosevic, J.,
 1283 Aguilar-Benitez, M., Alcaraz Maestre, J., Arce, P., Battilana, C., Calvo, E., Cerrada, M.,
 1284 Chamizo Llatas, M., Colino, N., De La Cruz, B., Delgado Peris, A., Domínguez Vázquez,
 1285 D., Fernandez Bedoya, C., Fernández Ramos, J. P., Ferrando, A., Flix, J., Fouz, M. C.,
 1286 Garcia-Abia, P., Gonzalez Lopez, O., Goy Lopez, S., Hernandez, J. M., Josa, M. I., Merino,
 1287 G., Puerta Pelayo, J., Quintario Olmeda, A., Redondo, I., Romero, L., Santaolalla, J.,
 1288 Soares, M. S., Willmott, C., Albajar, C., Codispoti, G., de Trocóniz, J. F., Brun, H.,
 1289 Cuevas, J., Fernandez Menendez, J., Folgueras, S., Gonzalez Caballero, I., Lloret Iglesias,
 1290 L., Piedra Gomez, J., Brochero Cifuentes, J. A., Cabrillo, I. J., Calderon, A., Chuang,
 1291 S. H., Duarte Campderros, J., Felcini, M., Fernandez, M., Gomez, G., Gonzalez Sanchez,
 1292 J., Jorda, C., Lopez Virto, A., Marco, J., Marco, R., Martinez Rivero, C., Matorras,
 1293 F., Munoz Sanchez, F. J., Rodrigo, T., Rodríguez-Marrero, A. Y., Ruiz-Jimeno, A.,
 1294 Scodellaro, L., Sobron Sanudo, M., Vila, I., Vilar Cortabitarte, R., Abbaneo, D., Auffray,
 1295 E., Auzinger, G., Baillon, P., Ball, A. H., Barney, D., Benitez, J. F., Bernet, C., Bianchi,
 1296 G., Bloch, P., Bocci, A., Bonato, A., Botta, C., Breuker, H., Camporesi, T., Cerminara,
 1297 G., Christiansen, T., Coarasa Perez, J. A., D'Enterria, D., Dabrowski, A., De Roeck,
 1298 A., Di Guida, S., Dobson, M., Dupont-Sagorin, N., Elliott-Peisert, A., Frisch, B., Funk,
 1299 W., Georgiou, G., Giffels, M., Gigi, D., Gill, K., Giordano, D., Giunta, M., Glege, F.,
 1300 Gomez-Reino Garrido, R., Govoni, P., Gowdy, S., Guida, R., Hansen, M., Harris, P.,
 1301 Hartl, C., Harvey, J., Hegner, B., Hinzmann, A., Innocente, V., Janot, P., Kaadze, K.,
 1302 Karavakis, E., Kousouris, K., Lecoq, P., Lee, Y.-J., Lenzi, P., Lourenço, C., Mäki, T.,
 1303 Malberti, M., Malgeri, L., Mannelli, M., Masetti, L., Meijers, F., Mersi, S., Meschi, E.,
 1304 Moser, R., Mozer, M. U., Mulders, M., Musella, P., Nesvold, E., Orimoto, T., Orsini, L.,
 1305 Palencia Cortezon, E., Perez, E., Perrozzi, L., Petrilli, A., Pfeiffer, A., Pierini, M., Pimiä,
 1306 M., Piparo, D., Polese, G., Quertenmont, L., Racz, A., Reece, W., Rodrigues Antunes, J.,
 1307 Rolandi, G., Rommerskirchen, T., Rovelli, C., Rovere, M., Sakulin, H., Santanastasio, F.,
 1308 Schäfer, C., Schwick, C., Segoni, I., Sekmen, S., Sharma, A., Siegrist, P., Silva, P., Simon,
 1309 M., Sphicas, P., Spiga, D., Spiropulu, M., Tsiros, A., Veres, G. I., Vlimant, J. R., Wöhri,
 1310 H. K., Worm, S. D., Zeuner, W. D., Bertl, W., Deiters, K., Erdmann, W., Gabathuler,
 1311 K., Horisberger, R., Ingram, Q., Kaestli, H. C., König, S., Kotlinski, D., Langenegger, U.,

1312 Meier, F., Renker, D., Rohe, T., Sibille, J., Bäni, L., Bortignon, P., Buchmann, M. A.,
 1313 Casal, B., Chanon, N., Deisher, A., Dissertori, G., Dittmar, M., Dünser, M., Eugster, J.,
 1314 Freudenreich, K., Grab, C., Hits, D., Lecomte, P., Lustermann, W., Martinez Ruiz del
 1315 Arbol, P., Mohr, N., Moortgat, F., Nägeli, C., Nef, P., Nessi-Tedaldi, F., Pandolfi, F.,
 1316 Pape, L., Pauss, F., Peruzzi, M., Ronga, F. J., Rossini, M., Sala, L., Sanchez, A. K.,
 1317 Starodumov, A., Stieger, B., Takahashi, M., Tauscher, L., Thea, A., Theofilatos, K.,
 1318 Treille, D., Urscheler, C., Wallny, R., Weber, H. A., Wehrli, L., Aguilo, E., Amsler, C.,
 1319 Chiochia, V., De Visscher, S., Favaro, C., Ivova Rikova, M., Millan Mejias, B., Otiougova,
 1320 P., Robmann, P., Snoek, H., Tupputi, S., Verzetti, M., Chang, Y. H., Chen, K. H., Kuo,
 1321 C. M., Li, S. W., Lin, W., Liu, Z. K., Lu, Y. J., Mekterovic, D., Singh, A. P., Volpe, R., Yu,
 1322 S. S., Bartalini, P., Chang, P., Chang, Y. H., Chang, Y. W., Chao, Y., Chen, K. F., Dietz,
 1323 C., Grundler, U., Hou, W.-S., Hsiung, Y., Kao, K. Y., Lei, Y. J., Lu, R.-S., Majumder, D.,
 1324 Petrakou, E., Shi, X., Shiu, J. G., Tzeng, Y. M., Wan, X., Wang, M., Adiguzel, A., Bakirci,
 1325 M. N., Cerci, S., Dozen, C., Dumanoglu, I., Eskut, E., Girgis, S., Gokbulut, G., Gurpinar,
 1326 E., Hos, I., Kangal, E. E., Karapinar, G., Kayis Topaksu, A., Onengut, G., Ozdemir, K.,
 1327 Ozturk, S., Polatoz, A., Sogut, K., Sunar Cerci, D., Tali, B., Topakli, H., Vergili, L. N.,
 1328 Vergili, M., Akin, I. V., Aliev, T., Bilin, B., Bilmis, S., Deniz, M., Gamsizkan, H., Guler,
 1329 A. M., Ocalan, K., Ozpineci, A., Serin, M., Sever, R., Surat, U. E., Yalvac, M., Yildirim,
 1330 E., Zeyrek, M., Gülmez, E., Isildak, B., Kaya, M., Kaya, O., Ozkorucuklu, S., Sonmez, N.,
 1331 Cankocak, K., Levchuk, L., Bostock, F., Brooke, J. J., Clement, E., Cussans, D., Flacher,
 1332 H., Frazier, R., Goldstein, J., Grimes, M., Heath, G. P., Heath, H. F., Kreczko, L.,
 1333 Metson, S., Newbold, D. M., Nirunpong, K., Poll, A., Senkin, S., Smith, V. J., Williams,
 1334 T., Basso, L., Bell, K. W., Belyaev, A., Brew, C., Brown, R. M., Cockerill, D. J. A.,
 1335 Coughlan, J. A., Harder, K., Harper, S., Jackson, J., Kennedy, B. W., Olaiya, E., Petyt,
 1336 D., Radburn-Smith, B. C., Shepherd-Themistocleous, C. H., Tomalin, I. R., Womersley,
 1337 W. J., Bainbridge, R., Ball, G., Beuselinck, R., Buchmuller, O., Colling, D., Cripps, N.,
 1338 Cutajar, M., Dauncey, P., Davies, G., Della Negra, M., Ferguson, W., Fulcher, J., Futyan,
 1339 D., Gilbert, A., Guneratne Bryer, A., Hall, G., Hatherell, Z., Hays, J., Iles, G., Jarvis,
 1340 M., Karapostoli, G., Lyons, L., Magnan, A.-M., Marrouche, J., Mathias, B., Nandi, R.,
 1341 Nash, J., Nikitenko, A., Papageorgiou, A., Pela, J., Pesaresi, M., Petridis, K., Pioppi,

M., Raymond, D. M., Rogerson, S., Rose, A., Ryan, M. J., Seez, C., Sharp, P., Sparrow,
A., Stoye, M., Tapper, A., Vazquez Acosta, M., Virdee, T., Wakefield, S., Wardle, N.,
Whyntie, T., Chadwick, M., Cole, J. E., Hobson, P. R., Khan, A., Kyberd, P., Leslie, D.,
Martin, W., Reid, I. D., Symonds, P., Teodorescu, L., Turner, M., Hatakeyama, K., Liu,
H., Scarborough, T., Charaf, O., Henderson, C., Rumerio, P., Avetisyan, A., Bose, T.,
Fantasia, C., Heiste (2012). Measurement of the pseudorapidity and centrality dependence
of the transverse energy density in pb-pb collisions at $\sqrt{s_{NN}} = 2.76$ TeV. *Phys. Rev. Lett.*,
109:152303. 6, 21

[13] Collaboration, T. A., Aamodt, K., Quintana, A. A., Achenbach, R., Acounis, S.,
Adamov, D., Adler, C., Aggarwal, M., Agnese, F., Rinella, G. A., Ahammed, Z., Ahmad,
A., Ahmad, N., Ahmad, S., Akindinov, A., Akishin, P., Aleksandrov, D., Alessandro,
B., Alfaro, R., Alfarone, G., Alici, A., Alme, J., Alt, T., Altinpinar, S., Amend, W.,
Andrei, C., Andres, Y., Andronic, A., Anelli, G., Anfreville, M., Angelov, V., Anzo, A.,
Anson, C., Antici, T., Antonenko, V., Antonczyk, D., Antinori, F., Antinori, S., Antonioli,
P., Aphecetche, L., Appelshuser, H., Aprodu, V., Arba, M., Arcelli, S., Argentieri, A.,
Armesto, N., Arnaldi, R., Arefiev, A., Arsene, I., Asryan, A., Augustinus, A., Awes, T. C.,
ysto, J., Azmi, M. D., Bablock, S., Badal, A., Badyal, S. K., Baechler, J., Bagnasco, S.,
Bailhache, R., Bala, R., Baldisseri, A., Baldit, A., Bn, J., Barbera, R., Barberis, P.-L.,
Barbet, J. M., Barnfoldi, G., Barret, V., Bartke, J., Bartos, D., Basile, M., Basmanov, V.,
Bastid, N., Batigne, G., Batyunya, B., Baudot, J., Baumann, C., Bearden, I., Becker, B.,
Belikov, J., Bellwied, R., Belmont-Moreno, E., Belogianni, A., Belyaev, S., Benato, A.,
Beney, J. L., Benhabib, L., Benotto, F., Beol, S., Berceanu, I., Bercuci, A., Berdermann,
E., Berdnikov, Y., Bernard, C., Berny, R., Berst, J. D., Bertelsen, H., Betev, L., Bhasin,
A., Baskar, P., Bhati, A., Bianchi, N., Bielik, J., Bielikov, J., Bimbot, L., Blanchard, G.,
Blanco, F., Blanco, F., Blau, D., Blume, C., Blyth, S., Boccioni, M., Bogdanov, A., Bggild,
H., Bogolyubsky, M., Boldizsr, L., Bombara, M., Bombonati, C., Bondila, M., Bonnet,
D., Bonvicini, V., Borel, H., Borotto, F., Borshchov, V., Bortoli, Y., Borysov, O., Bose,
S., Bosisio, L., Botje, M., Bttger, S., Bourdaud, G., Bourrion, O., Bouvier, S., Braem,
A., Braun, M., Braun-Munzinger, P., Bravina, L., Bregant, M., Bruckner, G., Brun, R.,

1371 Bruna, E., Brunasso, O., Bruno, G. E., Bucher, D., Budilov, V., Budnikov, D., Buesching,
 1372 H., Buncic, P., Burns, M., Burachas, S., Busch, O., Bushop, J., Cai, X., Caines, H.,
 1373 Calaon, F., Caldognio, M., Cali, I., Camerini, P., Campagnolo, R., Campbell, M., Cao,
 1374 X., Capitani, G. P., Romeo, G. C., Cardenas-Montes, M., Carduner, H., Carena, F.,
 1375 Carena, W., Cariola, P., Carminati, F., Casado, J., Diaz, A. C., Caselle, M., Castellanos,
 1376 J. C., Castor, J., Catanescu, V., Cattaruzza, E., Cavazza, D., Cerello, P., Ceresa, S.,
 1377 ern, V., Chambert, V., Chapeland, S., Charpy, A., Charrier, D., Chartoire, M., Charvet,
 1378 J. L., Chattopadhyay, S., Chattopadhyay, S., Chepurnov, V., Chernenko, S., Cherney,
 1379 M., Cheshkov, C., Cheynis, B., Chochula, P., Chiavassa, E., Barroso, V. C., Choi, J.,
 1380 Christakoglou, P., Christiansen, P., Christensen, C., Chykalov, O. A., Cicalo, C., Cifarelli-
 1381 Strolin, L., Ciobanu, M., Cindolo, F., Cirstoiu, C., Clausse, O., Cleymans, J., Cobanoglu,
 1382 O., Coffin, J.-P., Coli, S., Colla, A., Colledani, C., Combaret, C., Combet, M., Comets,
 1383 M., Balbastre, G. C., del Valle, Z. C., Contin, G., Contreras, J., Cormier, T., Corsi, F.,
 1384 Cortese, P., Costa, F., Crescio, E., Crochet, P., Cuautle, E., Cussonneau, J., Dahlinger,
 1385 M., Dainese, A., Dalsgaard, H. H., Daniel, L., Das, I., Das, T., Dash, A., Silva, R. D.,
 1386 Davenport, M., Daues, H., Caro, A. D., de Cataldo, G., Cuveland, J. D., Falco, A. D.,
 1387 de Gaspari, M., de Girolamo, P., de Groot, J., Gruttola, D. D., Haas, A. D., Marco, N. D.,
 1388 Pasquale, S. D., Remigis, P. D., de Vaux, D., Decock, G., Delagrange, H., Franco, M. D.,
 1389 Dellacasa, G., Dell'Olio, C., Dell'Olio, D., Deloff, A., Demanov, V., Dnes, E., D'Erasmus,
 1390 G., Derkach, D., Devaux, A., Bari, D. D., Bartolomeo, A. D., Giglio, C. D., Liberto,
 1391 S. D., Mauro, A. D., Nezza, P. D., Dialinas, M., Diaz, L., Valdes, R. D., Dietel, T., Dima,
 1392 R., Ding, H., Dinca, C., Divi, R., Dobretsov, V., Dobrin, A., Doenigus, B., Dobrowolski,
 1393 T., Domnguez, I., Dorn, M., Drouet, S., Dubey, A. E., Ducroux, L., Dumitrache, F.,
 1394 Dumonteil, E., Dupieux, P., Duta, V., Majumdar, A. D., Majumdar, M. D., Dyhre,
 1395 T., Efimov, L., Efremov, A., Elia, D., Emschermann, D., Engster, C., Enokizono, A.,
 1396 Espagnon, B., Estienne, M., Evangelista, A., Evans, D., Evrard, S., Fabjan, C. W.,
 1397 Fabris, D., Faivre, J., Falchieri, D., Fantoni, A., Farano, R., Fearick, R., Fedorov, O.,
 1398 Fekete, V., Felea, D., Feofilov, G., Tllez, A. F., Ferretti, A., Fichera, F., Filchagin, S.,
 1399 Filoni, E., Finck, C., Fini, R., Fiore, E. M., Flierl, D., Floris, M., Fodor, Z., Foka, Y.,
 1400 Fokin, S., Force, P., Formenti, F., Fragiaco, E., Fragiadakis, M., Fraissard, D., Franco,

1401 A., Franco, M., Frankenfeld, U., Fratino, U., Fresneau, S., Frolov, A., Fuchs, U., Fujita, J.,
 1402 Furget, C., Furini, M., Girard, M. F., Gaardhje, J.-J., Gabrielli, A., Gadrat, S., Gagliardi,
 1403 M., Gago, A., Gaido, L., Torreira, A. G., Gallio, M., Gandolfi, E., Ganoti, P., Ganti, M.,
 1404 Garabatos, J., Lopez, A. G., Garizzo, L., Gaudichet, L., Gemme, R., Germain, M., Gheata,
 1405 A., Gheata, M., Ghidini, B., Ghosh, P., Giolu, G., Giraudo, G., Giubellino, P., Glasow,
 1406 R., Glssel, P., Ferreira, E. G., Gutierrez, C. G., Gonzales-Trueba, L. H., Gorbunov, S.,
 1407 Gorbunov, Y., Gos, H., Gosset, J., Gotovac, S., Gottschlag, H., Gottschalk, D., Grabski,
 1408 V., Grassi, T., Gray, H., Grebenyuk, O., Grebieszko, K., Gregory, C., Grigoras, C.,
 1409 Grion, N., Grigoriev, V., Grigoryan, A., Grigoryan, C., Grigoryan, S., Grishuk, Y., Gros,
 1410 P., Grosse-Oetringhaus, J., Grossiord, J.-Y., Grosso, R., Grynyov, B., Guarnaccia, C.,
 1411 Guber, F., Guerin, F., Guernane, R., Guerzoni, M., Guichard, A., Guida, M., Guilloux,
 1412 G., Gulkanyan, H., Gulbrandsen, K., Gunji, T., Gupta, A., Gupta, V., Gustafsson, H.-
 1413 A., Gutbrod, H., Hadjidakis, C., Haiduc, M., Hamar, G., Hamagaki, H., Hamblen, J.,
 1414 Hansen, J. C., Hardy, P., Hatzifotiadou, D., Harris, J. W., Hartig, M., Harutyunyan, A.,
 1415 Hayrapetyan, A., Hasch, D., Hasegan, D., Hehner, J., Heine, N., Heinz, M., Helstrup, H.,
 1416 Herghelegiu, A., Herlant, S., Corral, G. H., Herrmann, N., Hetland, K., Hille, P., Hinke,
 1417 H., Hippolyte, B., Hoch, M., Hoebbel, H., Hoedlmoser, H., Horaguchi, T., Horner, M.,
 1418 Hristov, P., Hivnov, I., Hu, S., Guo, C. H., Humanic, T., Hurtado, A., Hwang, D. S.,
 1419 Ianigro, J. C., Idzik, M., Igolkin, S., Ilkaev, R., Ilkiv, I., Imhoff, M., Innocenti, P. G.,
 1420 Ionescu, E., Ippolitov, M., Irfan, M., Insa, C., Inuzuka, M., Ivan, C., Ivanov, A., Ivanov,
 1421 M., Ivanov, V., Jacobs, P., Jacholkowski, A., Janurov, L., Janik, R., Jasper, M., Jena, C.,
 1422 Jirden, L., Johnson, D. P., Jones, G. T., Jorgensen, C., Jouve, F., Jovanovi, P., Junique,
 1423 A., Jusko, A., Jung, H., Jung, W., Kadija, K., Kamal, A., Kamermans, R., Kapusta, S.,
 1424 Kaidalov, A., Kakoyan, V., Kalcher, S., Kang, E., Kapitan, J., Kaplin, V., Karadzhev, K.,
 1425 Karavichev, O., Karavicheva, T., Karpechev, E., Karpio, K., Kazantsev, A., Kebschull,
 1426 U., Keidel, R., Khan, M. M., Khanzadeev, A., Kharlov, Y., Kikola, D., Kileng, B., Kim,
 1427 D., Kim, D. S., Kim, D. W., Kim, H. N., Kim, J. S., Kim, S., Kinson, J. B., Kiprich, S. K.,
 1428 Kisel, I., Kiselev, S., Kisiel, A., Kiss, T., Kiworra, V., Klay, J., Bsing, C. K., Kliemant, M.,
 1429 Klimov, A., Klovning, A., Kluge, A., Kluit, R., Kniege, S., Kolevatov, R., Kollegger, T.,
 1430 Kolojvari, A., Kondratiev, V., Kornas, E., Koshurnikov, E., Kotov, I., Kour, R., Kowalski,

1431 M., Kox, S., Kozlov, K., Krlik, I., Kramer, F., Kraus, I., Kravkov, A., Krawutschke, T.,
 1432 Krivda, M., Kryshen, E., Kucheriaev, Y., Kugler, A., Kuhn, C., Kuijer, P., Kumar, L.,
 1433 Kumar, N., Kumpumaeki, P., Kurepin, A., Kurepin, A. N., Kushpil, S., Kushpil, V.,
 1434 Kutovsky, M., Kvaerno, H., Kweon, M., Labb, J.-C., Lackner, F., de Guevara, P. L.,
 1435 Lafage, V., Rocca, P. L., Lamont, M., Lara, C., Larsen, D. T., Laurenti, G., Lazzeroni,
 1436 C., Bornec, Y. L., Bris, N. L., Gailliard, C. L., Lebedev, V., Lecoq, J., Lee, K. S., Lee, S. C.,
 1437 Lefvre, F., Legrand, I., Lehmann, T., Leistam, L., Lenoir, P., Lenti, V., Leon, H., Monzon,
 1438 I. L., Lvai, P., Li, Q., Li, X., Librizzi, F., Lietava, R., Lindegaard, N., Lindenstruth, V.,
 1439 Lippmann, C., Lisa, M., Listratenko, O. M., Littel, F., Liu, Y., Lo, J., Lobanov, V.,
 1440 Loginov, V., Noriega, M. L., Lpez-Ramrez, R., Torres, E. L., Lorenzo, P. M., Lvhidden,
 1441 G., Lu, S., Ludolphs, W., Lunardon, M., Luquin, L., Lusso, S., Lutz, J.-R., Luvisetto,
 1442 M., Lyapin, V., Maevskaya, A., Magureanu, C., Mahajan, A., Majahan, S., Mahmoud,
 1443 T., Mairani, A., Mahapatra, D., Makarov, A., Makhlyueva, I., Malek, M., Malkiewicz,
 1444 T., Mal'Kevich, D., Malzacher, P., Mamonov, A., Manea, C., Mangotra, L. K., Maniero,
 1445 D., Manko, V., Manso, F., Manzari, V., Mao, Y., Marcel, A., Marchini, S., Mare, J.,
 1446 Margagliotti, G. V., Margotti, A., Marin, A., Marin, J.-C., Marras, D., Martinengo, P.,
 1447 Martnez, M. I., Martinez-Davalos, A., Garcia, G. M., Martini, S., Chiesa, A. M., Marzocca,
 1448 C., Masciocchi, S., Maser, M., Masetti, M., Maslov, N. I., Masoni, A., Massera, F., Mast,
 1449 M., Mastroserio, A., Matthews, Z. L., Mayer, B., Mazza, G., Mazzaro, M. D., Mazzoni,
 1450 A., Meddi, F., Meleshko, E., Menchaca-Rocha, A., Meneghini, S., Meoni, M., Perez, J. M.,
 1451 Mereu, P., Meunier, O., Miake, Y., Michalon, A., Michinelli, R., Miftakhov, N., Mignone,
 1452 M., Mikhailov, K., Milosevic, J., Minaev, Y., Minafra, F., Mischke, A., Mikowiec, D.,
 1453 Mitsyn, V., Mitu, C., Mohanty, B., Moisa, D., Molnar, L., Mondal, M., Mondal, N.,
 1454 Zetina, L. M., Monteno, M., Morando, M., Morel, M., Moretto, S., Morhardt, T., Morsch,
 1455 A., Moukhanova, T., Mucchi, M., Muccifora, V., Mudnic, E., Miller, H., Miller, W., Munoz,
 1456 J., Mura, D., Musa, L., Muraz, J. F., Musso, A., Nania, R., Nandi, B., Nappi, E., Navach,
 1457 F., Navin, S., Nayak, T., Nazarenko, S., Nazarov, G., Nellen, L., Nendaz, F., Nianine,
 1458 A., Nicassio, M., Nielsen, B. S., Nikolaev, S., Nikolic, V., Nikulin, S., Nikulin, V., Nilsen,
 1459 B., Nitti, M., Noferini, F., Nomokonov, P., Nooren, G., Noto, F., Nouais, D., Nyiri,
 1460 A., Nystrand, J., Odyniec, G., Oeschler, H., Oinonen, M., Oldenburg, M., Oleks, I.,

1461 Olsen, E. K., Onuchin, V., Oppedisano, C., Orsini, F., Ortiz-Velzquez, A., Oskamp, C.,
 1462 Oskarsson, A., Osmic, F., sberman, L., Otterlund, I., Ovrebekk, G., Oyama, K., Pachr,
 1463 M., Pagano, P., Pai, G., Pajares, C., Pal, S., Pal, S., Plla, G., Palmeri, A., Pancaldi,
 1464 G., Panse, R., Pantaleo, A., Pappalardo, G. S., Pastirk, B., Pastore, C., Patarakin, O.,
 1465 Paticchio, V., Patimo, G., Pavlinov, A., Pawlak, T., Peitzmann, T., Pnichot, Y., Pepato,
 1466 A., Pereira, H., Peresunko, D., Perez, C., Griffio, J. P., Perini, D., Perrino, D., Peryt, W.,
 1467 Pesci, A., Peskov, V., Pestov, Y., Peters, A. J., Petrek, V., Petridis, A., Petris, M., Petrov,
 1468 V., Petrov, V., Petrovici, M., Peyr, J., Piano, S., Piccotti, A., Pichot, P., Piemonte, C.,
 1469 Pikna, M., Pilastrini, R., Pillot, P., Pinazza, O., Pini, B., Pinsky, L., Morais, V. P.,
 1470 Pismennaya, V., Piuz, F., Platt, R., Ploskon, M., Plumeri, S., Pluta, J., Pocheptsov,
 1471 T., Podesta, P., Poggio, F., Poghosyan, M., Poghosyan, T., Polk, K., Polichtchouk, B.,
 1472 Polozov, P., Polyakov, V., Pommeresch, B., Pompei, F., Pop, A., Popescu, S., Posa, F.,
 1473 Pospil, V., Potukuchi, B., Pouthas, J., Prasad, S., Preghenella, R., Prino, F., Prodan, L.,
 1474 Prono, G., Protsenko, M. A., Pruneau, C. A., Przybyla, A., Pshenichnov, I., Puddu, G.,
 1475 Pujahari, P., Pulvirenti, A., Punin, A., Punin, V., Putschke, J., Quartieri, J., Quercigh,
 1476 E., Rachevskaya, I., Rachevski, A., Rademakers, A., Radomski, S., Radu, A., Rak, J.,
 1477 Ramello, L., Raniwala, R., Raniwala, S., Rasmussen, O. B., Rasson, J., Razin, V., Read,
 1478 K., Real, J., Redlich, K., Reichling, C., Renard, C., Renault, G., Renfordt, R., Reolon,
 1479 A. R., Reshetin, A., Revol, J.-P., Reygers, K., Ricaud, H., Riccati, L., Ricci, R. A., Richter,
 1480 M., Riedler, P., Rigalleau, L. M., Riggi, F., Riegler, W., Rindel, E., Riso, J., Rivetti, A.,
 1481 Rizzi, M., Rizzi, V., Cahuantzi, M. R., Red, K., Rhrich, D., Romn-Lpez, S., Romanato, M.,
 1482 Romita, R., Ronchetti, F., Rosinsky, P., Rosnet, P., Rossegger, S., Rossi, A., Rostchin,
 1483 V., Rotondo, F., Roukoutakis, F., Rousseau, S., Roy, C., Roy, D., Roy, P., Royer, L.,
 1484 Rubin, G., Rubio, A., Rui, R., Rusanov, I., Russo, G., Ruuskanen, V., Ryabinkin, E.,
 1485 Rybicki, A., Sadovsky, S., afak, K., Sahoo, R., Saini, J., Saiz, P., Salur, S., Sambyal,
 1486 S., Samsonov, V., ndor, L., Sandoval, A., Sann, H., Santiard, J.-C., Santo, R., Santoro,
 1487 R., Sargsyan, G., Saturnini, P., Scapparone, E., Scarlassara, F., Schackert, B., Schiaua,
 1488 C., Schicker, R., Schioler, T., Schippers, J. D., Schmidt, C., Schmidt, H., Schneider, R.,
 1489 Schossmailer, K., Schukraft, J., Schutz, Y., Schwarz, K., Schweda, K., Schyns, E., Scioli,
 1490 G., Scomparin, E., Snow, H., Sedykh, S., Segato, G., Sellitto, S., Semeria, F., Senyukov,

1491 S., Seppnen, H., Serici, S., Serkin, L., Serra, S., Sesselmann, T., Sevcenco, A., Sgura, I.,
 1492 Shabratova, G., Shahoyan, R., Sharkov, E., Sharma, S., Shigaki, K., Shileev, K., Shukla,
 1493 P., Shurygin, A., Shurygina, M., Sibiriak, Y., Siddi, E., Siemiarzczuk, T., Sigward, M. H.,
 1494 Silenzi, A., Silvermyr, D., Silvestri, R., Simili, E., Simion, V., Simon, R., Simonetti, L.,
 1495 Singaraju, R., Singhal, V., Sinha, B., Sinha, T., Siska, M., Sitr, B., Sitta, M., Skaali,
 1496 B., Skowronski, P., Slodkowski, M., Smirnov, N., Smykov, L., Snellings, R., Snoeys, W.,
 1497 Soegaard, C., Soerensen, J., Sokolov, O., Soldatov, A., Soloviev, A., Soltveit, H., Soltz,
 1498 R., Sommer, W., Soos, C., Soramel, F., Sorensen, S., Soyk, D., Spyropoulou-Stassinaki,
 1499 M., Stachel, J., Staley, F., Stan, I., Stavinskiy, A., Steckert, J., Stefanini, G., Stefanek,
 1500 G., Steinbeck, T., Stelzer, H., Stenlund, E., Stocco, D., Stockmeier, M., Stoicea, G.,
 1501 Stolpovsky, P., Strme, P., Stutzmann, J. S., Su, G., Sugitate, T., umbera, M., Suire, C.,
 1502 Susa, T., Kumar, K. S., Swoboda, D., Symons, J., Szarka, I., Szostak, A., Szuba, M.,
 1503 Szymanski, P., Tadel, M., Tagridis, C., Tan, L., Takaki, D. T., Taureg, H., Tauro, A.,
 1504 Tavlet, M., Munoz, G. T., Thder, J., Tieulent, R., Timmer, P., Tolyhy, T., Topilskaya,
 1505 N., de Matos, C. T., Torii, H., Toscano, L., Tosello, F., Tournaire, A., Traczyk, T., Trger,
 1506 G., Tromeur, W., Truesdale, D., Trzaska, W., Tsiledakis, G., Tsilis, E., Tsvetkov, A.,
 1507 Turcato, M., Turrisi, R., Tuveri, M., Tveter, T., Tydesjo, H., Tykarski, L., Tywoniuk, K.,
 1508 Ugolini, E., Ullaland, K., Urbn, J., Urciuoli, G. M., Usai, G. L., Usseglio, M., Vacchi, A.,
 1509 Vala, M., Valiev, F., Vyvre, P. V., Brink, A. V. D., Eijndhoven, N. V., Kolk, N. V. D.,
 1510 van Leeuwen, M., Vannucci, L., Vanzetto, S., Vanuxem, J.-P., Vargas, M. A., Varma,
 1511 R., Vascotto, A., Vasiliev, A., Vassiliou, M., Vasta, P., Vechernin, V., Venaruzzo, M.,
 1512 Vercellin, E., Vergara, S., Verhoeven, W., Veronese, F., Vetlitskiy, I., Vernet, R., Victorov,
 1513 V., Vidak, L., Viesti, G., Vikhlyantsev, O., Vilakazi, Z., Baillie, O. V., Vinogradov, A.,
 1514 Vinogradov, L., Vinogradov, Y., Virgili, T., Viyogi, Y., Vodopianov, A., Volpe, G., Vranic,
 1515 D., Vrlkov, J., Vulpescu, B., Wabnitz, C., Wagner, V., Wallet, L., Wan, R., Wang, Y.,
 1516 Wang, Y., Wheadon, R., Weis, R., Wen, Q., Wessels, J., Westergaard, J., Wiechula, J.,
 1517 Wiesenaecker, A., Wikne, J., Wilk, A., Wilk, G., Williams, C., Willis, N., Windelband, B.,
 1518 Witt, R., Woehri, H., Wyllie, K., Xu, C., Yang, C., Yang, H., Yermia, F., Yin, Z., Yin, Z.,
 1519 Ky, B. Y., Yushmanov, I., Yuting, B., Zabrodin, E., Zagato, S., Zagreev, B., Zaharia, P.,
 1520 Zalite, A., Zampa, G., Zampolli, C., Zanevskiy, Y., Zarochentsev, A., Zaudtke, O., Zvada,

1521 P., Zbroszczyk, H., Zepeda, A., Zeter, V., Zgura, I., Zhalov, M., Zhou, D., Zhou, S., Zhu,
1522 G., Zichichi, A., Zinchenko, A., Zinovjev, G., Zoccarato, Y., Zubarev, A., Zucchini, A.,
1523 and Zuffa, M. (2008). The alice experiment at the cern lhc. *Journal of Instrumentation*,
1524 3(08):S08002. 24

1525 [14] Connors, M., Nattrass, C., Reed, R., and Salur, S. (2017). Review of Jet Measurements
1526 in Heavy Ion Collisions. vi, 11, 13, 14

1527 [15] Elia, D. and the ALICE Collaboration (2013). Strangeness production in alice. *Journal*
1528 *of Physics: Conference Series*, 455(1):012005. 18

1529 [16] Evans, L. and Bryant, P. (2008). Lhc machine. *Journal of Instrumentation*,
1530 3(08):S08001. 9

1531 [17] Floris, M. (2014). Hadron yields and the phase diagram of strongly interacting matter.
1532 *Nuclear Physics A*, 931:103 – 112. QUARK MATTER 2014. 6

1533 [18] Foka, P. and Janik, M. A. (2016). An overview of experimental results from ultra-
1534 relativistic heavy-ion collisions at the cern lhc: Bulk properties and dynamical evolution.
1535 *Reviews in Physics*, 1:154 – 171. 10

1536 [19] Gyulassy, M. (2004). The QGP discovered at RHIC. In *Structure and dynamics*
1537 *of elementary matter. Proceedings, NATO Advanced Study Institute, Camyuva-Kemer,*
1538 *Turkey, September 22-October 2, 2003*, pages 159–182. 7

1539 [20] Heuser, J. M. (2013). The compressed baryonic matter experiment at fair. *Nuclear*
1540 *Physics A*, 904-905:941c – 944c. The Quark Matter 2012. 5

1541 [21] Hilke, H. J. (2010). Time projection chambers. *Reports on Progress in Physics*,
1542 73(11):116201. vii, 26, 27

1543 [22] Huovinen, P., Kolb, P. F., Heinz, U., Ruuskanen, P. V., and Voloshin, S. A. (2001).
1544 Radial and elliptic flow at RHIC: further predictions. *Physics Letters B*, 503:58–64. 16

1545 [23] Jacobs, P. and Wang, X.-N. (2005). Matter in extremis: ultrarelativistic nuclear
1546 collisions at RHIC. *Progress in Particle and Nuclear Physics*, 54:443–534. 15

- [24] Kapusta, J. I. (1979). Quantum chromodynamics at high temperature. *Nuclear Physics B*, 148(3):461 – 498. 3
- [25] Luo, X. (2016). Exploring the qcd phase structure with beam energy scan in heavy-ion collisions. *Nuclear Physics A*, 956:75 – 82. The XXV International Conference on Ultrarelativistic Nucleus-Nucleus Collisions: Quark Matter 2015. 19
- [26] Nattrass, C. (2009). System, energy, and flavor dependence of jets through di-hadron correlations in heavy ion collisions. *v*, 10, 26
- [27] Odyniec, G. (2013). The rhic beam energy scan program in star and what’s next ... *Journal of Physics: Conference Series*, 455(1):012037. 19
- [28] Ozaki, S. and Roser, T. (2015). Relativistic heavy ion collider, its construction and upgrade. *Progress of Theoretical and Experimental Physics*, 2015(3):03A102. vi, 8
- [29] Preghenella, R. (2011). Transverse momentum spectra of identified charged hadrons with the ALICE detector in Pb-Pb collisions at $\sqrt{s_{NN}} = 2.76$ TeV. *PoS, EPS-HEP2011:118*. 24
- [30] Qin, G.-Y. and Wang, X.-N. (2015). Jet quenching in high-energy heavy-ion collisions. *International Journal of Modern Physics E*, 24:1530014–438. 19
- [31] Satz, H. (2006). Colour deconfinement and quarkonium binding. *Journal of Physics G: Nuclear and Particle Physics*, 32(3):R25. 4, 6
- [32] Schenke, B. (2017). Origins of collectivity in small systems. *Nuclear Physics A*, 967:105 – 112. The 26th International Conference on Ultra-relativistic Nucleus-Nucleus Collisions: Quark Matter 2017. 15
- [33] Shao, M., Barannikova, O. Yu., Dong, X., Fisyak, Y., Ruan, L., Sorensen, P., and Xu, Z. (2006). Extensive particle identification with TPC and TOF at the STAR experiment. *Nucl. Instrum. Meth.*, A558:419–429. 26
- [34] Shuryak, E. V. (1988). The qcd vacuum and quark-gluon plasma. *Zeitschrift für Physik C Particles and Fields*, 38(1):141–145. 3

- 1573 [35] Snellings, R. (2011). Elliptic flow: a brief review. *New Journal of Physics*, 13(5):055008.
1574 16
- 1575 [36] Stock, R. (2004). Ultra-relativistic nucleus-nucleus collisions. Proceedings, 17th
1576 International Conference, Quark Matter 2004, Oakland, USA, January 11-17, 2004. *J.*
1577 *Phys.*, G30:S633–S648. 7
- 1578 [37] Strickland, M. (2014). Anisotropic hydrodynamics: Motivation and methodology.
1579 *Nuclear Physics A*, 926:92–101. 15
- 1580 [38] Stcker, H. (2005). Collective flow signals the quarkgluon plasma. *Nuclear Physics A*,
1581 750(1):121 – 147. Quark-Gluon Plasma. New Discoveries at RHIC: Case for the Strongly
1582 Interacting Quark-Gluon Plasma. Contributions from the RBRC Workshop held May 14-
1583 15, 2004. vii, 20
- 1584 [39] Vovchenko, V., Anchishkin, D., and Csernai, L. P. (2014). Time dependence of
1585 partition into spectators and participants in relativistic heavy-ion collisions. *Phys. Rev.*
1586 *C*, 90:044907. vi, 12
- 1587 [40] Wilde, M. (2013). Measurement of Direct Photons in pp and Pb-Pb Collisions with
1588 ALICE. *Nucl. Phys.*, A904-905:573c–576c. 17
- 1589 [41] Wong, C.-Y. (1994). *Introduction to high-energy heavy-ion collisions*. World scientific.
1590 vi, 12, 17, 18

Appendices